ATR

AUSTRALIAN TELECOMMUNICATION RESEARCH

ATR is published twice a year (in May and November) by the Telecommunication Society of Australia. In addition special issues may be published.
ATR publishes papers relating to research into telecommunications in Australia.

CONTRIBUTIONS: The editors will be pleased to consider papers for publication. Contributions should be addressed to the Secretary, ATR, c/- Telecom Australia Research Laboratories, 22 Winterton Rd., Clayton, Vic., 3168.

RESPONSIBILITY: The Society and the Board of Editors are not responsible for statements made or opinions expressed by authors of articles in this journal.

REPRINTING: Editors of other publications are welcome to use not more than one third of any article, provided that credit is given at the beginning or end as:- ATR, the volume number, issue and date. Permission to reprint larger extracts or complete articles will normally be granted on application to the General Secretary of the Telecommunication Society of Australia.

SUBSCRIPTIONS: Subscriptions for ATR may be placed with the General Secretary, Telecommunication Society of Australia, Box 4050, G.P.O., Melbourne, Victoria, Australia, 3001. The subscription rates are detailed below. All rates are post free. Remittances should be made payable to the Telecommunication Society of Australia, in Australian currency and should yield the full amount free of any bank charges.

Contents

Challenge . . .

It is now widely recognised that the information industry is a very significant part of our economy. Means of recording, storing, transferring and manipulating information are becoming more powerful and cheaper with astonishing rapidity.

We are also witnessing the growth of two opposing social attitudes towards information - freedom of information and privacy. These opposing views are progressively developing and lines of demarcation are becoming increasingly difficult to discern; in some cases they even overlap. A case in point is telephone numbers; in general, it is desirable that these should be publicly available so that calls can be made to people whom one wishes to contact. However, many people are prepared to pay a premium for an unlisted telephone number so that they will not be bothered with telephone calls. Taken to the ultimate, if the only purpose of a telephone were to originate a call and not to receive one, then the reason for existence of a telephone network becomes unclear. While there is universal acceptance of a telephone directory containing most telephone numbers, there appears to be considerable resistance to selections of that publicly available information being made available. Direct mail selling is becoming a way of life, and purveyors will need address lists; some people may wish to preserve their privacy in regard to not being included, yet others will wish to avail themselves of opportunities. Modern information processing equipment can sort available data, but what will be the guiding social pressures?

Commercial information, or data, can be regarded as a commodity; indeed, this is now recognised by the OECD, who are formulating rules about transnational data flows. How are these to be monitored, while respecting privacy? On the other side of the coin, how is commercial security (which is necessary to preserve the value of the commodity) to be maintained? Technology is available for encryption which can enable data, or information, to be openly concealed in publicly available or private data bases in a form which makes its recognition virtually impossible; similarly with information which is transmitted. Maintenance of security is vital to those handling the data or information; however, what are the rules of freedom of access for those genuinely concerned that the data may or may not refer, accurately or inaccurately, to themselves? Mention of Debt Collecting Agencies provides interesting speculation on the values of both commercial security of information and freedom of access.

The acceptability of methods of handling data and information is going to become more complex and have increasing significance as tools for handling them become (inevitably) cheaper and more powerful. Likewise, difficulties in policing rules are going to become more significant, both technically and in volume. It is to be hoped that we can develop a realistic attitude to the handling of information that will be acceptable to both the information industry and to individuals.

<div align="right">H.S. Wragge.</div>

A Computer Technique For The Frequency Response And Sensitivity Analysis Of Digital Filters: A Tutorial

P.R. HICKS
J.L. SNARE
Telecom Australia Research Laboratories

This paper describes a numerical technique (suitable for performing on a digital computer) to obtain the frequency response and make a sensitivity analysis of a wide variety of digital filter networks. The technique, which is based on well established theory, uses a simple matrix representation of the digital network, which is readily derived from a signal flow graph description of the network. Some practical results obtained in analysing the cascade form and parallel form realizations of an eighth order bandpass filter are presented.

1. INTRODUCTION

Fundamental to virtually all signal processing is the need for linear time invariant frequency selective filters. By implementing the filter using digital components performance criteria can often be satisfied which would be elusive using alternative classes of filter, such as passive LC or active filters. The past decade has seen a unification of the theoretical basis and the development of a wide variety of structures and design techniques for the implementation of digital filters. Presumably digital filtering will become common place in the next decade - particularly in view of the developments in digital hardware suitable for digital signal processing applications.

It is possible to realize a particular transfer function or filter specification by a number of different filter structures : direct form II, cascade form or parallel form for example.

Having obtained the filter coefficients for a particular structure it is likely that the designer would like to check the filter response and perhaps more importantly test either the sensitivity of the response to changes in the filter coefficients or test the effect of finite word length. This paper describes a technique for computing the frequency response and making a sensitivity analysis of digital filters. The technique provides the designer with a convenient method of comparing the responses of different filter structures for varying coefficient precision. The technique is based on some well established theory; however we feel that many engineers may not be aware that this theory can be applied to obtain the frequency response and make a sensitivity analysis of digital networks. We see its use as an analysis tool in the first stages of the design of a practical digital filter; ie. finding the minimum precision with which the filter coefficients must be specified.

The approach taken uses a simple matrix representation of digital networks, which is readily derived from a signal flow graph description, using z-transform techniques.

2. MATRIX REPRESENTATION OF DIGITAL NETWORKS

A digital network can be represented by a signal flow graph. The signal flow graph consists of nodes and directed branches with all branches connected between nodes. The transmission from node j to node k is denoted f_{jk} ie. a branch in a signal flow graph joining node j to node k is drawn as shown below

$$
\begin{array}{ccc}
w_j & & w_k \\
\underline{}\!\!\longrightarrow\!\!\underline{} & & \\
j & f_{jk} & k
\end{array}
$$
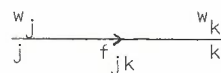
Associated with each node j there is a node variable, w_j. Associated with each branch jk there is an input (w_j) and output (v_{jk}). w_j is commonly referred to as the node input variable; v_{jk} is referred to as the branch output variable. The dependence of a branch output upon the branch input is denoted

$$ v_{jk} = f_{jk}[w_j] $$

The [] notation represents the transformation from branch input to branch output.

In the common realizations of digital filters the branch transmittances (f_{jk}) are restricted to either,

(i) multiplication by a scalar

(ii) a delay element (shift operation)

The node value at each node in the network is given by the sum of the outputs of all branches

entering the node (similar to Kirchoffs current law).

If we define a source node as one at which we can inject external inputs into the graph and a sink node as one at which an output can be extracted

assuming N network nodes (numbered 1 to N) in the graph

        M source nodes

        P sink nodes

a graph can be represented by the following set of equations (Ref.1).

$$w_k = \sum_{j=1}^{N} v_{jk} + \sum_{j=1}^{M} s_{jk} \qquad k=1,2,3, \ .. \ N$$
$$\text{(network} \qquad \text{(source}$$
$$\text{nodes)} \qquad \text{nodes)}$$

$$y_k = \sum_{j=1}^{N} r_{jk} \qquad k=1,2, \ .. \ P$$
$$\text{(network}$$
$$\text{nodes)}$$

where s_{jk} denotes the output of the branch connecting source node j to network node k

r_{jk} denotes the output of the branch connecting network node j to sink node k .

A convenient way of representing a network containing delay elements is to use the z-transform. The z-transform of a unit delay is z^{-1} .

In terms of the z-transform the above set of equations may be written

$$W_k(z) = \sum_{j=1}^{N} V_{jk}(z) + \sum_{j=1}^{M} S_{jk}(z) \qquad k=1,2, \ .. \ N$$

$$Y_k(z) = \sum_{j=1}^{N} R_{jk}(z) \qquad k=1,2, \ .. \ P$$

Assuming the branches connecting the source and sink nodes to the network have constant transmittances b_{jk} and c_{jk} respectively, then

$$V_{jk}(z) = F_{jk}W_j(z)$$

$$S_{jk}(z) = b_{jk}X_j(z)$$

$$R_{jk}(z) = c_{jk}W_j(z)$$

where F_{jk} is either a scalar or the unit delay operator z^{-1} .

Thus

$$W_k(z) = \sum_{j=1}^{N} F_{jk}(z)W_j(z) + \sum_{j=1}^{M} b_{jk}X_j(z)$$

$$Y_k(z) = \sum_{j=1}^{N} c_{jk}W_j(z)$$

The notation used in this paper so far has used lower case symbols to denote sequences in the time domain and upper case symbols to denote their z-transforms. To simplify the notation in the following discussion, all variables are assumed to be in the z domain. Matrices are denoted by uppercase italic unsubscripted symbols with specific elements identified by subscript.

In matrix form the network equations in the z domain may be written:

$$W = F^{\dagger}W + B^{\dagger}X$$

$$Y = C^{\dagger}W$$

where W is the column vector W_k of signals at the network nodes $k=1,2, \ .. \ N$

X is the column vector X_j of sources $j=1,2, \ .. \ M$

Y is the column vector Y_k of sinks (outputs) $j=1,2, \ .. \ P$

$F^{\dagger}$ is the $N{\times}N$ transpose of the transmittance matrix

$B^{\dagger}$ is the $N{\times}M$ transpose of the source connection matrix

$C^{\dagger}$ is the $P{\times}N$ transpose of the sink connection matrix

The transpose notation is necessary for subscript consistency between the network description and matrix representation.

Solving for W(z)

$$W = [I - F^{\dagger}]^{-1} B^{\dagger}X$$

$$= T^{\dagger}X$$

where $T^{\dagger} = [I - F^{\dagger}]^{-1} B^{\dagger}$ is defined as the transfer function matrix of the system.

If we assume that there are N source nodes and there are N network nodes (ie. each network node has a source connected to it) then $B^{\dagger} = I$ the unit matrix

and

$$X_N = \begin{bmatrix} X_1 \\ X_2 \\ . \\ . \\ X_N \end{bmatrix}$$

Thus

$$T^\dagger = [I - F^\dagger]^{-1}$$

Then the transfer function from node j to node k may be determined from the matrix $T^\dagger$ by setting all sources to zero except the one connected to node j. For example: assume a source is connected to node j, then the transfer function between node j and arbitrary node k is the element k,j of $T^\dagger$.

3. NETWORK SENSITIVITY

Using Tellegens theorem (Ref.1) a general expression may be derived which relates the sensitivity of the transfer function for a given network to changes in the branch transmittances.

We will consider the transfer function between an arbitrary pair of nodes a and b in the network, see Fig.1. T_{ab} is then the system transfer function from node a to node b. The sensitivity of this function to changes in a branch transmittance F_{nm} is defined as

$$\frac{\partial T_{ab}}{\partial F_{nm}}$$

It has been shown (Ref.2) that

$$\frac{\partial T_{ab}}{\partial F_{nm}} = T_{an} \, T_{mb}$$

where T_{an} is the system function between node a and node n
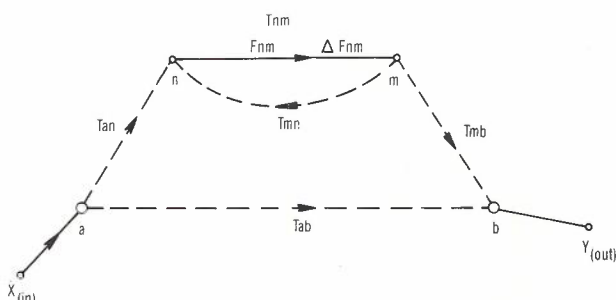
and T_{mb} is the system function between node m and node b.

Fig.1 - *Signal flow graph conventions.*

The sensitivity of T_{ab} to a large scale change in F_{nm} can be determined by writing ΔT_{ab} as a Taylor Series Expansion

$$\Delta T_{ab} = \frac{\partial T_{ab}}{\partial F_{nm}} \Delta F_{nm} + \frac{1}{2} \frac{\partial^2 T_{ab}}{\partial F^2_{nm}} (\Delta F_{nm})^2 + \ldots$$

It follows that (see Appendix 1)

$$\Delta T_{ab} = \frac{T_{an} \, T_{mb} \, \Delta F_{nm}}{1 - T_{mn} \, \Delta F_{nm}}$$

This expression relates a change in the system function T_{ab} to a large scale change in the branch transmittance $F_{nm},(\Delta F_{nm})$.

4. PRACTICAL ADVANTAGES OF THE MATRIX APPROACH

It is of course possible to compute the transfer function response and calculate sensitivities using so called direct methods. From the signal flow graph representation of the digital network the system transfer function is obtained. This will usually involve either solving a series of network equations or breaking the filter structure down into a number of canonic form sections whose transfer functions are readily known. For example the transfer function of a direct form II section is of the form

$$H(z) = \frac{1 + C_2 z^{-1} + C_4 z^{-2}}{1 - C_1 z^{-1} - C_3 z^{-2}}$$

The overall transfer function of say a cascade form (of direct form II sections) is then the product of such terms. The frequency response may be computed by setting $z^{-1} = e^{-s} = e^{-j\omega}$ and calculating the magnitude as the frequency is varied. This process will generally involve a fair amount of tedious algebra especially for complicated filter structures.

In regard to calculating sensitivities it should be noted that the sensitivity expression developed in section 3 is valid regardless of how the transfer functions are calculated. However in calculating ΔT_{ab} it is necessary to know the values of several internal transfer functions for each coefficient change. Direct method calculation of these internal transfer functions may be quite difficult. Typically a sensitivity analysis would require the effects of changes in many/all of the filter coefficients to be considered. Also each coefficient may be varied over a range of values. Thus a large amount of algebraic and computational effort may be required when using the direct method approach.

With the matrix approach, the values of all possible required transfer functions at a particular frequency can be obtained using information gained from a single evaluation of the system transfer function matrix $T^\dagger$. If efficient matrix inversion techniques are used a considerable saving in computational effort is made. Having obtained the required transfer functions the effect of changing a particular branch transmittance over a range of values, (at one particular frequency), is then a relatively simple calculation using the sensitivity expression. The calculation may be readily repeated for each of the coefficients in turn.

Of course it is possible to calculate $\Delta T_{ab}/\Delta F_{nm}$ directly; however this would involve many evaluations of the transfer function in order that all coefficients are varied by a desired amount over the frequency range of interest.

5. NUMERICAL EVALUATION

A computer program has been written to calculate the transfer function of a digital network and the sensitivity of that network to coefficient changes. The program is not an implementation of the filter but uses the theory outlined in sections 2 and 3 to enable the required calculations to be made.

It has been noted that sensitivity (ΔT_{ab}) and transfer function can be calculated by selecting appropriate elements from the $(I - F^\dagger)^{-1}$ matrix calculated for the overall network. The z-transform domain description of this matrix is not convenient for numerical computation. A satisfactory way to perform the required calculations is to consider the case where a steady state sinusoidal input is assumed. Under these conditions

$$z^{-1} = e^{-j\omega} = \cos\omega - j\sin\omega$$

where ω is the radian frequency.

The main feature of the computer program is evaluation of $[I - F^\dagger]^{-1}$. In general, $F^\dagger(z)$ contains complex elements, so the matrix inversion technique used must be able to handle complex variables. Since it is common to specify the digital filter coefficients to a large number of significant figures (e.g. 10), double precision arithmetic may be required.

Subroutines exist that will perform either complex or double precision matrix inversions but not both. To achieve the desired inversion an algorithm was used that separately handles the real and imaginary parts of a complex matrix in double precision form and produces an inverse consisting of two matrices – the real part and the imaginary part. Details are shown in Appendix 2. A simple calculation can then be performed to find the magnitude and phase of the elements of the complex inverse.

Filter configuration details and coefficient values are entered in special subroutines rather than being input variables. This has two main advantages (at the cost of loss of generality).

Firstly, the program is simpler and secondly, large amounts of data do not need to be entered for each run. The subroutine for a filter configuration is simply structured and additional subroutines can be readily added.

The network defining subroutine is constructed such that firstly the numerical values of the network coefficients are entered. Next the elements of the transpose of the transmittance matrix $F^\dagger$ are entered. Now since the network will contain delay elements ie. z^{-1}, the transmittance matrix is complex since $z^{-1} = e^{-j\omega} = \cos\omega - j\sin\omega$.

$F^\dagger$ is stored as two matrices:

FTR represents the real part of $F^\dagger$

FTI represents the imaginary part of $F^\dagger$

For example if we have a branch

$$j \xrightarrow{\quad C_x \quad} k$$
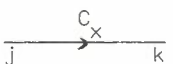
where C_x is a real constant $\quad$ FTR$(k,j) = + C_x$

if we have

$$1 \xrightarrow{\quad z^{-1} \quad} m$$
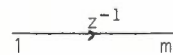
$$\text{FTR}(m,1) = + \cos\omega$$
$$\text{FTI}(m,1) = - \sin\omega$$

Since any network is completely specified by the transpose of the transmittance matrix ie. $F^\dagger$, the numbering of the nodes of any signal flow graph can be done quite arbitrarily. However in order that no node is overlooked it is best to adopt a logical or sequential numbering scheme. The convention adopted was that the input node was specified as node #1 and the output node as node #2.

As an example, the transpose of the transmittance matrix $F^\dagger$ for the cascade form structure shown in Fig.2a is as shown below.

This matrix typically contains few non-zero elements and hence sparse matrix inversion techniques enable the inverse to be efficiently computed.

$F^\dagger$ is readily obtained when it is realized that the columns of $F^\dagger$ are the branch input nodes and the rows are the branch output nodes. Thus the transmittance of the branch joining node j to node k is the element k,j of $F^\dagger$.

$$
F^\dagger(z) = \begin{bmatrix}
0 & 0 & 0 & 0 & 0 & 0 & 0 & 0 & 0 & 0 & 0 & 0 & 0 & 0 & 0 & 0 & 0 \\
0 & 0 & 0 & 0 & 0 & 0 & 0 & 0 & 0 & 0 & 0 & 0 & 0 & 0 & 1 & C_{11} & 1 \\
K & 0 & 0 & C_1 & C_3 & 0 & 0 & 0 & 0 & 0 & 0 & 0 & 0 & 0 & 0 & 0 & 0 \\
0 & 0 & z^{-1} & 0 & 0 & 0 & 0 & 0 & 0 & 0 & 0 & 0 & 0 & 0 & 0 & 0 & 0 \\
0 & 0 & 0 & z^{-1} & 0 & 0 & 0 & 0 & 0 & 0 & 0 & 0 & 0 & 0 & 0 & 0 & 0 \\
0 & 0 & 1 & C_2 & 1 & 0 & 0 & 0 & 0 & 0 & 0 & 0 & 0 & 0 & 0 & 0 & 0 \\
0 & 0 & 0 & 0 & 0 & 1 & 0 & C_4 & C_6 & 0 & 0 & 0 & 0 & 0 & 0 & 0 & 0 \\
0 & 0 & 0 & 0 & 0 & 0 & z^{-1} & 0 & 0 & 0 & 0 & 0 & 0 & 0 & 0 & 0 & 0 \\
0 & 0 & 0 & 0 & 0 & 0 & 0 & z^{-1} & 0 & 0 & 0 & 0 & 0 & 0 & 0 & 0 & 0 \\
0 & 0 & 0 & 0 & 0 & 0 & 1 & C_5 & 1 & 0 & 0 & 0 & 0 & 0 & 0 & 0 & 0 \\
0 & 0 & 0 & 0 & 0 & 0 & 0 & 0 & 0 & 1 & 0 & C_7 & C_9 & 0 & 0 & 0 & 0 \\
0 & 0 & 0 & 0 & 0 & 0 & 0 & 0 & 0 & 0 & z^{-1} & 0 & 0 & 0 & 0 & 0 & 0 \\
0 & 0 & 0 & 0 & 0 & 0 & 0 & 0 & 0 & 0 & 0 & z^{-1} & 0 & 0 & 0 & 0 & 0 \\
0 & 0 & 0 & 0 & 0 & 0 & 0 & 0 & 0 & 0 & 1 & C_8 & 1 & 0 & 0 & 0 & 0 \\
0 & 0 & 0 & 0 & 0 & 0 & 0 & 0 & 0 & 0 & 0 & 0 & 0 & 1 & 0 & C_{10} & C_{12} \\
0 & 0 & 0 & 0 & 0 & 0 & 0 & 0 & 0 & 0 & 0 & 0 & 0 & 0 & z^{-1} & 0 & 0 \\
0 & 0 & 0 & 0 & 0 & 0 & 0 & 0 & 0 & 0 & 0 & 0 & 0 & 0 & 0 & z^{-1} & 0
\end{bmatrix}
$$

Transmittance Matrix for filter structure shown in Figure 2a.

k = 0·005656462366

C1 = 0·2855823838
C2 = 0·4512591755
C3 = ⁻0·9116360616
C4 = 0·4457342317
C5 = ⁻1·09869455
C6 = ⁻0·913078673

C7 = 0·196901665
C8 = ⁻0·0099665157
C9 = ⁻0·9695353354
C10 = 0·5515388641
C11 = ⁻0·7304169706
C12 = ⁻0·9705899009
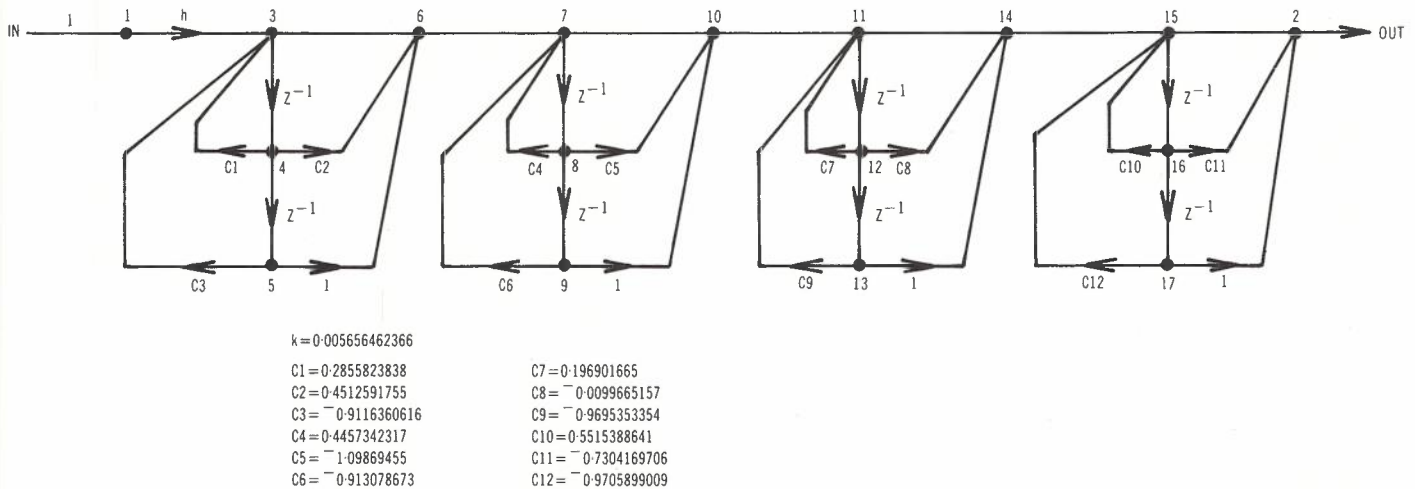
Fig.2a   -   Cascade form (direct form II sections) realization.

6. APPLICATIONS

The program can be used to investigate the aspects of digital filter performance given in sections 6.1 and 6.2. As an example, the cascade form and parallel form realizations of an eighth order bandpass filter are considered.

6.1 Frequency Response

The specification of the bandpass filter example chosen is shown in Fig.3. From the filter specification the filter passband is (1.2915436 to 1.466077) Radian/Sec and the response must lie within the limits (1.03156, 0.9684368). The stopbands are (0 to 1.2086) and (1.553 to π) Radian/ Sec where the response must be less than 0.01052.

A cascade form realization of the specification is shown in Fig.2a. A parallel form realization is shown in Fig.2b. The frequency response was computed using the nominal coefficient values as specified in Fig.2. A plot of the frequency response is shown in Fig.4. It can be seen that the achieved response meets the specification.

K = 0·10000
C1 = ⁻0·2034508401
C2 = 0·2855823838
C3 = 0·9026252904
C4 = ⁻0·9116860616
C5 = 0·182701196
C6 = 0·4457342317
C7 = ⁻0·9457352763
C8 = ⁻0·913078673

D = 0·07220910762
C9 = ⁻0·2052671178
C10 = 0·196901665
C11 = ⁻0·2413054652
C12 = ⁻0·9695353354
C13 = ⁻0·1965294023
C14 = 0·5515388641
C15 = 0·298888793
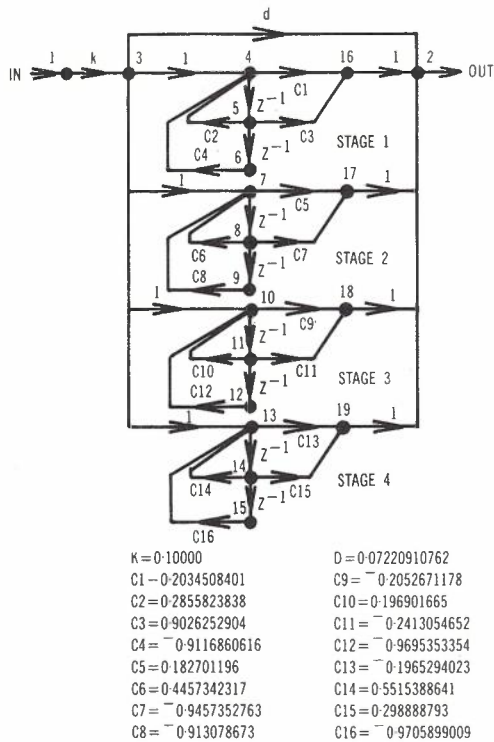C16 = ⁻0·9705899009

Fig.2b – *Parallel form realization.*

$\epsilon_p = 0{\cdot}0157816$ $\epsilon_s = 0{\cdot}00526063$

$\omega_{p1} = 0{\cdot}4111111\pi$ $\omega_{s1} = 0{\cdot}3847015\pi$

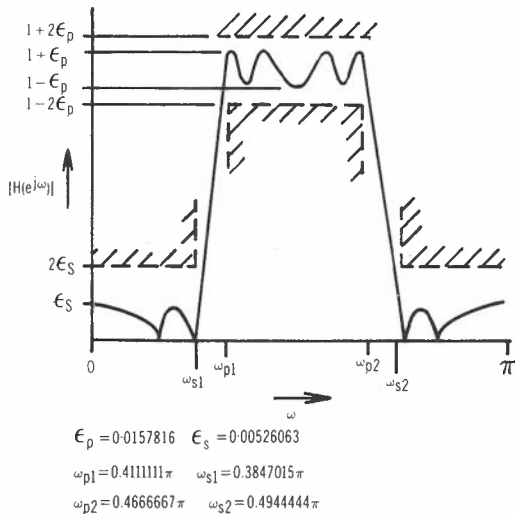$\omega_{p2} = 0{\cdot}4666667\pi$ $\omega_{s2} = 0{\cdot}4944444\pi$

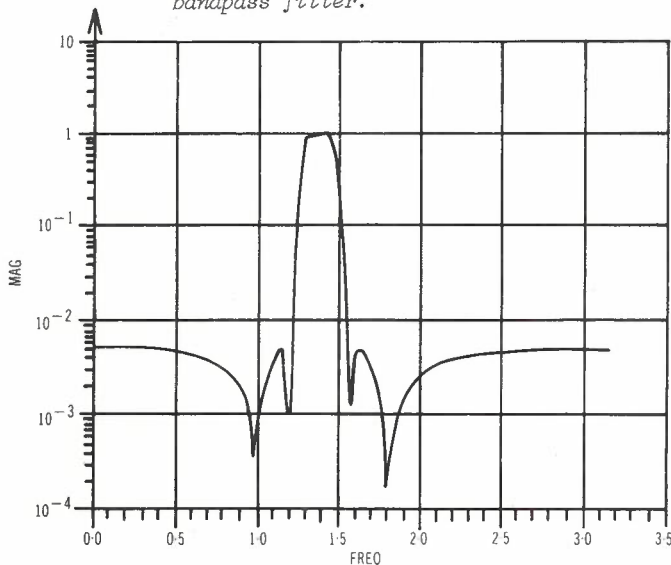*Fig.3* – *Design specification for eighth-order bandpass filter.*

Fig.4a – *Frequency response of cascade form realization (nominal coefficients).*
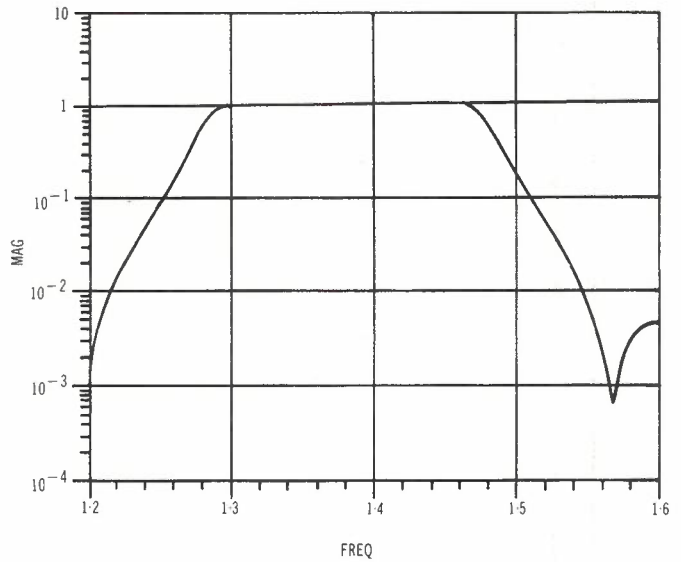

Fig.4b – *Passband frequency response of cascade form realization (nominal coefficients).*

6.2 Effect of Finite Word Length/Sensitivity Analysis

(a) Finite Word Length Effect

In implementing a digital filter structure the designer is restricted to a finite register length and hence one can not assume infinite precision in the filter coefficients.

The filter coefficients may for example be specified to 10 significant figures. For integer arithmetic a working rule is that you require approximately three binary bits/decimal digit plus one bit. Also it is usual that an extra bit is required to represent the sign.

Hence by truncating the filter coefficients to say 5 decimal digits we could see the effect of implementing the filter with 16 bit precision arithmetic.

The following table gives the approximate number of binary bits required to represent a decimal number.

Number of decimal digits	Number of bits (sign + magnitude)
3	1 + 10
4	1 + 13
5	1 + 16

In order to see the effect of finite word length the filter coefficients of the cascade form filter shown in Fig.2 were truncated to 3, 4 and 5 decimal digits. Plots of the response of the passband are shown in Fig.5.

With the coefficients specified to 3 decimal digits the passband specification is not met for the cascade realization. If the passband specification is critical but some relaxation in the stopband is allowed another structure might be considered. For example, with the parallel form realization of the filter, with the coefficients specified to 3 decimal digits, the passband speci-
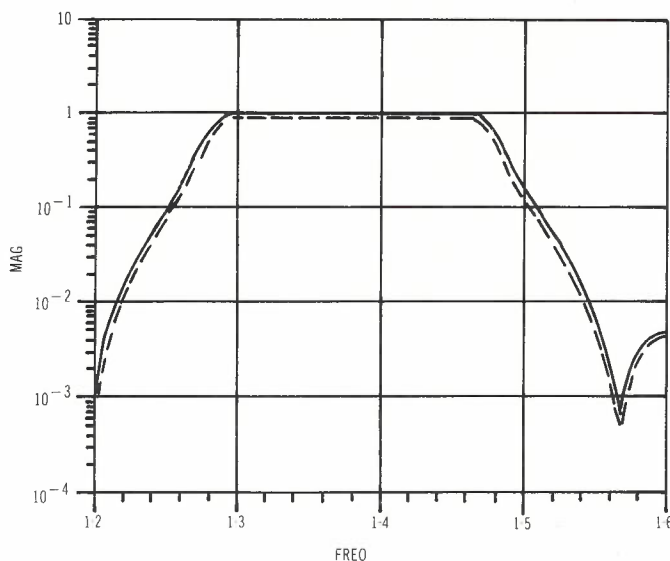
10
MAG

*Fig.5 - Effect of finite word length on fre-
quency response of cascade form real-
ization.*

fication is now met. However the stop band speci-
fication is not met.

Alternatively we can increase the precision
with which the coefficients are specified. The
filter specification is met using 4 decimal digits
for both the cascade form and parallel form real-
izations.

Considering the specific frequency $\omega = 1.3823$,
the difference between the magnitude response us-
ing the nominal coefficients and the response us-
ing 5 digit coefficients is 0.01 dB. Hence it is
seen that it is only required to specify the co-
efficients to 5 decimal places to get an excellent
response. Practically one could use 4 decimal dig-
its. The cascade form filter could certainly be
implemented using 16 bit arithmetic.

The filter coefficients for the 3, 4 and 5
decimal digit specification were just straight
truncations and no rounding was performed. With
rounding the 4 decimal specification would appear
to be adequate. A design approach might be to use
16 bit arithmetic (including sign bit) and fill
the register to the precision provided by 15 mag-
nitude bits.

(b) Sensitivity Analysis

A more formal method of studying the effect
of coefficient changes on the achieved transfer

function is by applying the sensitivity formula of
section 3. This enables changes in the transfer
function to be calculated directly from changes in
the coefficients. It is interesting to note that
for non recursive filter structures with no feed-
back paths, the T_{mn} term in the sensitivity
equation is always zero and hence the change in
the overall transfer function is directly propor-
tional to the change in a branch transmittance.

Sensitivity analysis can be used to find those
coefficients which are sensitive to change and
thus cause the specification not to be met as the
coefficient precision is decreased. As an applica-
tion of the sensitivity formula using the matrix
approach, sensitivity analyses were performed for
variations of each coefficient in both the cascade
and parallel form realizations of the filter. The
change in the system transfer function was com-
pared to the filter specification given in Fig.3.

The sensitivity analysis was carried out in
the following manner. All filter coefficients were
rounded to 4 decimal digits since this precision
was the minimum required to meet the filter speci-
fication. Each coefficient was then varied in turn
by the same amount. The variation chosen was
$\delta = 2^{-9} = .001953$. This variation represents the
effect of truncating the coefficients after the
9th bit. It should be noted that because of the
nature of digital filters any variation in the
filter coefficient must be a discrete amount.
Hence we do not consider percentage changes in the
coefficients as we might do with a passive LC fil-
ter.

Detailed results of the magnitude of the var-
iation in the cascade filter response at some
specific frequencies of interest are given in
Table 1.

As can be seen from Table 1 the cascade form
realization is characterized by having the pass-
band more sensitive to coefficient variation then
than the stopband. The stopband variations are 2-3
orders of magnitude below the passband variations.
Also we see that the variations due to changes in
coefficients C_7 and C_{10} would cause the filter
specification not to be met. For $\delta = 2^{-12}$ the
filter specification was met. Thus we see that
with coefficients C_7 and C_{10} specified to 12
bits and the other coefficients specified to 10
bits the filter specification would be met.

A more refined sensitivity analysis would pro-
duce the minimum precision required for each co-

TABLE 1 - Transfer Function Variation for Coefficient Change
$\delta = 2^{-9}$ - Cascade Filter

Frequency rad/sec	Transfer Function Variation (ΔT_{ab})					
	$\Delta C_3 = \delta$	$\Delta C_4 = \delta$	$\Delta C_6 = \delta$	$\Delta C_7 = \delta$	$\Delta C_9 = \delta$	$\Delta C_{10} = \delta$
.4	6×10^{-6}	7.4×10^{-6}	6.7×10^{-6}	6×10^{-6}	5.4×10^{-6}	7.7×10^{-6}
.651	5.1×10^{-6}	7.6×10^{-6}	5.6×10^{-6}	6×10^{-6}	4.4×10^{-6}	8×10^{-6}
1.29434	.0005	.0068	.0136	.0018	.0048	.061 *
1.30062	.0007	.0056	.0157	.0013	.0054	.044 *
1.38230	.01	.016	.0014	.011	.0009	.01
1.45142	.016	.0017	.0083	.032 *	.029	.0044
1.4577	.014	.0025	.0079	.048 *	.023	.0053

* Indicates filter specification will not be met.

efficient. A suggested technique is to first cal-
culate the binary equivalent of each coefficient
to say k bits, and then apply the change δ
equivalent to truncating the coefficient after
the nth bit.

ie. $\delta = \sum\limits_{i=n+1}^{k} x_i W_i$

where x_i is the ith bit - 1 or 0

W_i is the weight of the ith bit.

In relation to the parallel form realization,
we find that the situation is reversed - ie. the
stopband is more sensitive to coefficient change.
Hence, if the pass-band specification is critical
the parallel form structure may be desirable but
if the stop-band specification is critical the
cascade form structure may be a better choice.

7. CONCLUSIONS

The design of digital filters remains a rel-
atively complex subject. However the advent of
suitable digital hardware and catalogue designs
greatly aids the implementation of digital fil-
ters. A potential user is still faced with the
problems of how to compare alternative digital
filter realizations and how to determine the com-
putational precision required for their implemen-
tation. This paper has demonstrated how the appli-
cation of some relatively simple theory enables
these problems to be solved. Numerical calcula-
tions based on this theory can be performed using
a computer program that can be readily adapted to
analyse a wide range of digital filter networks.

A sensitivity analysis can be used for a de-
tailed study of a particular digital filter imple-
mentation to investigate in depth the effects in-
dicated by the simpler truncation analysis.

8. ACKNOWLEDGEMENT

9. REFERENCES

1. Oppenheim, A.V. and Schafer, R.W., "Digital
   Signal Processing", Prentice Hall, N.J., 1975.

2. Seviora, R.E. and Sablatash, M., "A Tellegen's
   Theorem for Digital Filters", IEEE Trans. Cir-
   cuit Theory, Vol.CT-18, No.1, Jan. 1971.
   pp.201-203.

APPENDIX 1 : Derivation of the Sensitivity Equation

We have

$$\Delta T_{ab} = \frac{\partial T_{ab}}{\partial F_{nm}} \Delta F_{nm} + \frac{1}{2} \frac{\partial^2 T_{ab}}{\partial F_{nm}^2} (\Delta F_{nm})^2$$

$$+ \dots \text{ Taylor Series Expansion}$$

From

$$\frac{\partial T_{ab}}{\partial F_{nm}} = T_{an} T_{mb} \qquad (1)$$

$$\therefore \frac{\partial^2 T_{ab}}{\partial F_{nm}^2} = \frac{\partial}{\partial F_{nm}} (T_{an} T_{mb})$$

$$= T_{an} \frac{\partial T_{mb}}{\partial F_{nm}} + T_{mb} \frac{\partial T_{an}}{\partial F_{nm}} \qquad (2)$$

From equation (1)

$$\frac{\partial T_{mb}}{\partial F_{nm}} = T_{mn} T_{mb} \quad , \quad \frac{\partial T_{an}}{\partial F_{nm}} = T_{an} T_{mn}$$

Substitute into equation (2)

$$\therefore \frac{\partial^2 T_{ab}}{\partial F_{nm}^2} = 2. T_{an} T_{mn} T_{mb}$$

$$\frac{1}{2} \frac{\partial^3 T_{ab}}{\partial F_{nm}^3} = \frac{2}{2} . \frac{\partial(T_{an} T_{mn} T_{mb})}{\partial F_{nm}}$$

$$= T_{an} T_{mb} \frac{\partial T_{mb}}{\partial F_{nm}} + T_{an} T_{mb} \frac{\partial T_{mn}}{\partial F_{nm}} + T_{an} T_{mb} \frac{\partial T_{an}}{\partial F_{nm}}$$

ie. $\dfrac{\partial^3 T_{ab}}{\partial F^3_{nm}} = 2.3\ T^2_{mn}\ T_{an}\ T_{mb}$

Generalizing

$$\dfrac{\partial^k T_{ab}}{\partial F^k_{nm}} = k!\ T_{mn}^{k-1}\ T_{an}\ T_{mb}$$

$\therefore\quad \Delta T_{ab} = \displaystyle\sum_{k=1}^{\infty} \dfrac{1}{k!}\ \dfrac{\partial^k T_{ab}}{\partial F^k_{nm}}\ \left[\Delta F_{nm}\right]^k$

$= \displaystyle\sum_{k=1}^{\infty} \dfrac{1}{k!}\ k!\ T^{k-1}_{mn}\ T_{an}\ T_{mb}\ \left[\Delta F_{nm}\right]^k$

$= \displaystyle\sum_{k'=0}^{\infty} T^{k'}_{mn}\ T_{an}\ T_{mb}\ \Delta F^{k'}_{nm}.\Delta F_{nm}$

$= \dfrac{T_{an}\ T_{mb}\ \Delta F_{nm}}{1\ -\ T_{mn}\ \Delta F_{nm}}$

ie. $\Delta T_{ab} = \dfrac{T_{an}\ T_{mb}\ \Delta F_{nm}}{1\ -\ T_{mn}\ \Delta F_{nm}}$

APPENDIX 2 : Inversion of Complex Matrices

Consider that we wish to invert the matrix $[A+jB]$

Define

$[A + jB]^{-1} \triangleq [C + jD]$ (1)

by definition of the inverse

$[A + jB][C + jD] = I$ (2)

Hence equating real and imaginary parts

$AC - BD = I$ (3)

$AD + BC = 0$ (4)

From equation (4)

$D = -A^{-1}.B.C =$ imaginary part of the inverse   (5)

From equations (3) and (5)

$AC + BA^{-1}BC = I$

$\therefore\quad C = (A + BA^{-1}B)^{-1} =$ real part of the inverse.

Hence the inversion procedure is as follows:

(i)   Compute A^{-1}

(ii)   Compute $C = (A + BA^{-1}B)^{-1}$

(iii) Compute $D = -A^{-1}BC$

It should be noted that a necessary condition for this matrix inversion algorithm to function is that both the Matrices A and C must be non-singular. In digital filters this will usually be the case since $A = R_e\{I-F^{\dagger}(z)\}$ and is forced to have unity elements on the leading diagonal. Alternative formulations of the solution place non-singular requirements on B and D .

BIOGRAPHIES

JOHN SNARE received the Bachelor of Engineering degree with Honours from Monash University in 1973 and joined the Transmission Systems Branch of the Telecom Australia Research Laboratories the same year. While in the Transmission Branch he studied filter and equalizer design in the Network Theory Section and aspects of digital transmission relating to data services and PCM in the Line and Data Systems Section. In July 1979 he joined the Switching and Signalling Branch and is currently investigating packet-switching techniques. He is presently undertaking part-time post-graduate studies for a Master of Engineering Science degree.

PETER R. HICKS was educated at Monash University, Clayton, Victoria where he was awarded the degree of Bachelor of Engineering (Electrical) in 1971 and the degree of Bachelor of Science (Applied Mathematics) in 1975. He commenced work as an Engineer with the APO Research Laboratories, Equipment Development Sub-section in March 1971. Between February 1972 and January 1981 he worked in the Radio Systems Section of the Laboratories' Transmission Branch. His work in that section was mainly concerned with the design of special equipment and the development of techniques to evaluate the service areas of mobile radio systems. He is currently working in the Line and Data Systems Section on the synchronization of digital networks. He is presently undertaking part-time post-graduate studies for a Master of Engineering Science degree.

The Chernoff Bound Applied To Error Rate Measurements

A. HAIME
Telecom Australia Engineering Department
Western Australia

A simple expression has been derived from the Chernoff bound, which enables a rapid determination of the number of errors which are required to be observed in a data transmission system to ensure, with a given statistical certainty, that the true mean error rate lies within a specified confidence interval.

1. INTRODUCTION

One of the fundamental tests applied to practical data communication systems is the measurement of the bit error rate. A bit error rate versus signal-to-noise ratio curve provides a basis for the relative comparison of systems, a measure of how well the system error rate approaches theoretical expectations, and a relative figure on which to base system degradation introduced by transmission perturbations such as amplitude and phase distortion, phase jitter etc.

We are dealing with a statistical concept when measuring the bit error rate. Theoretically the observed relative frequency of error only converges to the true mean error rate of a system as the observation period tends to infinity. One may ask how closely does the relative frequency approach the true mean after a finite (and practical) observation period. Alternatively, we may ask what is the minimum number of errors one should observe to be sure, with a given statistical certainty, that the relative frequency of error is as close as required to the true mean error rate.

One approach would be, using the normal or Poisson approximation to the binomial distribution (Ref.1) to determine the probability (ie. statistical certainty) that the true mean error rate lies within a given confidence interval about the measured relative frequency of error following a series of independent binary transmissions. This method provides useful results - see Fig.3-2 of (Ref.2) for example - but suffers from the drawback of requiring relatively long and time consuming calculations or reference to look-up tables. Where a requirement exists to quickly determine the minimum number of errors which is required to be observed, then a more direct and simple approach becomes necessary.

The statistical limit theorems which include the weak law of large numbers, the central limit theorem, and the Chernoff bound (Ref.3) provide the answer in that they can be used to derive simple expressions for the rapid determination of an upper bound on the number of errors required to be observed for any specified confidence interval and statistical certainty. The weak law and central limit theorems provide simpler expressions,

but the Chernoff bound generally provides by far the tightest bound.

This paper deals with the solution of an equation derived from the Chernoff bound to find the required number of transmissions and hence the number of errors required to be observed so that, with a given statistical certainty, we can say that the true mean error rate lies within a specified confidence interval for a data transmission system, where it is assumed that the occurrence or non-occurrence of an error is statistically independent for each transmission. The results are tabulated to provide a useful reference, and an example of a practical error rate versus signal to noise ratio curve is presented.

2. THE CHERNOFF BOUND

A statistically independent random variable x_i is defined such that:

$$x_i = \begin{cases} 1 & \text{with probability } p \\ 0 & \text{with probability } 1 - p \\ \quad i = 1, 2, \ldots\ldots\ldots\ldots N \end{cases} \qquad (1)$$

where $x_i = 1$ is interpreted as an error in transmission with probability p, and $x_i = 0$ as a correct transmission.

The mean of x_i is given by

$$\bar{x} = p \qquad (2)$$

A new random variable m is defined as the normalised sum of N identically distributed statistically independent random variables:

Error Rate Measurements

$$m = \frac{1}{N} \sum_{i=1}^{N} x_i \qquad (3)$$

In keeping with the above interpretation of x_i, m is then the relative frequency of error over N transmissions, which approaches the true mean error rate p as N becomes large.

A parameter d is defined as follows

$$d = \bar{x} + \beta p$$

$$= (1 + \beta)\, p \qquad (4)$$

Where β is the percentage variation of the estimated mean m from the true mean p.

From the definition of the Chernoff bound for the sum of N random variables (Ref.3) we have

$$P\big[(m-p) \geq \beta p\big] \leq e^{-NX} \quad ; \quad 0 < \beta \leq 1$$

$$P\big[(m-p) \leq \beta p\big] \leq e^{-NX} \quad ; \quad -1 \leq \beta < 0 \qquad (5)$$

where

$$X = -\left[d \ln \frac{p}{d} + (1-d) \ln \left(\frac{1-p}{1-d}\right)\right] \qquad (6)$$

This definition requires that $(1-p) > p$ which is entirely satisfactory for most practical purposes.

Using the power series expansion of the logarithmic function, X can be expanded as follows

$$X = \frac{\beta^2 p}{2(1-p)} - \frac{\beta^3 p^3}{6}\left[\frac{1}{p^2} - \frac{1}{(1-p)^2}\right] + \frac{\beta^4 p^4}{12}\left[\frac{1}{p^3} + \frac{1}{(1-p)^3}\right] -$$

$$\ldots\ldots + \frac{\beta^n p^n}{n(n-1)}\left[\frac{(-1)^n}{p^{n-1}} + \frac{1}{(1-p)^{n-1}}\right] + \ldots\ldots$$

$$(7)$$

which is convergent for $-1 \leq \beta \leq 1$ and $0 \leq p \leq 0.5$.

For values of $p \ll 1$ the expansion of X can be approximated by the following

$$X \approx p\big[(1+\beta)\ln(1+\beta) - \beta\big] \qquad (8)$$

It is clear from equation (7) that for a given value of p, two values of β equal in magnitude but different in sign will yield different values of X; the positive value of β yields a smaller value of X than the negative β. The values of X derived from positive and negative β are denoted as follows

$$X_1 \triangleq X \; ; \; \beta + ve$$

$$X_2 \triangleq X \; ; \; \beta - ve$$

It follows that for a given absolute value of β

$$e^{-NX_1} \geq e^{-NX_2} \quad ; \quad -1 \leq \beta \leq 1$$

$$; \quad 0 \leq p \leq 0.5 \qquad (9)$$

We now obtain a single bound for both negative and positive β.

The union of the two events

$$y = (m-p) \geq \beta p \qquad (10)$$

$$z = (m-p) \leq \beta p \qquad (11)$$

is used to define a joint Chernoff bound

$$P\big[y \cup z\big] \leq e^{-NX_1} + e^{-NX_2} \qquad (12)$$

which, from equations (5) and (9) above, can be written

$$P\big[|m-p| \geq \beta p\big] \leq 2e^{-NX_1} \quad ; \quad 0 < \beta \leq 1$$

$$; \quad 0 \leq p \leq 0.5 \qquad (13)$$

The equality of expression (13) yields the required bound on N. By taking natural logarithms and rearranging (13), the following equation results

$$N = \frac{\ln\{P\big[|m-p| \geq \beta p\big]\} - \ln 2}{-p\big[(1+\beta)\ln(1+\beta) - \beta\big]} \quad ; \quad 0 < \beta \leq 1$$

$$; \quad p \ll 1 \qquad (14)$$

It is convenient to define the following

$$P\big[|m-p| \geqslant \beta p\big] = 1 - C \qquad (15)$$

where C is interpreted as the statistical certainty that the observed relative frequency of error m is within ±β of the true mean error rate p . Since for most practical purposes we are dealing with values of m which tend to closely approximate p , we can also interpret C as the certainty that the true mean error rate p is within ±β of the observed relative frequency of error m , ie. within the confidence interval (−βm, βm). Substituting equation (15) into (14) yields

$$N = \frac{\ln(\frac{2}{1-C})}{p\big[(1+\beta)\ln(1+\beta)-\beta\big]} \quad ; \quad \begin{matrix} 0 < \beta \leqslant 1 \\ p << 1 \end{matrix} \qquad (16)$$

which is of the form

$$N = \frac{k}{p} \qquad (17)$$

where k is a constant.

If we now consider the error rate

$$m = \frac{\varepsilon}{N} \qquad (18)$$

where ε is equal to number of errors observed over N transmissions, we note that since m→p it follows that ε→k and therefore

$$\varepsilon = \frac{\ln(\frac{2}{1-C})}{(1+\beta)\ln(1+\beta) - \beta} \quad ; \quad \begin{matrix} 0 < \beta \leqslant 1 \\ p << 1 \end{matrix} \qquad (19)$$

This is the required expression which relates the number of errors required to be observed to the confidence interval defined by β and the statistical certainty C , for values of p<<1 .

Equation (19) can be readily solved using, for example, a hand calculator. Table 1 lists ε as a function of some typical values of C and β . Due to the approximation of equation (8) the results obtained from (19) are roughly 10 and 1 percent high for values of p = 0.1 and 0.01 respectively. For smaller values of p equation (8) is an excellent approximation and the error in equation (19) is negligible.

3. AN APPLICATION OF THE RESULTS

Here we discuss the relevance of equation (19) by considering the noise performance of a typical modem. When noise is added to the modem line signal, the measured error rate, m , is related to the signal to noise ratio, SNR, by the curve shown in Figure 1. We wish to be certain, with statistical certainty C , that the true mean error rate, p , versus SNR curve lies within the shaded confidence region shown above and below the m versus SNR curve.* This region corresponds to the ±βm confidence interval along the ordinate where β is a function of m as shown by the values of

---

* It will be noted that this margin has been chosen to represent a variation of 0.25dB SNR on the abcissa about the m versus SNR curve, for all m .

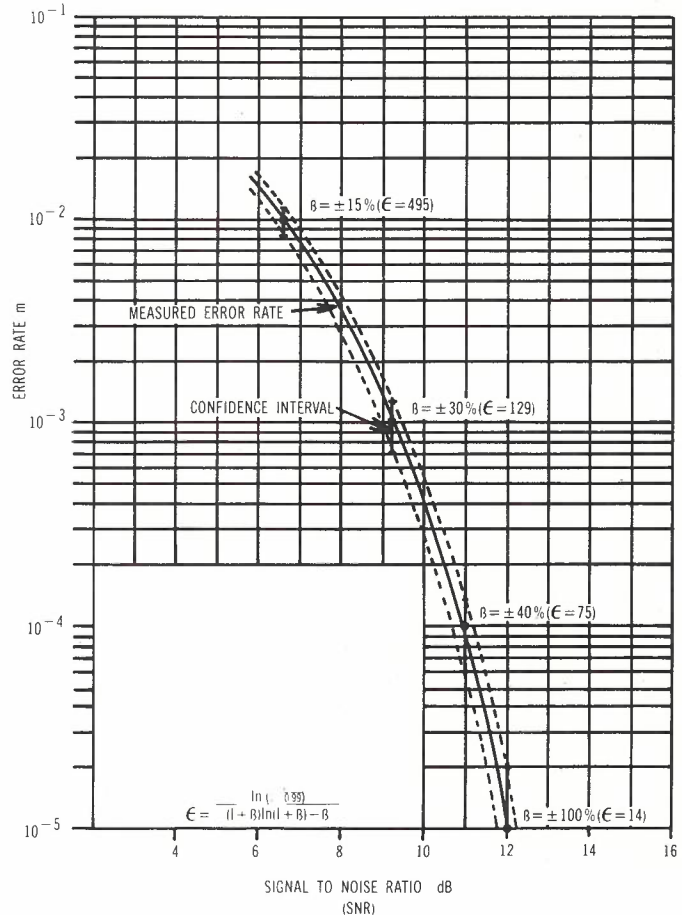

Fig.1 - *Typical error rate versus signal to noise ratio curve for a VF data modem, showing the number of errors ε which are required to be observed to ensure that the true mean error rate lies within the confidence interval (−βm, βm) with 99% certainty. The shaded interval represents ±0.25 dB variation in SNR and*

$$\varepsilon = \frac{ln(\frac{2}{1-0.99})}{(1+\beta)\,ln(1+\beta) - \beta}$$

Error Rate Measurements

TABLE 1 — The minimum number of errors ε which are required to be observed to ensure that the true mean error rate p of a data communications system is within $\pm\beta$ of the measured error rate m with statistical certainty C.

C(%)	99.9	99.0	95.0	90.0
$\beta(\%)$				
1	152500	106300	74020	60110
5	6181	4309	3000	2436
10	1570	1094	762	619
20	405	282	197	160
30	185	129	90	73
40	107	75	52	42
50	70	49	34	28
60	50	35	24	20
70	38	26	18	15
80	30	21	14	12
90	24	17	12	9
100	20	14	10	8

$$\varepsilon = \frac{\ln(\frac{2}{1-C})}{(1+\beta)\ln(1+\beta) - \beta} \quad ; \quad \begin{array}{l} 0 < \beta \leqslant 1 \\ p \ll 1 \end{array}$$

β inserted alongside the measurement points on the curve. If we choose $C = 99\%$, the minimum number of errors, ε , we must observe at each measurement point are calculated from equation (19) or read from Table 1 for each relevant value of β . These values of ε are shown in parenthesis in Figure 1. The significance of having to measure fewer errors as p is decreased, is that considerable measurement time is saved when the mean time between errors is substantial, ie. when p is small.

4. ACKNOWLEDGEMENTS

The subject matter for this paper stems from a Master of Engineering Science project completed at the University of Western Australia under the supervision of Dr. J. Hullett. The author is indebted to the reviewers for suggested improvements to the paper.

5. REFERENCES

1. Miller, I. and Freund, J.E., "Probability and Statistics for Engineers", New Jersey, Prentice Hall, 1965.

2. Wandel and Goltermann Description and Operating Manual 692/1B, "PCM Regenerator Tester PRT-1", Federal Republic of Germany, Wandel and Goltermann Co., 1977.

3. Wozencroft, J.M. and Jacobs, G.W., "Principles of Communications Engineering", New York, Wiley, 1965.
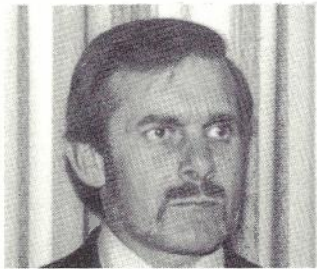
BIOGRAPHY

ALAN HAIME joined the PMG Department as a Technician-in-Training in 1958 and qualified as a Senior Technician in 1965. During this period he was associated with transmission measurements. During 1966 he worked for some time with the Muirhead group of companies in London, England. He became a Cadet Engineer in 1968 and completed degrees of Bachelor of Engineering and Master of Engineering Science at the University of Western Australia in 1971 and 1977 respectively. He was awarded the 1970 IREE Fisk prize. Mr. Haime has been with the Radio Section, Western Australia since 1974 and is currently the Senior Engineer, Radiocom Design.

Ray Tracing On Tropospheric Radio Paths

W.S. DAVIES
Telecom Australia Research Laboratories

T.A. EVANS
Anderson Digital Equipment

The paper presents two approaches used in developing desk-calculator ray-tracing programs for tropospheric radio propagation studies. One technique uses standard integral results for the ray-trajectory in a parabolic refractive index profile. The other, based on Taylor series, can be applied to any profile for which all derivatives exist. However the detailed development of this second method has again been for a parabolic profile. In both techniques arbitrary profiles are represented as sequences of parabolic sub-profiles. The example ray plots shown use refractive index profiles taken from actual microwave radio paths, and include tracings that are compared with the results of an earlier investigator. A feature of some example plots is the high sensitivity of certain ray trajectories to small variations in the refractive index profile.

1. INTRODUCTION

The study of radio wave propagation in the troposphere is one of the many areas where ray concepts have proved most naturally useful and effective. The ray paths of interest in this field can be determined by relatively straightforward techniques. Consequently their prediction is a task ideally suited for programmable desk calculators and plotters. The basic formulations used in two programs developed for this purpose are presented here, together with examples of the ray tracings obtained.

The work follows the development of an earlier Fortran program by Rosman (Ref.1) for microwave radio system path studies. Experience with Rosman's program (Refs.2&3) and with a modified version due to Tang (Ref.4) demonstrated its considerable value as an aid to assessing tropospheric propagation phenomena. In a like manner the two new programs have proved similarly useful in some recent investigations by Harvey (Ref.5). Other examples illustrating the application of ray-tracing to tropospheric radio propagation problems are the works of Ikegami (Ref.6), Baker (Ref.7) and Barton (Ref.8). A complete review of the numerous publications reporting similar specific applications has been deemed outside the scope of the present paper, since it is the ray-tracing technique itself that is of central interest.

Ray-tracing or geometric optics methods for regions of continuously varying refractive index n may be based equivalently on Fermat's principle, the eikonal equation, Hamiltonian optics, or the generalised form of Snell's law. In regions where n is anisotropic and varies along more than one co-ordinate, and where arbitrary ray trajectories are of interest, the approach developed by Hazelgrove (Ref.9) from Hamiltonian optics is generally recognized to be the best for computational purposes (Refs.7,10-13). However in media which are isotropic, and in which n varies along only one co-ordinate the simplifications thereby made possible permit various other techniques to be employed. Notable examples are the exact solutions of Thayer (Ref.14) Croft and Hoogasian (Ref.15) and Westover (Ref.16) for power law, quasi-parabolic, and quasi-linear n height dependencies respectively.

Within the troposphere n is very close to unity; furthermore on most terrestrial radio system paths operating at VHF or above, the rays of interest are near horizontal. Under these additional constraints simple approximate formulations giving very good estimates are easily obtained. The two methods described in Section 2 below for a parabolic n profile, and employed in the two new programs, are in this category. Arbitrary profiles are approximated by a sequence of parabolic subprofiles.

The development of two different mathematical techniques, and consequently of two programs, arose primarily from the individual preferences of the two authors. In the first method the ray path and delay relative to a reference ray are determined from standard integrals. The basic approach is similar to that first developed by Försterling and Lassen (Ref.17) and later refined by Appleton and Beynon (Ref.18) and Rawer (Ref.19) for ionospheric propagation studies. In the second method corresponding expressions are found using Taylor series.

Although attention here is essentially restricted to the solutions for parabolic profiles, the second method can be applied to a much wider class of function. As indicated in Section 2, it will yield the ray path for any profile for which all derivatives exist. So far as the authors are aware the second technique is original in this respect.
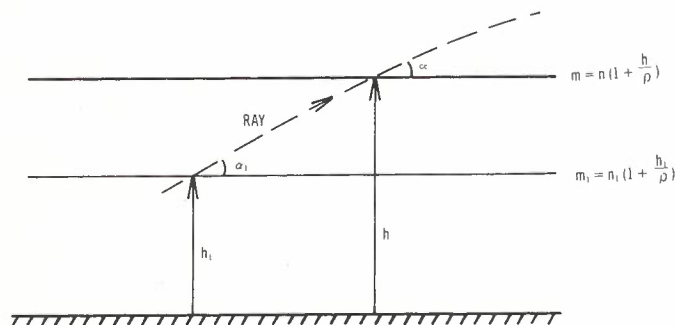
Tropospheric Ray Tracing

The first of the two new programs developed in these studies traces rays on paths where the refractive index n depends only on height. In the second this same dependence has been assumed to apply locally, however along the whole path n may vary in a number of discrete steps. Thus the second program gives ray trajectory estimates for paths where n is a function of both height and lateral distance.

The first program operates at a higher speed and requires less memory storage than the second. It should therefore find application where these advantages are important, and when there is little variation of the n profile along the path. More involved situations require the more versatile second program. Examples of tracings produced for both types of path are presented in Section 3.

The example tracings have been obtained from a desk calculator and plotter operating with HPL, a high-level programming language. Complete HPL listings of the two programs, and detailed operating instructions, are contained in a separate report (Ref.20).
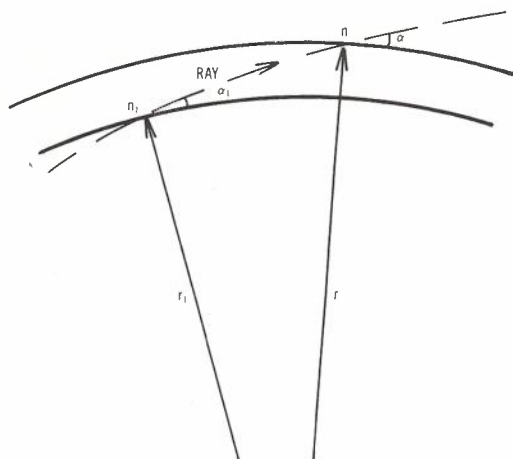
(a) SPHERICAL EARTH MODEL

(b) EQUIVALENT FLAT EARTH MODEL

Fig.1 - Physical Models.

2. RAY TRACING FORMULATIONS

The generalization of Snell's law to describe refraction in a continuously-varying spherically-stratified isotropic medium, is due to Rayleigh, and is described for example by Försterling and Lassen (Ref.17) and by Humphreys (Ref.21). It states that a ray path as depicted in Fig.1 is characterized by

$$n \, r \, \cos \alpha = n_1 \, r_1 \, \cos \alpha_1 \qquad (1)$$

where r = radius from sphere centre

n = refractive index at radius r

α = angle between ray and the sphere tangent plane at the field point

n_1, r_1 and α_1 denote reference or starting point values.

If the radii to the field and reference points are expressed in terms of heights above some datum radius ρ , equation (1) becomes

$$n(1 + \frac{h}{\rho}) \, \cos \alpha = n_1(1 + \frac{h_1}{\rho}) \, \cos \alpha_1$$

or equivalently

$$m \cos \alpha = m_1 \cos \alpha_1 \qquad (2)$$

where

$$m = n(1 + \frac{h}{\rho}) \qquad (3)$$

is the so-called modified refractive index.

Since equation (2) is the generalized form of Snell's law for propagation above an equivalent flat earth having a stratified refractive index m , the conversion (3) enables one to replace the spherical model of Fig.1a with an equivalent flat earth model as shown in Fig.1b. For such a conversion it is usual to set ρ = earth radius. Note that α and h both remain unchanged by the transformation.

In practice n or m differ from unity by only very small amounts. Hence it is usual to work with so called N or M units, which magnify the difference by a factor of one million. Thus

$$M = (m - 1) \, 10^6 \qquad (4)$$

with an identical relation defining N in terms of n .

As they stand, equation (1) or (2) could be used iteratively to extrapolate the ray path through the appropriate stratified atmosphere. However if a suitable functional variation of n or m is assumed within each layer, the ray path may be specified in analytic form. This approach was adopted by Rosman, and is used in the first of the two programs developed during these studies. The second program employs a different technique based on Taylor series. In both programs the n, and hence the m profiles, are modelled by a set of parabolic sub-profiles as depicted in Fig.2.

From this point on it is appropriate to present the two formulations in separate subsections.

2.1 First Formulation

If x is chosen as the map distance (ie. the horizontal distance in the flat earth model) then

$$\frac{dx}{dh} = \cot \alpha \qquad (5a)$$

$$\simeq \frac{1}{\alpha} - \frac{\alpha}{3} \quad , \qquad \text{for} \quad |\alpha| << 1 \qquad (5b)$$

Thus between any two heights h_1 and h_2, the horizontal distance traversed is

$$X = x_2 - x_1 \simeq \int_{h_1}^{h_2} \frac{dh}{\alpha} - \frac{1}{3} \int_{h_1}^{h_2} \alpha dh \quad , \text{ for } |\alpha| << 1$$
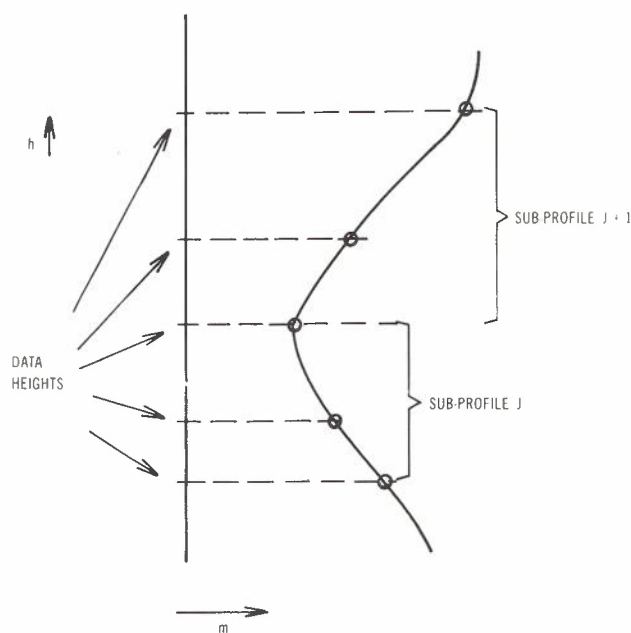
$$(6)$$

Fig.2 - Parabolic Sub-Profiles.

The requirement that $|\alpha|$ be small clearly makes the first term on the right of equation (6) dominant. That is to say if equation (6) is written as

$$X \simeq I_1 - \frac{1}{3} I_2 \qquad (7)$$

$$I_2 << I_1 \qquad \text{for} \quad |\alpha| << 1$$

In fact for calculations of ray geometry on tropospheric paths in relatively flat regions, where $|\alpha|$ remains below about 2 deg., the first order approximation

$$X \simeq I_1 \quad , \qquad \text{for} \quad |\alpha| << | \qquad (8)$$

is entirely adequate. Within the program based on this first approach, both orders of approximation are used at different stages.

The restriction to $|\alpha|$ small also permits the cosine factors in equation (2) to be replaced by the first two terms of their series expansions. With equation (4) this yields

$$\alpha^2 \simeq 2(M-M_1)10^{-6} + \alpha_1^2 \quad , \qquad \text{for} \quad |\alpha| << 1 \qquad (9)$$

where terms of orders α^4 and $\alpha^2 M\, 10^{-6}$ are neglected.

Now if h_1 and h_2 are heights between which

$$2(M-M_1) \cdot 10^{-6} = Ah^2 + Bh + C \qquad (10)$$

successive substitution into equation (9) and then into the terms of equation (6) gives

$$I_1 = \pm \int_{h_1}^{h_2} \left[A(h + D)^2 + E \right]^{-\frac{1}{2}} dh \quad ,$$

$$\text{for} \quad h_2 \overset{\geq}{\underset{<}{}} h_1 \qquad (11a)$$

$$I_2 = \pm \int_{h_1}^{h_2} \left[A(h + D)^2 + E \right]^{\frac{1}{2}} dh \quad ,$$

$$\text{for} \quad h_2 \overset{\geq}{\underset{<}{}} h_1 \qquad (11b)$$

where

$$D = \frac{B}{2A}$$

Tropospheric Ray Tracing

$$E = C + \alpha_1^2 - AD^2$$

The above two integrals are standard forms, which yield expressions as set out in Appendix A.

When a ray path is predicted in successive stages, through a medium of the form represented in Fig.2, the following three different types of extrapolation are generally needed:

(i) x_2 and α_2 to be found for a given h_2 .

(ii) h_2 and α_2 to be found for a given x_2

(iii) x_2 and h_2 to be found for $\alpha_2 = 0$.

Of these types, (i) is a normal sub-profile crossing extrapolation as shown in Fig.3a, (ii) is used either to shorten a long plotting step, or at the end of the path, as indicated in Fig.3b, while (iii) is required when turning points occur as shown in Fig.3c.
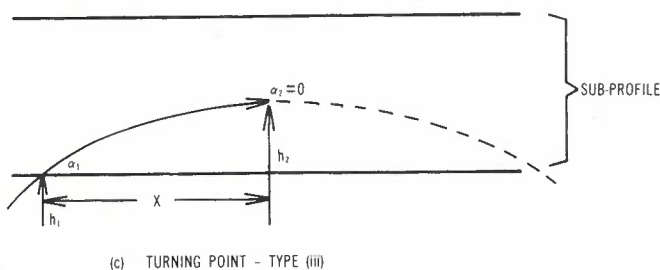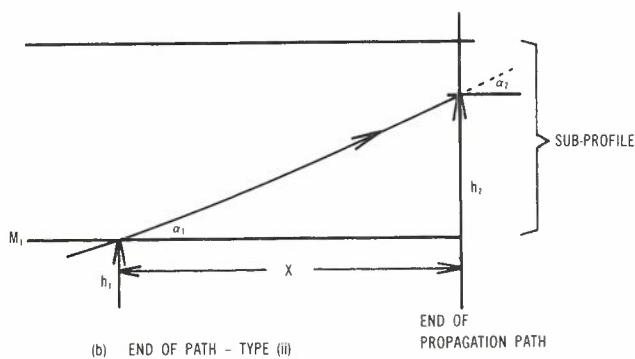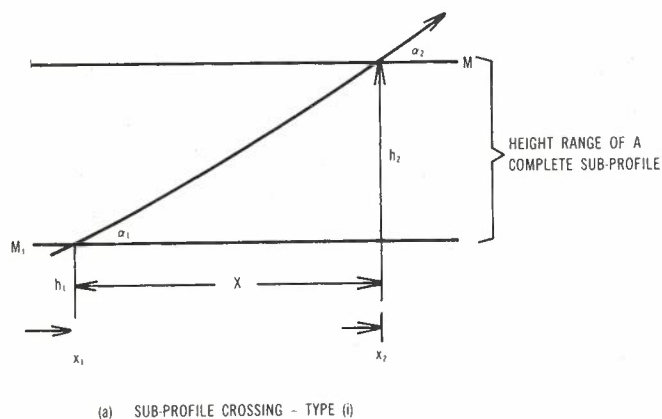

(a)   SUB-PROFILE CROSSING – TYPE (i)

(b)   END OF PATH – TYPE (ii)

(c)   TURNING POINT – TYPE (iii)

Fig.3 – Types of Extrapolation.

Extrapolation type (i) can be performed directly using equation (7) or (8), together with equations (10) and (9). In the program these calculations are performed using equation (7) rather than the less accurate (8).

In order to perform the type (ii) extrapolations directly, an inverted form of equation (7) or (8) is required. With the more accurate expression (7), this is only possible for linear or constant M subprofiles, since the others yield transcendental equations for h_2 . For this reason the inverted forms of equation (8) have been employed for plotting intermediate points between the more accurately determined points of type (i), whereas at the end of the path a correction based on equation (7) is made to the first order point predicted by equation (8).

The type (iii) extrapolation is performed by determining M at the turning point from equation (9), then (10) is used to find h_2 . The results are

$$h_2 = -D \pm (-\frac{E}{A})^{\frac{1}{2}} \quad , \qquad \text{for } A \neq 0 \text{ and } \alpha_1 A \lessgtr 0$$

$$(12a)$$

and

$$h_2 = -(\alpha_1^2 + C)/B \quad , \qquad \text{for } A = 0 \text{ , } B \neq 0$$

$$(12b)$$

The map distance increment X is then found using equation (7).

In summary then, the X increments for the main ray-path characterizing points (ie. the sub-profile boundary crossings and the turning points) are found using the second order equation (7). The intermediate points, determined optionally if a smooth appearance to the tracings is required, employ the first order equation (8) in inverted form. Finally the end-of-path point is found in two stages by applying the first and second order solutions sequentially.

It has already been seen that the ray height and angle are unaltered by the transformation from the spherical to the equivalent flat earth model. In a like manner, it is a straightforward matter to show that no change occurs in the trajectory transit delay.

In radio system propagation studies, the quantities of interest are the relative delays between different ray trajectories, rather than the absolute delays. In practice this means one requires to resolve differences of around 10^{-10} to 10^{-11} seconds, between absolute delays of about 10^{-4} seconds.

On some early computing machines working to a relatively low accuracy it was imperative to employ equations which gave the relative delay directly, rather than as the difference between two almost equal absolute values (Ref.22). Although this is no longer necessary with modern desk calculators, which typically retain 12 significant figures, it is still a desirable feature for mathematical elegance.

Let ℓ be the distance along the ray trajectory in the equivalent flat earth model. An elemental trajectory segment $\Delta \ell$, and a corresponding reference path segment Δx , chosen to be at

the transmitter height h_t , are shown in Fig.4. Since the wave velocity is $v = c_0/m$ (where c_0 = free space velocity of light) the relative transit time delay along $\Delta\ell$ is

$$\Delta t_r \simeq (\Delta\ell m - \Delta x m_t)/c_0$$

$$= \Delta\ell(m - m_t)/c_0 + (\Delta\ell - \Delta x)m_t/c_0 \qquad (13)$$

The relation is exact in the geometric optics sense, in the limit as $\Delta\ell$ and Δx tend to zero. Therefore

$$\frac{dt_r}{dh} = \frac{(m-m_t)}{c_0}\frac{d\ell}{dh} + \frac{m_t}{c_0}\frac{d(\ell-x)}{dh} \qquad (14)$$

From the trajectory

$$\frac{d\ell}{dh} = \operatorname{cosec}\alpha \simeq \frac{1}{\alpha} + \frac{\alpha}{6} \quad , \qquad \text{for } |\alpha| << 1$$

Hence with equation (5b)

$$\frac{d(\ell-x)}{dh} \simeq \frac{\alpha}{2} \quad , \qquad \text{for } |\alpha| << 1$$

Substituting into equation (14) and integrating yields

$$t_r \simeq \int_{h_1}^{h_2}\frac{(M-M_t)10^{-6}}{c_0\alpha}\,dh + \int_{h_1}^{h_2}(1 + M_t 10^{-6})\frac{\alpha}{2c_0}\,dh \quad ,$$

$$\text{for } |\alpha| << 1 \qquad (15)$$

The first term in equation (13), and hence that in equation (15), gives the relative delay contribution due to the differing m values at h and h_t respectively. The second term in each equation gives the contribution due to the geometric path difference. Notice that although m and m_t are very nearly equal, M and M_t are generally quite different. Thus equation (15) avoids the inelegant differencing of nearly identical quantities.
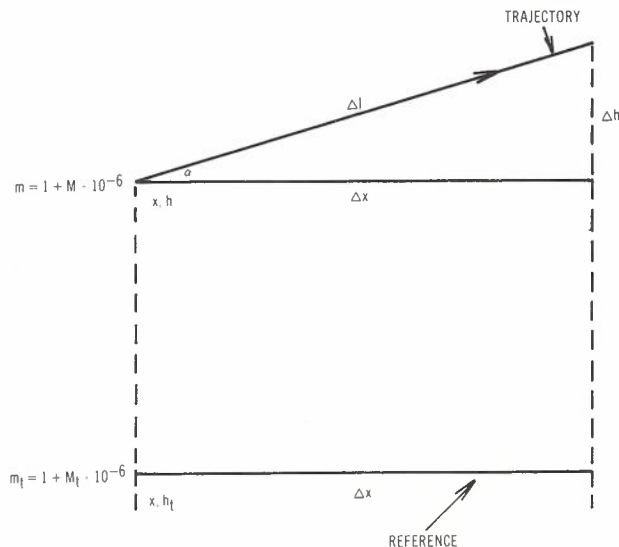

Fig.4 - Model for Relative Delay Derivation.

By substituting for M from equations (9) and (10), and with some rearrangement, equation (15) becomes

$$t_r \simeq \left\{\left[(M_1-M_t)10^{-6} - \frac{\alpha_1^2}{2}\right]I_1 + (1 + \frac{M_t 10^{-6}}{2})I_2\right\}/c_0 \;\; ,$$

$$\text{for } |\alpha| << 1 \qquad (16)$$

2.2 Second Formulation

Since the gradient at any point (x, h) on the ray trajectory is the tangent of the ray angle,

$$\frac{d^2 h}{dx^2} = \sec^2\alpha\,\frac{d\alpha}{dx} \qquad (17)$$

From equation (2) the derivative on the right may be shown to be

$$\frac{d\alpha}{dx} = \frac{1}{m}\frac{dm}{dh}$$

Hence equation (17) becomes

$$\frac{d^2 h}{dx^2} = \frac{\sec^2\alpha}{m}\frac{dm}{dh} \qquad (18)$$

The second method uses the approximation that the quotient term on the right is almost unity for small ray angles, and for practical values of m . That is

$$\frac{d^2 h}{dx^2} \simeq \frac{dm}{dh} \quad , \quad |\alpha| << 1 \;, \; m \simeq 1 \qquad (19)$$

To calculate the ray path a double integration of equation (19) is necessary. For the general class of m profiles in which derivatives of all orders exist, the integrations can be effectively performed by the use of the Taylor series, applied successively over map distance increments $X = x_2 - x_1$. Thus for the first integration, the Taylor series representation is

$$h^{(1)}(x_2) = h^{(1)}(x_1) + X h^{(2)}(x_1) + \frac{X^2}{2!}h^{(3)}(x_1) + \dots$$

$$(20)$$

where

$$h^{(1)}(x_1) = h_1^{(1)} \quad , \quad \text{the known initial gradient}$$

$$h^{(2)}(x_1) = \left.\frac{dm}{dh}\right|_{h(x_1)} \qquad , \quad \text{from equation (19)}$$

and with successive differentiation

$$h^{(3)}(x_1) = h^{(1)}(x_1)\left.\frac{d^2 m}{dh^2}\right|_{h(x_1)}$$

$$h^{(4)}(x_1) = \left[h^{(1)}(x_1)\right]^2 \left.\frac{d^3 m}{dh^3}\right|_{h(x_1)}$$

$$+ h^{(2)}(x_1) \left.\frac{d^2 m}{dh^2}\right|_{h(x_1)}$$

etc.

Likewise for the second integration

$$h(x_2) = h(x_1) + X h^{(1)}(x_1) + \frac{X^2}{2!} h^{(2)}(x_1) + \ldots \quad (21)$$

In the program developed using this Taylor series technique, the profile representation employed is identical to that used for the first method (ie. a sequence of parabolic sub-profiles as in Fig.2). Thus of all possible functions in the admissible class referred to above, attention from this point on is confined to

$$M.10^{-6} = A_1 h^2 + B_1 h + C_1 \quad (22)$$

where the subscript 1 has been used to distinguish the coefficients here from those in equation (10).*

---

* It should be noted that the parabolic profile (22) reduces (19) to a second order differential equation, which has a closed form solution given by standard analytical methods. The results are similar to those given by inverting the expressions for I_2 in the method of section 2.1. The Taylor series method is thus not essential for the solution of equation (19) in this particular case. It is rather that the parabolic profile provides a convenient m dependence with which to assess the new technique.

With equation (22), the successive derivatives of h in equations (20) and (21) become

$$h^{(2)}(x_1) = 2A_1 h(x_1) + B_1$$

$$h^{(3)}(x_1) = 2A_1 h^{(1)}(x_1)$$

$$\vdots$$

$$h^{(n)}(x_1) = 2A_1 h^{(n-2)}(x_1) \qquad \text{for } n \geq 3$$

In both equations (20) and (21), the higher order terms are included until their contribution becomes negligible.

Note that this second formulation enables extrapolations of the type (ii) listed in Section 2.1 to be made directly. That is, h_2 and α_2 may be found for a specified x_2. However as the order at which truncation of the Taylor series is best performed in practice is variable, it is not easy to devise inversion formulae to treat the type (i) and type (iii) extrapolations. For this reason the second program uses a procedure of successively improved trial approximations to find x_2 and α_2 when h_2 is given (ie. for the type (i) extrapolation).

In principle a similar technique could be used for the type (iii) extrapolations, which terminate at the ray turning points. This has not been done however, since by keeping x small, it is possible to avoid any serious errors, which could otherwise occur when extrapolating through turning points.

The distance through a vacuum that would give the same transit times as the real ray path is given by the integral:

$$s = \int_{x_1}^{x_2} m \left[1 + \left(\frac{dh}{dx}\right)^2\right]^{\frac{1}{2}} dx \quad (23)$$

The evaluation of equation (23) by Taylor series is performed in Appendix B.

The reference distance against which s is to be compared is $X m_t$. Hence the relative time delay over the path increment is

$$t_r = (s - X m_t) / c_0 \quad (24)$$

3. EXAMPLE RESULTS

3.1 Comparison with Rosman's Program

Two ray tracings produced by Rosman's earlier Fortran program are shown in Figs.5a and 5b. The first is from Warhaft and Van Dijks' study of "space-wave fadeout" phenomena on the Nullarbor plain, South Australia (Ref.3), while the second is from unpublished work.

TABLE 1 — Ray Data for Tracing of Fig.6

RAY No.	HEIGHT (M)	REC.ANG. (mrad)	REL.DEL. (nanosec)
1	ray escapes		
2	ray escapes		
3	ray escapes		
4	ray escapes		
5	ray escapes		
6	95.41	2.676	2.9785
7	ray escapes		
8	ray escapes		
9	ray escapes		
10	ray escapes		
11	ray escapes		
12	ray escapes		
13	ray escapes		

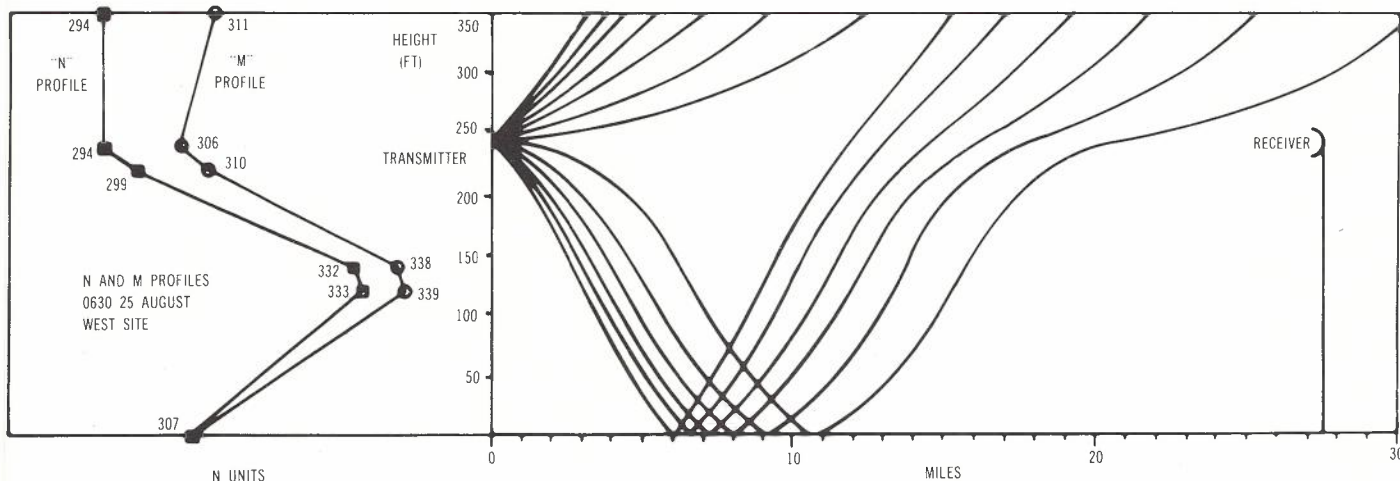(Tx. Ant. Ht. = 75.3 m. launching 13 rays from −5.527 to 5.527 mrad.)

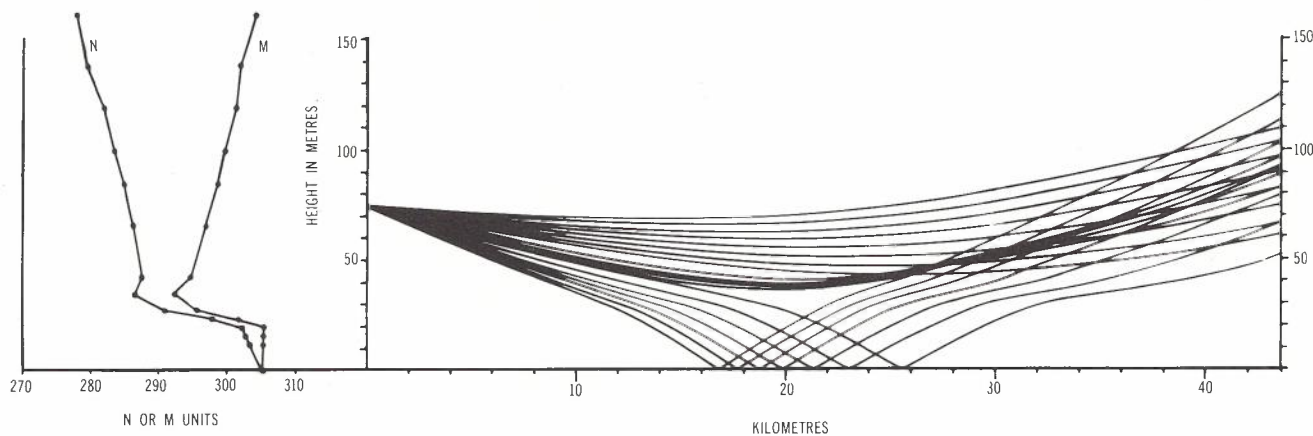*Fig.5a - Example tracing produced by Rosman's program showing "Space Wave Fadeout" phenomenon (Ref.3).*

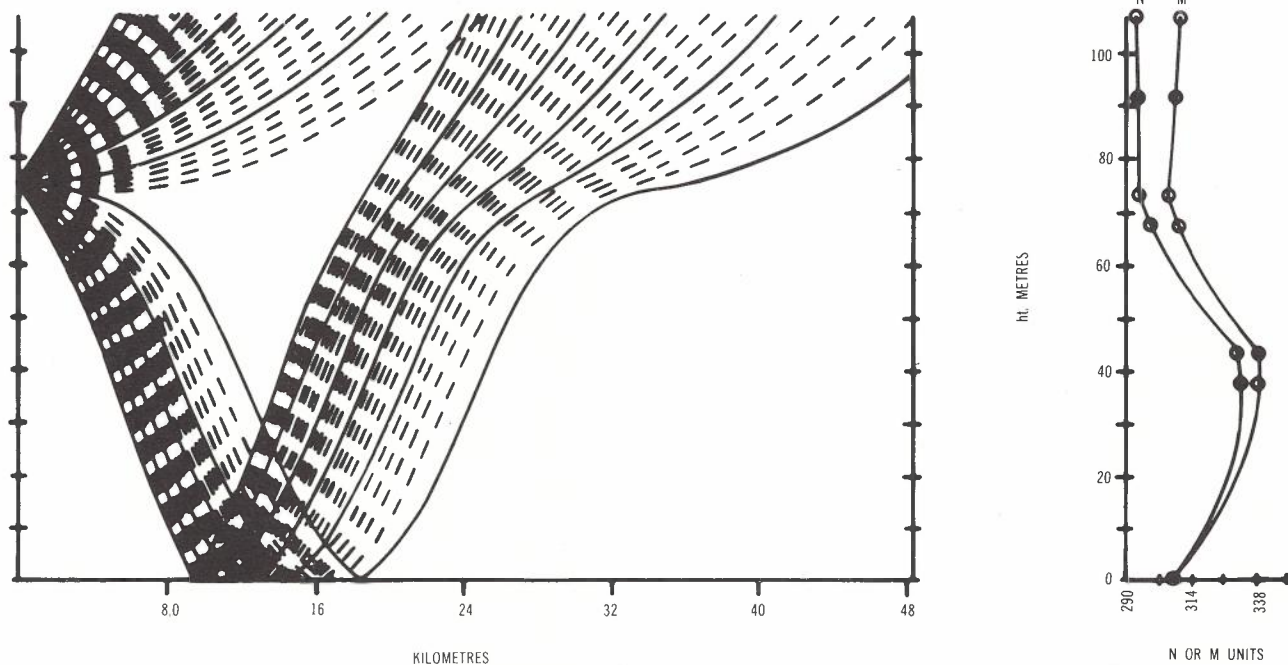*Fig.5b - Second example tracing from Rosman's program.*

Fig.6 - Tracing for path of Fig.5a as produced by first new program (full line ray data as per Table 1).

The results obtained by the first new program for the first example are shown in Fig.6 and Table 1. The data point heights used for the N profile were scaled from Warhaft and Van Dijks' diagram. As with the other new program results given here, the numerical values are given in (Ref.20). Notice that the full-line ray trajectories agree very well with those predicted by Rosman's program. The intermediate broken-line rays were added to emphasise the completeness of the "fadeout" phenomenon in this example. These latter rays are not tabulated.

Figure 7 and Table 2 show the results obtained for the second example. In this case a listing of the original N and height values was available; yet on comparison with Fig.5b it is evident that considerably different trajectories are predicted for a number of rays.

The differences here are apparently due to small variations in the refractive index profiles, caused by different curve fitting techniques used in Rosman's program and in our own. The rays most affected are those most nearly horizontal over much of their path. Their sensitivity to small changes in the N gradient is demonstrated by comparing the rays of Fig.7 and Table 2, with those of Fig.8 and Table 3, which were obtained by including only two additional interpolation points in the original data set.

Ray tracings made for the examples described here using the second new program have produced results almost identical to those given by the first program, the maximum differences from the end-of-path quantities of Tables 1 and 2 being less than 0.01 metres in height, 0.001 millirad. in receive angle, and 0.0001 nanosec. in relative delay.

3.2 Higher Speed Tracing

The ray trajectories shown in Figs.6, 7 and 8 were obtained with small plotting increments, the maximum values being no greater than 2.5 percent of the path length. Such a choice ensures an adequately smooth trajectory for final display pur-

poses. However, it does not permit the tracings to be performed in the fastest time.

To obtain a high speed run with the first program, the plotting increment should be made larger, even greater than the path length. This causes the program to estimate trajectory co-ordinates only at the crossings of subprofile boundaries, and at ray turning points.

TABLE 2 - Ray Data for Tracing of Fig.7

RAY No.	HEIGHT (M)	REC.ANG. (mrad)	REL.DEL. (nanosec)
1	126.22	5.318	1.6386
2	115.11	5.031	1.4466
3	103.52	4.652	1.2593
4	91.31	4.284	1.0777
5	77.85	3.847	0.8950
6	61.86	3.384	0.7049
7	35.99	1.088	0.4718
8	103.74	3.833	0.2436
9	100.07	3.578	0.1982
10	96.32	3.354	0.1549
11	92.46	3.118	0.1132
12	88.46	2.863	0.0734
13	84.30	2.584	0.0355
14	79.93	2.269	0.0002
15	75.32	1.896	-0.0319
16	70.49	1.417	-0.0587
17	65.90	0.801	-0.0757
18	60.17	0.445	-0.0884
19	115.96	2.784	0.2197

(Tx. Ant. Ht. = 75.29 m. launching 19 rays from -4.5455 to -1.1364 mrad.)
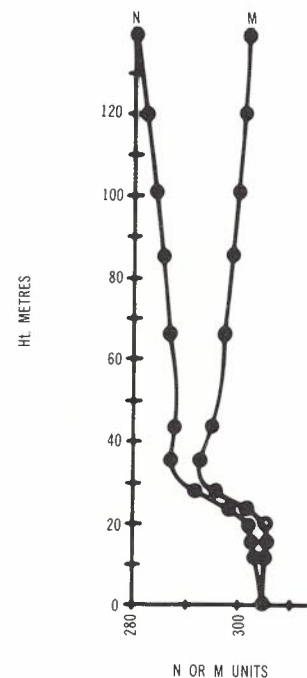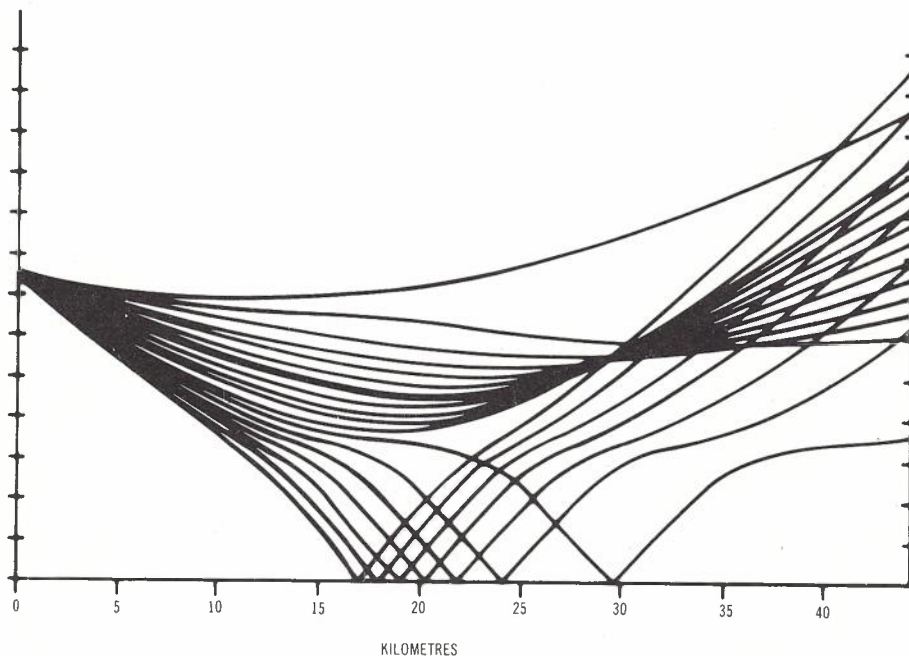

Fig.7 - Tracing for path of Fig.5b as produced by first new program (ray data as per Table 2).

TABLE 3 - Ray Data for Tracing of Fig.8

RAY No.	HEIGHT (M)	REC.ANG. (mrad)	REL.DEL. (nanosec)
1	124.14	5.300	1.5792
2	112.82	4.996	1.3846
3	101.04	4.594	1.1960
4	88.60	4.240	1.0127
5	74.98	3.781	0.8302
6	59.31	3.141	0.6490
7	38.89	0.993	0.4761
8	114.65	4.079	0.3189
9	114.82	3.934	0.3217
10	106.63	3.602	0.2190
11	92.36	3.115	0.0601
12	60.92	1.813	-0.2067
13	69.30	2.008	-0.1534
14	77.70	2.183	-0.0946
15	85.97	2.314	-0.0325
16	93.97	2.407	0.0306
17	101.64	2.484	0.0929
18	109.60	2.685	0.1616
19	115.96	2.784	0.2197

(Tx. Ant. Ht. = 75.29 m. launching 19 rays from
-4.5455 to -1.1364 mrad.)

An illustration of the ray plots obtained with a large plotting increment is shown in Fig.9 which employs the same N profile as Fig.7. Each piece-wise-linear trace segment in Fig.9 is a chord on the true continuously turning ray trajectory. The ray output listing for Fig.9 is identical to Table 2, since large increment plotting has no effect on the end-of-path estimates.

The speed advantage gained by large increment plotting over normal small increment tracing is illustrated in Table 4, which compares the first program times for the two cases. Small increment tracing times for the second program are also included in the table for comparison. Note that large increment plotting times for the latter program have been omitted, because as indicated in Section 2.2, significant errors can then develop.

TABLE 4 - Program Tracing Speeds

DIAGRAM	PROGRAM No.	INCREMENT X (m)	MEAN SPEED (Km/sec)
Fig.6	1	500	2.67
Fig.7	1	500	2.61
Fig.9	1	50,000 (high speed)	10.0
Fig.6	2	500	0.70
Fig.7	2	500	0.74
Fig.6	2	500 (delays not calc.	1.42

Note : (does not include plotting of axes and
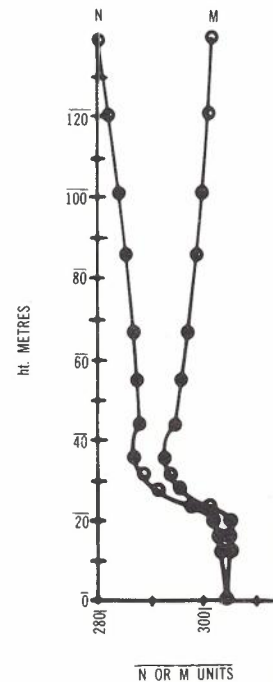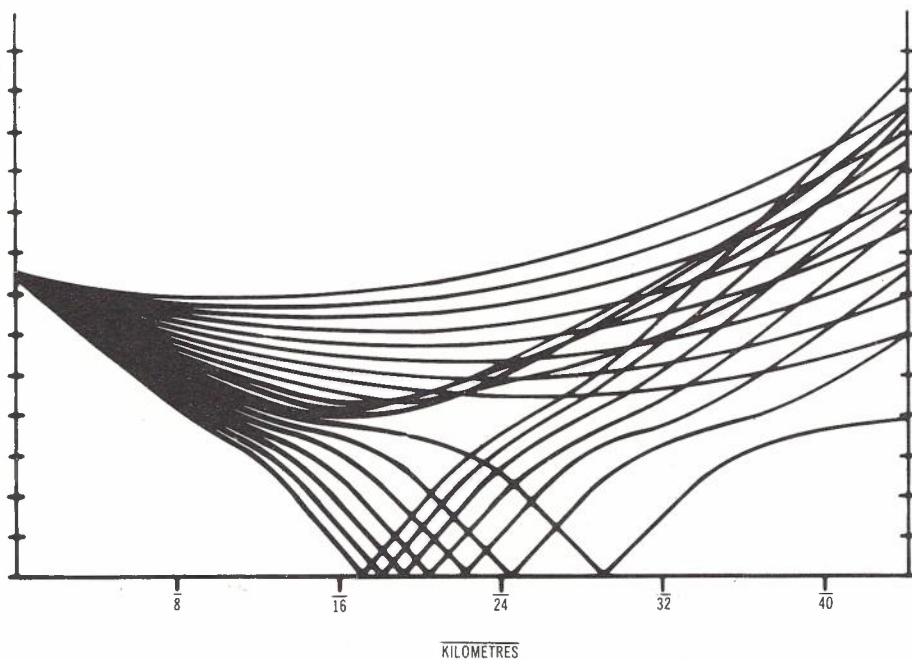profiles or labelling)

Fig.8 - *Tracing for path of Fig.7 with two addi-tional profile data points (ray data as per Table 3).*

Tropospheric Ray Tracing

3.3 Paths with Multiple N Profiles

The results shown in Fig.10 and Table 5 illustrate the use of the second program for a path where N depends on both height and map distance. The particular example chosen uses profiles derived by Harvey (Ref.5) in studies of microwave propagation in Queensland, Australia.

TABLE 5 — Ray Data for Tracing of Fig.10

6 Rays from -8.50 to -7.50 by 0.20 m.rad.					
RAY	GDH	TX.ANG.(mrad)	REC.ANG.(mrad)	REC HEIGHT	DELAY (ns)
1	1	-8.50000	6.60524		0.836
2	1	-8.30000	5.76774		0.760
3	1	-8.10000	4.94544		0.669
4	1	-7.90000	4.06296		0.554
5	1	-7.70000	7.80532		0.406
6	1	-7.50000	4.03461		0.342
11 Rays from -7.45 to -6.95 by 0.05 m.rad.					
RAY	GDH	TX.ANG.(mrad)	REC.ANG.(mrad)	REC HEIGHT	DELAY (ns)
1	1	-7.45000	3.18916		0.317
2	1	-7.40000	8.27918	76.64	0.123
3	1	-7.35000	6.80230	50.25	-0.564
4	1	-7.30000	2.81923	28.06	-0.944
5	1	-7.25000	0.94532	19.76	-0.991
6	1	-7.20000	0.55724	13.02	-1.008
7	1	-7.15000	0.08948	6.37	-1.016
8	1	-7.10000	0.52420	5.64	-1.015
9	1	-7.05000	1.18705	2.28	-1.026
10	0	-7.00000	4.38245	35.05	-0.953
11	0	-6.95000	2.09105		0.164
6 Rays from -6.90 to -5.90 by 0.20 m.rad.					
RAY	GDH	TX.ANG.(mrad)	REC.ANG.(mrad)	REC HEIGHT	DELAY (ns)
1	0	-6.90000	3.20348		0.183
2	0	-6.70000	7.00088		0.162
3	0	-6.50000	2.01078		0.216
4	0	-6.30000	2.51283		0.234
5	0	-6.10000	3.40714		0.238
6	0	-5.90000	4.36905		0.224

(Tx Ant. Ht. = 63.0 m. launching 23 rays as indicated)

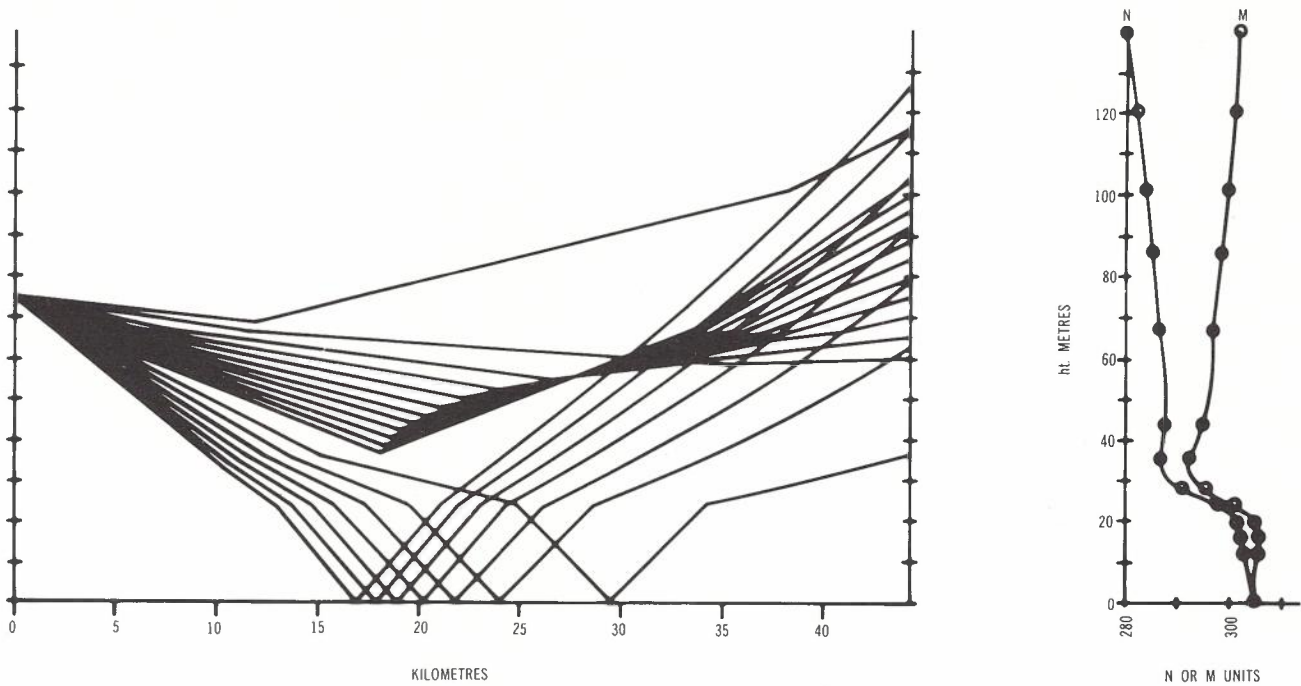(GDH = 1 for a ground reflection, = 0 otherwise)

Fig.9 - High speed tracing for path of Fig.7 (ray data unchanged from Table 2).

In view of the earlier noted sensitivity of certain rays through some N profiles, there is clearly a question as to the number of steps required for an adequate representation on paths of the type considered here. If the highest accuracy is sought, repeated tracings should be made using successively larger numbers of profiles giving correspondingly refined results; the process being taken to the stage where satisfactory convergence is obtained.

In other situations, where either only a general picture is required, or where the changes in N with path distance are relatively small, the results of a single tracing will prove adequate.

The tracings of Figs.11 and 12 have been produced to show how the ray paths of Fig.10 vary with different numbers of profiles. Figure 11 uses only the centre of path profile, and while the detail differs significantly from the other two plots, it still shows the same general defocussing action which is the main feature of all three tracings. This overall similarity of Fig.11 to the other two tracings supports the use of the single profile model for at least some actual path studies.

4. CONCLUSIONS

The most generally informative examples given in the paper are probably those showing how ray detail can change significantly with small variations in the path refractive index. It is important therefore, that when ray tracing programs are used to study tropospheric radio propagation phenomena, due account should be taken of the likely inaccuracies in the assumed path refractive index data. Repeated tracings covering the range of probable profiles will establish the stability or otherwise of any given mechanism. For example, Warhaft and Van Dijk have tested their "fadeout" phenomenon this way (Ref.3).
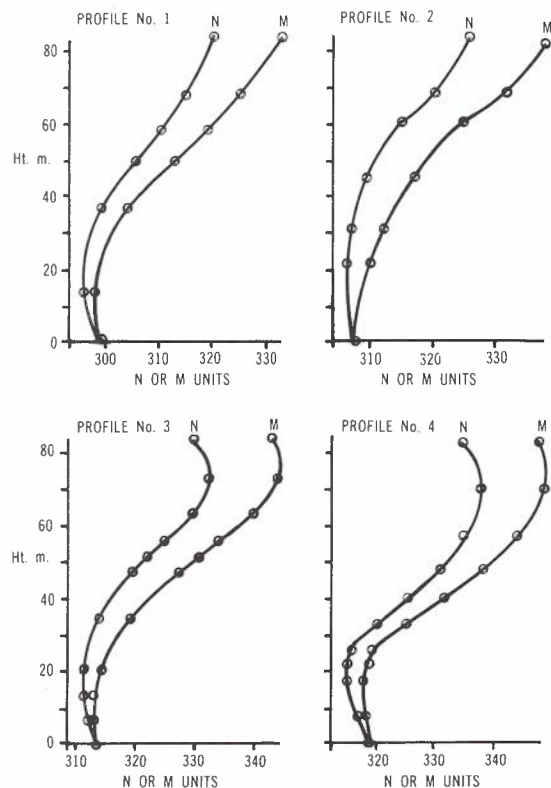
Fig.10a - Multiple profiles for Julia Creek (Qld.) path after Harvey (Ref.5).

Although both techniques described here give strictly accurate results for only small ray angles, comparisons made with a precise though very slow numerical routine have shown that the errors are less than 2 percent for $\alpha = 20°$ (Ref.20). It follows therefore that either program will give sufficiently accurate results for the practical investigation of almost all tropospheric paths.

Fig.10b — Multiple profile tracing for data of Fig.10a as produced by second new program (ray data as per Table 5).
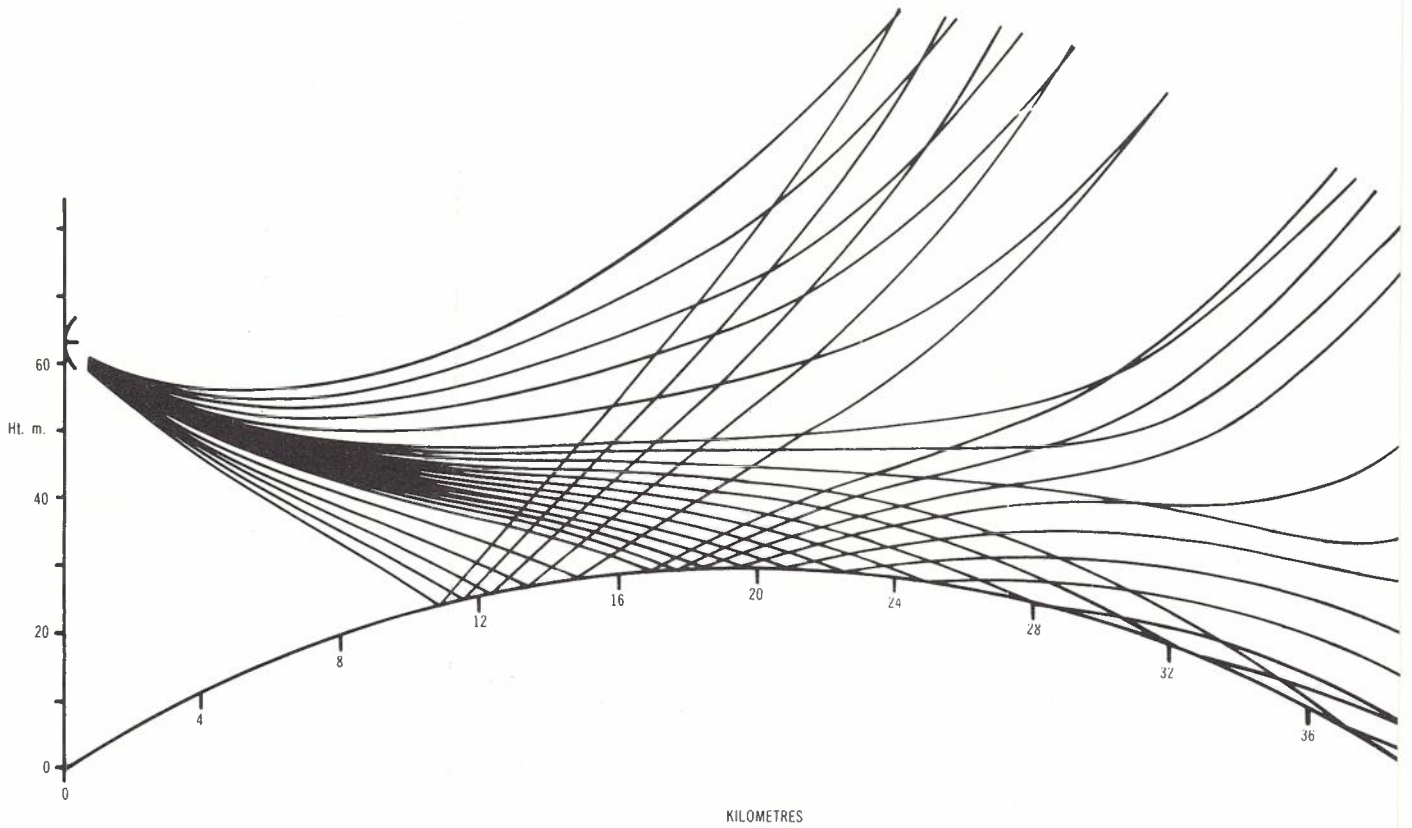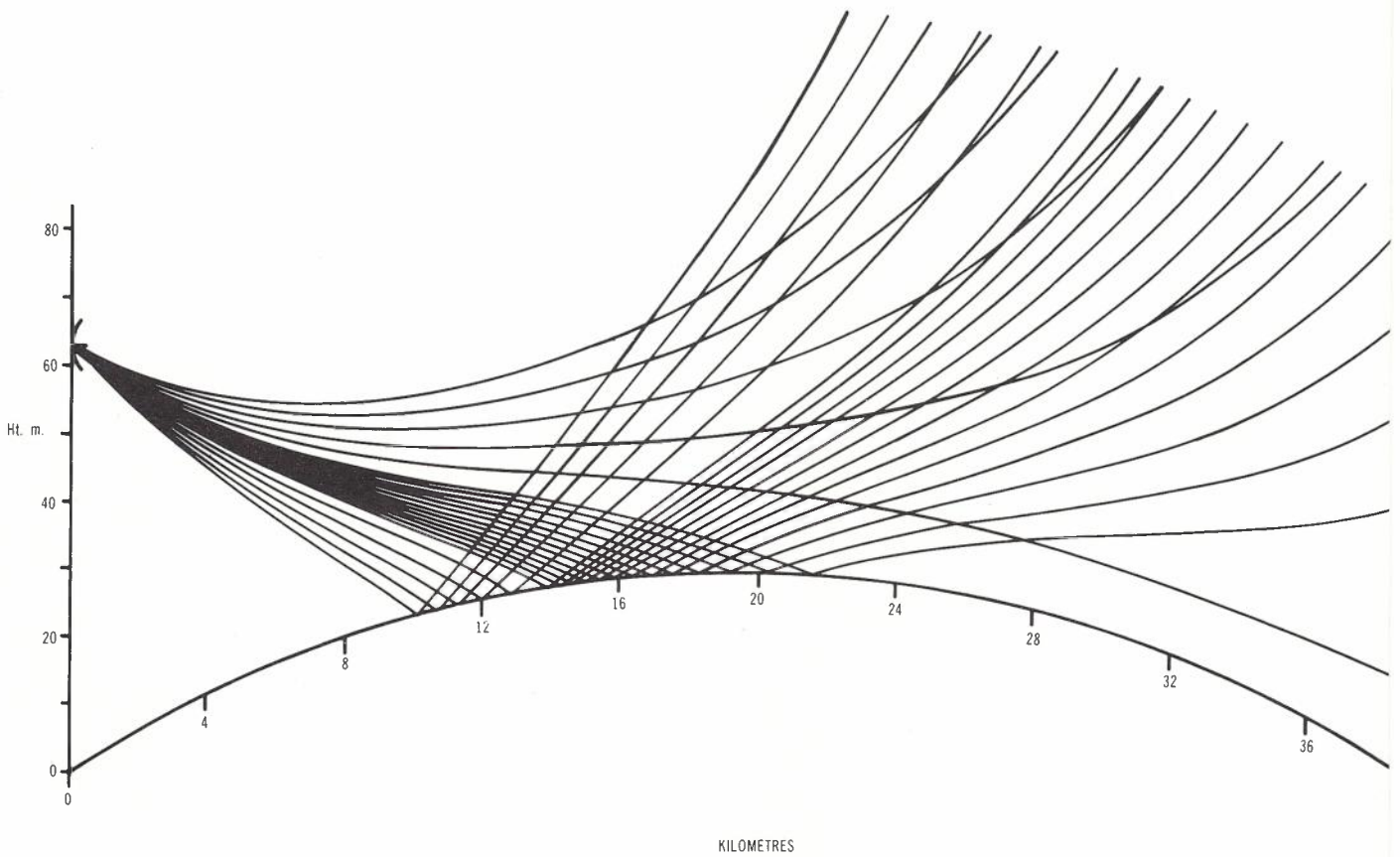

Fig.11 — Comparison tracing for path of Fig.10 using a single centre-of-path profile.

Various aspects of these investigations are considered worthy of further study or extension. The application of the Taylor series technique to arbitrary profiles is warranted, in order to explore its full capabilities. It would also be an advantage to modify the profile curve fitting approach used with the present methods, so that tracings could be made either with the form of Fig.2, or with sub-profiles having no splines, or cusps, at the odd data points. This would greatly facilitate the resolution of any questions as to the possible effects of such discontinuities in the refractive index gradient. Another worthwhile feature of any future program would be to provide for the identification of interference and attenuation regions as Ikegami has done (Ref.6).

5. ACKNOWLEDGEMENTS

6. REFERENCES

1. Rosman, G.E., "APO Research Fortran Program 2055", (unpublished studies) Australian Post Office Research Laboratories, Melbourne 1966.

2. Warhaft, Z. and Van Dijk, M.H., "Desert Microwave Propagation Studies - Report 1", Australian Post Office Research Laboratories, Report No.6244, Melbourne 1968.

3. Warhaft, Z. and Van Dijk, M.H., "Space Wave Fadeouts on a Line of Sight Path with Equal Terminal Heights", Australian Telecommunication Research, 1970, Vol.4, No.1, pp.16-22.

4. Tang, T., "Programme C2055A - Field Strength Estimation Using Ray Tracing Technique", Australian Post Office Research Laboratories, Student Report, Melbourne 1970.

5. Harvey, R.A., "Propagation Effects in Outback Areas", Telecom Australia Colloquium on New Propagation and System Techniques for Non-Trunk Radio Applications in the 1980s. 30th April-1st May 1980. Melbourne.

6. Ikegami, F., "Analysis of Microwave Fading due to Laminar Structure of the Atmospheric Refractive Index", Review of the Electrical Communication Laboratory, Vol.15, Nos.7-8, (July-August 1967), pp.483-506.

7. Baker, P.W., "Ray Tracing in the Troposphere", Department of Supply, Australian Defence Scientific Service, Weapons Research Establishment, WRE - Technical Note - A220(AP) Salisbury, S.A. 1972.

8. Barton, I.J., "The Importance of Tilted Layers in the Tropospheric Ducting of Radio Waves over the Timor Sea", Radio Science, 1973, Vol. 8, Nos.8 and 9, pp.727-732.

9. Haselgrove, J., "Ray Theory and a New Method for Ray Tracing", Proc. Camb. Conf. Phys. Ionosphere, The Physical Society, London, 1955, pp.355-364.
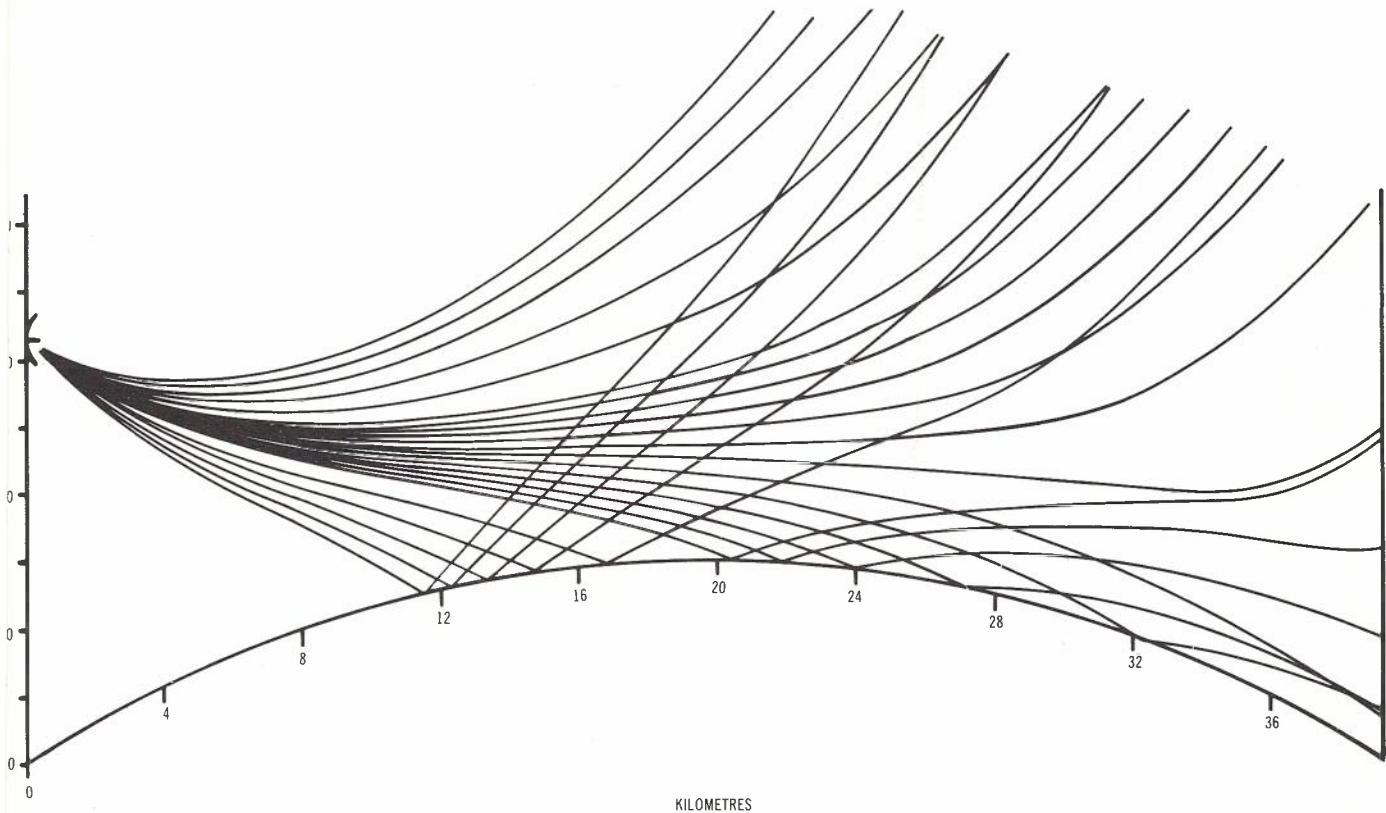
KILOMETRES

Fig.12 - Comparison tracing for path of Fig.10 using twelve multiple profiles.

10. Kelso, J.M., "Ray Tracing in the Ionosphere", Radio Science (New Series), Vol.3, No.1, 1968, pp.1-12.

11. Kopka, H. and Möller, H.G., "MUF Calculations Including the Effect of the Earth's Magnetic Field", ibid, pp.53-56.

12. Jones, R.M., "A Three-Dimensional Ray-Tracing Computer Program (Digest of ESSA Technical Report, ITSA No.17)", ibid, pp.93-94.

13. Jones, R.M. and Stephenson, J.J., "A Versatile Three-Dimensional Ray Tracing Computer Program for Radio Waves in the Ionosphere", U.S. Department of Commerce, Office of Telecommunications, OT Report 75-76, 1975.

14. Thayer, G.D., "A Rapid and Accurate Ray Tracing Algorithm for a Horizontally Stratified Atmosphere", Radio Science (New Series), Vol. 2, No.2, 1967, pp.249-252.

15. Croft, T.A. and Hoogasian, H., "Exact Ray Calculations in a Quasi-Parabolic Ionosphere with No Magnetic Field", Radio Science (New Series), Vol.3, No.1, 1968, pp.69-74.

16. Westover, D.E., "Exact Ray-Path Solutions in a Quasi-Linear Ionosphere", ibid, pp.75-79.

17. Försterling Von, K. and Lassen, H., "Die Ionisation der Atmosphäre und die Austreitung der kurzen elektrischen Wellen (10-100 m) über die Erde. III", Zeitschrift fur technische Physik, Vol.12, No.11, 1931, pp.502-527.

18. Appleton, E.V. and Beynon, W.J.G., "The Application of Ionospheric Data to Radio-Communication Problems : Pt.I", Proc. Phys. Soc. London, Vol.52, No.202, 1940, pp.518-533.

19. Rawer, K., "Optique Géométrique De l'Ionosphére", Rev. Sci. Paris, No.3298, 1948, pp.585-600.

20. Davies, W.S. and Evans, T.A., "Desk Calculator Ray-Tracing Programs for Tropospheric Radio Propagation Studies", Telecom Australia Research Laboratories Report No.7456, 1981.

21. Humphreys, W.J., "Physics of the Air", Dover, 1964 ed., pp.455-457.

22. Hartree, D.R., Michel, J.G.L. and Nicolson, P., "Practical Methods for the Solution of the Equations of Tropospheric Refraction", Conf. on Meteorological Factors in Radio-Wave Propagation, The Physical Society and The Royal Meteorological Society, London, 8th April 1946, pp.127-168.

APPENDIX A : Expressions for I_1 and I_2

Each of the integrals I_1 and I_2 yield different explicit expressions for the four possible types of m subprofile. The results for I_1 are as follows:

(a) $A > 0$; defocussing profile

$$I_1 = \pm A^{-\frac{1}{2}} \log_e \left[\frac{(h_2+D) + \{(h_2+D)^2 + E/A\}^{\frac{1}{2}}}{(h_1+D) + \{(h_1+D)^2 + E/A\}^{\frac{1}{2}}} \right] ,$$

for $h_2 \gtrless h_1$

(b) $A < 0$; focussing profile

$$I_1 = |A|^{-\frac{1}{2}} \left[\theta(h_2) - \theta(h_1) \right]$$

where

$$\theta(h) = \sin^{-1} \frac{|A|^{\frac{1}{2}}(h+D)}{E^{\frac{1}{2}}} , \quad \text{for } h+D \geq 0$$

$$\theta(h) = \pi - \sin^{-1} \frac{|A|^{\frac{1}{2}}(h+D)}{E^{\frac{1}{2}}} , \quad \text{for } h+D < 0$$

(c) $A = 0$; $B \neq 0$, linear profile

$$I_1 = \pm \frac{2}{B} \left[(\alpha_1^2 + C + Bh_2)^{\frac{1}{2}} - (\alpha_1^2 + C + Bh_1)^{\frac{1}{2}} \right] ,$$

for $h_2 \gtrless h_1$

(d) $A = 0$, $B = 0$; constant profile, hence from equation (10) $C = 0$

$$I_1 = \pm \frac{h_2 - h_1}{\alpha_1} , \quad \text{for } h_2 \gtrless h_1$$

The corresponding results for I_2 are:

(a) $A > 0$; defocussing profile

$$I_2 = \pm \frac{A^{\frac{1}{2}}}{2} (h_2+D)\{(h_2+D)^2 + \frac{E}{A}\}^{\frac{1}{2}}$$

$$- (h_1+D)\{(h_1+D)^2 + \frac{E}{A}\}^{\frac{1}{2}} \pm \frac{E}{2} I_1 ,$$

for $h_2 \gtrless h_1$

(b) $A < 0$; focussing profile

$$I_2 = [(h_2+D)\{A(h_2+D)^2 + E\}^{\frac{1}{2}}$$

$$- (h_1+D)\{A(h_1+D)^2 + E\}^{\frac{1}{2}} + EI_1]/2 \ ,$$

for $h_2 \gtrless h_1$

(c) $A = 0$, $B \neq 0$; linear profile

$$I_2 = \pm \frac{2}{3B}\left[(Bh_2+C+\alpha_1^2)^{3/2} - (Bh_1+C+\alpha_1^2)^{3/2}\right] \ ,$$

for $h_2 \gtrless h_1$

(d) $A = 0$, $B = 0$; constant profile

$$I_2 = \alpha_1(h_2 - h_1)$$

Note that the $\pm$ signs, where they appear, are equivalent to taking the absolute values, for in equation (6) dh and α are always of the same sign, hence I_1 and I_2 are always positive.

APPENDIX B : Expressions Employed in Taylor Series Method

To evaluate equation (23) let

$\xi = x - x_1$; then

$$\frac{dh}{dx} = h^{(1)}(x_1) + \xi h^{(2)}(x_1) + \frac{\xi^2}{2!} h^{(3)}(x_1) + \ldots$$

$$= 0 + \xi T + \frac{\xi^2}{2!} U + \frac{\xi^3}{3!} V + \frac{\xi^4}{4!} W \ldots \quad (25)$$

$$1 + (\frac{dh}{dx})^2 = 1 + 0^2 + 2\xi TO + \xi^2(\frac{2UO}{2!} + T^2)$$

$$+ \xi^3(\frac{2VO}{3!} + \frac{2TU}{2!}) + \xi^4(\frac{2WO}{4!} + \frac{3VT}{3!} + \frac{U^2}{4}) + \ldots$$

$$\simeq (1 + 0^2)(1 + a_1\xi + a_2\xi^2 + a_3\xi^3 + a_4\xi^4 + a_5\xi^5)$$

for ξ small $\quad (26)$

$$\left[1 + (\frac{dh}{dx})^2\right]^{\frac{1}{2}} \simeq (1+0^2)^{\frac{1}{2}} \left[1 + \xi\frac{a_1}{2} + \xi^2(\frac{a_2}{2} - \frac{a_1^2}{8})\right.$$

$$+ \xi^3(\frac{a_3}{2} - \frac{a_1 a_2}{4} + \frac{a_1^3}{16})$$

$$\left. + \xi^4(\frac{a_4}{2} - \frac{a_1 a_3}{4} - \frac{a_2^2}{8} + \frac{3a_1 a_2}{16} - \frac{5a_1^4}{12})\right]$$

$$= b_0 + \xi b_1 + \xi^2 b_2 + \xi^3 b_3 + \xi^4 b_4$$

$$(27)$$

The integration of equation (25) by the Taylor series method yields

$$h(x) = h_1 + 0\xi + \frac{\xi^2}{2!} T + \frac{\xi^3}{3!} U + \frac{\xi^4}{4!} V + \frac{\xi^5}{5!} W + \ldots$$

Now from equations (22) and (4)

$$m(x) = 1 + A_1 h^2(x) + B_1 h(x) + C_1$$

Hence with the above $h(x)$

$$m(x) \simeq 1 + A_1 h_1^2 + B_1 h_1 + C_1 + \xi(2A_1 h_1 0 + B_1 0)$$

$$+ \xi^2 \left[A_1(0^2 + h_1 T) + B_1 T/2\right]$$

$$+ \xi^3 \left[A_1(h_1 U/3 + 0T) + B_1 U/6\right]$$

$$+ \xi^4 \left[A_1(h_1 V/12 + 0U/3 + T^2/4) + B_1 V/24\right]$$

$$+ \xi^5 \left[A_1(h_1 W/60 + 0V/12 + TU/3) + B_1 W/120\right] \ ,$$

for ξ small

$$= c_0 + c_1\xi + c_2\xi^2 + c_3\xi^3 + c_4\xi^4 + c_5\xi^5 \tag{28}$$

Hence from equations (27) and (28)

$$m(x)\left[1 + \left(\frac{dh}{dx}\right)^2\right]^{\frac{1}{2}} \simeq \sum_{i=0}^{4} \sum_{j=0}^{5} b_i \, c_j \, \xi^{i+j} \quad ,$$

for ξ small

$$= F_0 + \xi F_1 + \ldots + \xi^9 F_9 \tag{29}$$

Thus integrating equation (29) over the range x_1, x_2, and using $X = x_2 - x_1$, gives the required result for s as

$$s \simeq X F_0 + X^2 F_1/2 + X^3 F_2/3 + \ldots + X^{10} F_9/10$$

for X small

In the program developed on the Taylor series method this last polynomial has been truncated at the term of order X^6.

BIOGRAPHIES

WILLIAM STANLEY DAVIES received his secondary education at Northam High School, in his home town of Northam, Western Australia.

During that period he was awarded the J.A. Wood Country Scholarship in 1954. He was appointed as a Cadet Engineer with the Australian Post Office in 1957, while studying for the B.E. degree at the University of Western Australia. Upon graduation in 1961, he was employed with Post Office Lines Divisions in Western Australia until 1962. During that year he transferred to the Post Office Research Laboratories in Melbourne, where he worked on various M.F., H.F. and microwave antenna projects until 1965, when he was granted an Australian Government Full-Time Free-Place, for studies towards the degree of M.Eng.Sc. at the University of Melbourne. Mr. Davies' thesis project was on Yagi-Uda antenna arrays. He was awarded the degree with honours, and the Ormsby Hamilton Radio Prize in 1967.

From 1968-70 Mr. Davies studied under a Commonwealth Public Service Board Overseas Postgraduate Scholarship at the Department of Electronic and Electrical Engineering, University of Sheffield, England. He received the degree of Ph.D. in 1973 for his thesis on microwave arrays with low-level low-order side-lobes. More recently Dr. Davies' activities have included transmission studies of optical fibres, further antenna and electromagnetic field investigations, and studies of the phenomenon and effects on communications systems of the electromagnetic pulse generated by a nuclear detonation (EMP). In this last mentioned context, Dr. Davies was leader of the Telecom team which participated in a Joint Electromagnetic Effects Project in Canberra in 1978. Dr. Davies' leisure-time interests include youth work and theology.
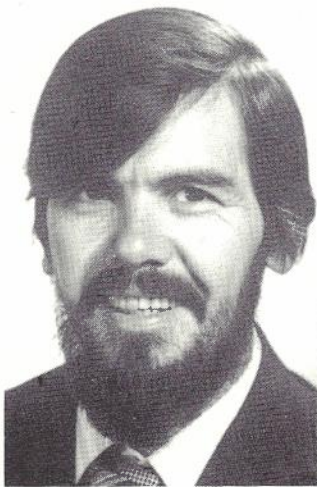
THOMAS A. EVANS attended the Carey Baptist Grammar School, Melbourne, where he obtained high distinction in the Higher School Certificate in 1974. He was awarded the degree of B.E. (hons) by the University of Melbourne, for studies completed at the Department of Electrical Engineering in 1978. Since graduating Mr. Evans has spent short periods of time with the Trunk Services Section of Telecom Australia, working on electrical safety compliance tests and switching-mode power supplies; and with the Datatronics Research and Development Department of A.T.L. Ltd., Melbourne, where he was mainly engaged on various microprocessor software and hardware projects. In August 1979 he was appointed to his current position as an Engineer in the National Support Group of Anderson Digital Equipment, where his duties include the evaluation and modification of various computers and peripheral equipment, fault diagnosis and chip-level repairs.

The ray-tracing programming work described in the present paper, was undertaken while Mr. Evans was on vacation employment with the Unguided Media Section at the Telecom Australia Research Laboratories in 1977-78.

Mr. Evans has shown considerable interest in home-computers as a hobby. His other recreational activities include skiing, bush walking and cycling. He is a member of both the Australian Computer Society, and the Microcomputer Club of Melbourne.

Reflections In A Crystal Ball
The Technologist as Prophet In A Turbulent Society

L.A. ALBERTSON
Telecom Australia Research Laboratories

Telecommunications engineers who participated in a Delphi forecasting study conducted by the former Australian Post Office in 1975 were found to have highly optimistic images of the future and to employ longer time perspectives than non-engineers. The present paper attempts to explain these concordant readings of the future by considering the socio-psychological origins of the engineer's career choice. After critical analysis of several streams of vocational research, the paper argues that the making of engineers begins with fixation during the developmental stage of latency. Professional education then consolidates the engineer's intellectual stance, and also subtly reinforces a set of assumptions that ultimately enter into the very fabric of his experience of reality. Unless these assumptions can be opened to re-assessment in light of changing circumstances, the paper concludes, technology-based organizations such as Telecom Australia will be ill-equipped to survive the environmental turbulence of the late twentieth century.

1. FIRST, FIND YOUR FORECASTER

When King Croesus of Lydia was seeking a consultant seer, he compiled a short list of seven noted oracles practising in the region and despatched to each an ambassador who, after a hundred days, was to pose the question: 'What is King Croesus, son of Alyattes, now doing?'. Only the Pythia at Delphi passed the test - the King, improbably enough, was cooking rabbit and tortoise together in a brazen pot - and she was duly awarded the contract.

Today, although prediction is still considered an important aspect of government, it is no longer carried out by mystics. The modern Delphi forecasting technique, for example, which was developed from the work of Olaf Helmer for the RAND corporation, has little in common with the methods of the famous oracle; and, paradoxically, the widespread popularity of the technique since it was first publicly described (Dalkey & Helmer (Ref.11)) has depended less upon rigorous proofs of its efficacy than upon belief in its scientific credentials. It employs a panel of people chosen for their expertise in a particular field - frequently a technological one - who respond anonymously to a written questionnaire dealing with potential developments in their field. In a second questionnaire, the panelists are asked to reconsider their forecasts in the light of their colleagues' responses. This procedure may be repeated for several more rounds in an attempt to reach consensus.

As part of their research into Australia's future needs for telecommunications, the National Telecommunications Planning Branch of the (then) Australian Post Office carried out two Delphi forecasting studies. The first, begun in 1974, was conducted in the classic manner with a panel constituted from a group deemed to have the relevant expertise: the organization's senior management (Second Division). The second, begun in 1975, made

use of a technique known as SPRITE, a modification of the Delphi developed by members of Bell Canada's Business Planning Group. This study took the form of a written dialogue between two panels: Telecom engineers at middle-management level and a group of women - librarians and housewives - representing potential consumers. To explore the role of psychological factors in forecasting, the questionnaire administered in the first round of each study included a semantic differential on which each panelist was asked to indicate his or her concept of the future. Two further groups - political science students from Monash University and a younger group of American Field Scholars - also completed the semantic differential, making a total of 189 respondents divided into five *a priori* social groups.

This aspect of the study, which is fully described in a previous paper (Albertson & Cutler (Ref.3)), showed that each group could be statistically separated from the others solely on the basis of its members' responses to the semantic differential. Engineers recorded the highest scores on the underlying dimension labelled 'essence' optimism/pessimism - defined as beliefs about the intrinsic nature of human events - and were second only to the senior managers (roughly half of whom were trained as engineers) in their scores on 'influence' optimism/pessimism - defined as a belief in man's capacity to influence the future. Moreover, differences in the image of the future held by the three Delphi panels correlated with differences in their numerical forecasts. The engineers' median forecasts were almost always longer than those of the other two panels, and they used the NEVER option significantly less often. However, a reversal of this pattern was observed in a six-item section dealing with future trends in work, travel and leisure. In the first round, for example, a majority of the engineers (56%) forecast that women would NEVER occupy 25%

of positions carrying an annual salary of $10,000 or more (then equivalent to the salary of a Clerk Class 6 in the Public Service), while only 12% of the senior managers and 20% of the consumers gave this response. Except for an item dealing with union representation on boards of management, the other items in this section evoked responses that were similarly untypical of the forecasting style the engineers had evidenced in the technological items.

Although 'optimism' has been variously described and measured, other studies have confirmed both the optimism of engineers (Barling (Ref.9); Luten (Ref.22)), and the link between optimism and forecasting (Loye (Ref.21); Schmidt et al. (Ref.29)). Loye, an American psychologist who had access to extensive data collected from 61 Californian males in the course of two other studies (one concerning the effects of television, the other a study of political forecasting), found that optimists - those who expected America in the year 2000 to be better than at present - made different forecasts for the immediate and short-term political future than did the pessimists - those who expected it to be worse. Schmidt et al., in a European study of forecasting and future time orientation, drew a sample of 125 adults from respondents to a newspaper appeal for volunteers. Defining as optimists those who rated the future either five or twenty years hence more positively than the present, they found that optimists possessing a college degree (but not those with only a high school diploma) had longer time perspectives than pessimists.

Other findings from these studies also cast greater light on the reasons for the differences between the groups in their images of the future. Schmidt et al. found that compared with the working-class participants in their study, the middle-class participants were more likely to be optimistic in their evaluation of the future, and more inclined to believe that they could influence public events. The researchers propose that middle-class membership and optimism are causally linked:

...it can be conjectured that the conviction that one himself can influence future events in specific spheres of life leads to an optimistic evaluation of events in that sphere (Schmidt et al. (Ref.29) p.75).

Although class was not a variable in the Australian study, this interpretation appears to offer a partial explanation for the findings. The senior managers, whose higher organizational status implies that they have greater control than the engineers over the events they are forecasting, scored highest of the five groups on the 'influence' dimension. Their neutral position as a group on the 'essence' dimension, however, shows that the power differential cannot fully account for the observed differences in optimism. It is in accounting for the differences along this second dimension that the evidence gathered by Loye concerning the personality differences of optimists and pessimists appears to hold promise. He found, for example, that optimists are significantly more likely than pessimists to be emotionally stable and less likely to exhibit anomie; and, (at a lower level of statistical significance) that optimists were more imaginative and less alienated than pessimists. (Loye (Ref.21)).

Nevertheless, to argue that the engineers' concordant readings of the future are due in part to personality traits raises a further question: why would one expect to find similar personalities among telecommunications engineers?

2. THE MAKING OF ENGINEERS

While the psychology of the practising Australian engineer is a largely unresearched territory, studies at university level have found that attitudes common among engineering students are not shared by students in other faculties.

In a study encompassing five Australian universities, Anderson and Western (Ref.6) measured the attitudes of 3146 students entering four professional faculties (engineering, law, medicine, teaching) both during their initial weeks at university and again at intervals throughout their university courses. Only minor differences were found between universities, but there were marked differences between the faculties - the majority arising from differences between the engineering students and one or more of the other groups (see Table 1). Engineering students scored lowest on intellectual interests (such as art, literature and the life of the mind), and highest on pragmatism and on dogmatism (the acceptance of authority and a tendency to prejudge issues). Together with the teaching students, they were the most conservative on social issues (such as censorship and sexual mores), and also the most politically conservative (the teaching students, on the other hand, were the most politically liberal). The follow-up studies showed that, compared with the initial study, the students generally had become more politically and socially liberal, more interested in intellectual pursuits and less dogmatic and pragmatic; nonetheless, the relative differences between the faculties remained unchanged.

Accounting for these differences is far from simple. Given that retrospective studies and biographies of eminent people often claim that the seeds of future greatness were manifest in their subjects from an early age, one might begin by hypothesizing that the observed attitudinal similarities are a product of the aptitudes that led the student to select one faculty rather than another. However, the consistently poor record of studies concerned with vocational prediction - including those that have attempted to find indicators of future high achievement among students in their final years of secondary school - provide little support for this hypothesis.

2.1 The View in the Rear-vision Mirror

In the atmosphere of heightened interest in science and technology that followed the second world war, the scientist became a popular subject for psychological and sociological research. Two well-regarded pieces of research dating from this period are Anne Roe's social profiles of eminent men of science - physical scientists, biologists, psychologists and anthropologists; and David McClelland's studies of the motivations of creative physical scientists (Refs.28&25). These studies, based primarily on data gathered from interviews and from projective tests, present clear-cut and generally consistent pictures of the gifted physical scientist and his childhood development (see Table 2 for a summary of McClelland's findings).

TABLE 1 - Attitudinal Differences Between Students in Four Professions

Scale	ENGINEERING	LAW	MEDICINE
LAW			
Intellectual interests	*		
Academic activities			
Political-economic liberalism			
Social liberalism			
Pragmatism	*r		
Dogmatism	*r		
Cynicism			
MEDICINE			
Intellectual interests	*		
Academic activities			
Political-economic liberalism	*	*	
Social liberalism			
Pragmatism			
Dogmatism	*r		
Cynicism			
TEACHING			
Intellectual interests	*		*
Academic activities	*r	*r	*r
Political-economic liberalism	*	*	*
Social liberalism		*r	
Pragmatism			
Dogmatism	*r		
Cynicism			*

Note: An asterisk (*) indicates that the faculty shown on the left
       of the table has a significantly higher score (at the 5% level
       of confidence) than the faculty shown in the columns;
       (*r) indicates significant differences in the opposite direc-
       tion (Scheffe tests).

       Source: Anderson & Western (Ref.6)

2.2 Through a Glass Darkly

The dramatic successes of the Russian space program in the mid-fifties lent new urgency to the American studies of the psychological properties of the scientist, with special attention being focussed on the early identification of scientific giftedness. The clear profile of the gifted scientist that had emerged from the retrospective studies carried an implicit promise that the task of identifying high achievers would be relatively simple; but experience proved otherwise. Certainly, measures of general intelligence (IQ) proved to be of surprisingly little value. While IQ tests are a useful means of quickly distinguishing between the bright and the dull in a large population, they simply fail to discriminate between those intelligent people who will realize their potential in a concrete form, and those intelligent people who will not. MacKinnon (Ref.26) concluded that beyond a certain minimum level - probably in the region of 115 to 125 IQ points - conventional IQ tests have little bearing on subsequent academic or career achievement.

Other measures fared little better. Despite the onslaught of studies which cross-correlated almost every imaginable variable with later career success, only a study of home environment conducted by Getzels and Jackson (Ref.12) attained a useful level of predictive power. Although attempts to replicate their general findings had mixed results, a Getzels and Jackson test for 'creativity' became part of a more successful line of inquiry pursued by the British psychologist and educator Liam Hudson.

TABLE 2 - Psychological Characteristics of Creative Physical Scientists

*Men are more likely than women to be creative scientists

*Experimental physical scientists come from a background of radical Protestantism more often than would be expected by chance, but are not themselves religious

*Scientists avoid interpersonal contact

*Creative physical scientists are unusually hardworking to the extent of appearing almost obsessed with their work

*Scientists avoid and are disturbed by complex human emotions, perhaps particularly interpersonal aggression

*Physical scientists are intensely masculine (engineers score even more highly than physicists on measures of masculinity)

*Physical scientists like music and dislike art and poetry

*Physical scientists develop a strong interest in analysis, in the structure of things, early in life.

Source: D. McClelland (Ref.25)

Hudson, whose work is discussed in greater detail below, not only endorses MacKinnon's view of the value of IQ scores (Hudson (Ref.19)), but points out that by the time a student is in the sixth form the main distinguishing characteristics of future high achievers are 'breadth of interest outside the curriculum and a tendency to work hard' (Hudson (Ref.16) p.43). His conclusions are supported by the monumental study of 1,528 American children with IQs of more than 135 (which places them in the top 1% of the population, and is generally characterized as the 'genius' range). Begun by Lewis Terman in 1921, this study now spans six decades, the most recent follow-up being conducted in 1977 when most of the participants had reached retirement age. Preliminary reports from the follow-up (Goleman (Ref.13)), show that although most had done well in careers and had incomes higher than the national average, none had manifested recognizable genius (there were, for example, no Nobel prizewinners in the group); moreover, among the participants were semi-skilled workers and people who had been unemployed for much of their working life. But those in the sample who did succeed in careers were rated by parents and teachers at age ten and again at age eighteen as higher than their classmates in such qualities as persistence and the desire to excel.

2.3 Refractory Evidence

Despite the failure to find the kinds of indicators of future high achievement that many researchers hoped for, a different stream of research was successful in identifying among schoolchildren broad differences in cognitive style that correlate well with their subject specialization at secondary school level and hence general direction of their career choice. Much of this evidence derives from the sustained research effort of Liam Hudson and his associates.

Hudson's work began in the late 1950s, and over many years followed the same pattern. He studied boys in the fourth, fifth and sixth forms of London schools he describes as 'privileged', restricting the size of the group to no more than about 200 in any given year so that he could interview and recall each boy individually. Over time, however, relatively large numbers accumulated in most of his categories. After experimenting with a variety of tests, Hudson settled upon the two which form the basis of his work: a high-level test of reasoning ability (the AH5) and the Getzels and Jackson test known as the Uses of Objects, which simply asks respondents to list as many uses as they can think of for common objects such as a brick, a paper-clip or a barrel. Hudson (Ref.16) demonstrated that useful predictions of career choice could be obtained by considering biases in the boys' scores (rather than absolute scores), and argued that these biases reveal underlying cognitive styles. 'Convergent' thinkers (those who scored relatively better on the reasoning test) typically specialized in physical sciences or classics; 'divergent' thinkers (those who score better on the Uses of Objects) in history or modern languages.

Without Australian research that directly replicates these findings, it cannot be demonstrated conclusively that what applies to Hudson's convergent thinkers also applies to the Australian engineer. Nevertheless, the available evidence points strongly in this direction. Hudson found, for example, that the attitudes of convergers differed from those of divergers along three dimensions: authoritarianism, rigidity of attitude and social conformity. Convergers were more likely, for example, to approve of being obedient, of accepting expert advice and of being a good team member; and more likely to disapprove of artistic sensitivity and of being highly imaginative (Hudson (Ref.16)). These attitudes closely resemble those found to obtain among Australian engineering students (Anderson & Western (Ref.6)).

In one of his earliest papers, Hudson (Ref.18) stated his basic thesis that the origins of the abilities and interests which distinguish arts specialists from science specialists originate in childhood personality differences. In his later works, he elaborates upon this thesis using diverse sources of evidence. A first building block in his argument is the evidence that stereotypes of the professions are both widely held and cross-culturally consistent. Scientists, for example, are regularly rated as 'hard, cold and valuable', while artists are seen as 'soft, warm and exciting'. A second building block is the psychoanalytic notion of fixation: the idea that a person's frame of mind takes on enduring shape during one of three developmental stages: infancy, latency or adolescence (see Fig.1). It is not accidental, argues Hudson, that the image of the scientist first emerges during the latency stage (which occurs roughly between the ages of five and ten) since it reflects the primary concern of this stage: the righteous subjugation of impulse in the service of impersonal, objective skill. It is during this stage, too, that future physical scientists (a category in which Hudson includes engineers) show a marked interest in the structure of the material world, although their developmental patterns are less extreme than those of mathematicians, who are often child prodigies. By contrast, the stereotype of the artist does not appear until adolescence, and reflects the dominant concerns of that age: the conflict of intensely personal desires and sensitivities with the puritanical system of values established during latency.

Hudson emphasizes that he is not attempting to invent another simple dichotomy for the human race, but rather to characterize two extremes that account for 30% of the population range. He also devotes attention to those students who score equally well (or badly) on both types of test: the 'hybrid all-rounders'. Psychologists, he argues, fall within this group and their genesis is complex. As a child, the future psychologist adopts the objective
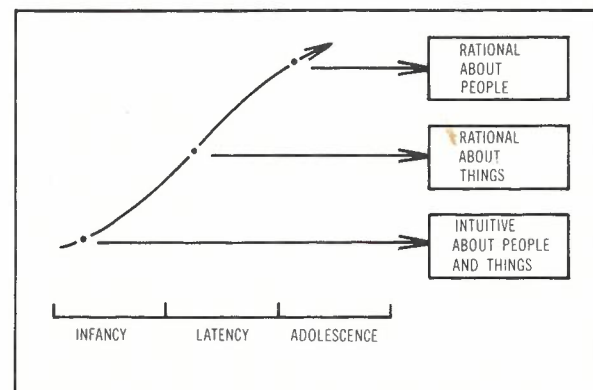

Fig.1 - The fixation hypothesis.

stance of the physical scientist, then, in late adolescence, attempts to apply scientific principles to human behaviour. This developmental shift, according to Hudson, explains why psychology is often a late career choice, and why many famous psychologists have come into the subject from a more orthodox form of science: medicine, biology, chemistry, even physics and engineering – but rarely, it seems, mathematics (Hudson (Ref.17)).

Within the framework of his study, Hudson has convincingly portrayed the psychodynamics of vocational choice. But his explanations become strained to the utmost when applied to vocational choice in the general population. It seems implausible to argue, for example, that girls are less likely to become fixated in latency than boys; or that the stereotype of the doctor or lawyer has intrinsically less appeal for the working-class child than for his middle-class counterpart. Yet the Australian Bureau of Census and Statistics figures show that only 3.8% of engineering students enrolled in 1978 were women (although women then constituted 39.9% of all Australian university students). Anderson and Western (Ref.7) also found that students from families where the parents have received higher education, and where the father either belongs to a profession or is a senior manager, are more likely to enter medicine or law than teaching or engineering.

Indeed, linking their attitudinal research with data such as these, Anderson and Western (Ref.7) claim that the differences in attitudes observed between the faculties are a product of the students social origins. Further, they suggest that these social origins can irrevocably affect one's professional performance. The 'presumably more limited experiences' of country children recruited into the teaching profession, for example, may unfit them for 'transmitting the culture of society to successive generations'; and they warn of increasing the difficulties in maintaining staff continuity in secondary schools if the balance of the sexes among teaching recruits continued to swing away from men (women then constituted 57% of teaching recruits).

Whereas Anderson and Western consider it necessary to discourage girls from entering teaching, McClelland (Ref.25) argues that the virtual absence of women from the physical sciences is a natural phenomenon. Observing that women have failed to flock into experimental physical science as opportunities for higher education for women have been more nearly equalized, he suggests that the reason is not social restriction, but a 'personality factor – women's lack of interest in physical science' (McClelland (Ref.25) p.144).

2.4 Resolution

That there are inequalities in the distribution of class and sex among faculties is undeniable; yet it does not necessarily follow that the inequalities are directly determined by properties intrinsic to either class or sex. Anderson and Western's claim that there is a causal link between social origins and attitudes is apparently based only on the correlation between social class and faculty membership and between faculty membership and attitudes: they offer no supporting evidence either from their own data (such as a demonstration that the correlation between social origins and attitudes also applies within faculties), or from other studies. Both sources, however, yield evidence that runs counter to their

claim. Table 1, for example, shows that the attitudes of teaching students differ significantly from those of engineering students, despite the similar class backgrounds of the two groups. The demonstration by Hudson (Ref.16) that a similar division of attitudes exists among English schoolboys attending privileged schools (which suggests that their class backgrounds may be more homogeneous than those of the Australian university students) also argues against any simple connection between social origins and attitudes.

International comparisons cast further doubt on the validity of Anderson and Western's suggestion that sex or social class represent reasonable criteria for assessing an individual's suitability for a given profession. The mobility of members of the working class into the professions and the extent to which occupational status is inherited vary considerably even between the industrialized nations. While it is difficult to make strict comparisons – not least because of differing rates of change in occupational structures – most of the general indices of occupational mobility that have been used would place Australia in the middle range of industrialized western nations (see, for example, Hazelrigg and Garnier, (Ref.14)).

Although it is difficult to apply the concept of class to communist countries, Parkin (Ref.23) points out that in such countries transitions between the lowest occupations and the highest commonly take place in a single generation. By contrast, professional occupations in western countries typically show a high inheritance rate. Turner (Ref.31) showed that in Australia the rate of inheritance of professional occupations was high: while 44.8% of the sons of university-trained professionals entered tertiary institutions (where they comprised 8% of the student body), only 4.4% of the sons of unskilled and semi-skilled workers did so (comprising 13% of the student body). Figures for eight European countries circa 1960 show a range from 5% (Italy and West Germany) to 25% (Great Britain and Norway) in the proportion of working-class students entering university (Parkin (Ref.23)).

Women's participation in the professions McClelland characterizes as 'masculine' also varies markedly between nations. Only five (0.8%) of the 631 engineering students who took part in Anderson and Western's studies of Australian university students were women, while figures presented in The Australian Engineer for March, 1969, showed that of the then 17,000 members of the Institute of Engineers (Australia), women accounted for only thirty-six, of whom twenty were migrants. These figures contrast sharply with figures supplied by the Association of Professional Engineers, Australia for women engineers in communist countries. In the USSR, 30% of the engineers were women (1959 figures) and in Poland 11% (1964 figures).

Given these disparities in the participation rate of both the working class and women in the professions, it becomes increasingly difficult to maintain that class or sex make one intrinsically unsuited to entering a specific profession. Nevertheless, society's expectations for a child are not independent of class and sex; and these expectations may filter the career-related information that the child receives and hence filter his or her career aspirations. A letter published in the New Scientist of 28 February 1980 suggests how such filtering might operate:

Reflections In A Crystal Ball

*I encourage my daughter aged six to look through
the New Scientist. I was surprised one day when
seeing diagrams about the Universe she said 'oh
they are only for boys'. When questioned about
this she told me that this was the view of her
friends at school.*

While the representativeness of such attitudes
is not easy to determine, where such attitudes do
exist they may discourage girls from expressing
the interests during the latency stage that,
according to Hudson, are central to the develop-
ment of the future physical scientist. It is at
least premature to conclude that intrinsic factors
alone account for the small numbers of women in
such courses as engineering.

The evidence thus shows that career choice has
been the subject of many transactions between the
individual and his social milieu long before his
enrolment in an engineering course. But it is with
the beginning of formal professional education
that the socialization of the engineer begins in
earnest.

3. CREATING CONSENSUS: THE ORIGINS OF THE OBVIOUS

The intellectual influences that enter into
the professional socialization of the engineer can
be identified fairly readily. Less apparent are
the effects of the socialization process on the
engineer's conception of reality.

3.1 The Intellectual Foundations

Engineering knowledge, as the sociologist
Holzner (Ref.15) points out, is structured by two
main considerations: the expected applications of
the knowledge, and the need to rapidly communicate
a body of information to the learner. The engin-
eering student, for example, gathers much of his
information from textbooks, whereas arts students
are often required to consult original sources.
The bulk of engineering knowledge is thus removed
even from the way in which new knowledge is ob-
tained in the physical sciences; yet many engin-
eering students and graduates are confident that
their methods represent the best - perhaps the
only - way of gaining knowledge in any sphere,
including the social and political. Anderson and
Western (Ref.8) found that engineering students
interviewed in the third and fourth years of their
courses expressed greater confidence in their own
ability to define the community's interests and
perceived less conflict between their own inter-
ests and those of the community than did third or
fourth year students in the other faculties.

Similar attitudes were evinced in interviews
designed to probe the attitudes of members of the
groups which participated in the National Tele-
communications Planning Branch Delphi studies
(Albertson & Cutler (Ref.4)). A Telecom engineer,
now in his forties and occupying a middle-manage-
ment position, elaborates:

*When I was doing engineering, or just subsequently,
I believed that the Government should be run by
engineers and scientists - the rational people who
could set the world on the right track, and keep
it on the right track with industry and productiv-
ity. What was needed was highly objective people -
we wouldn't have used the word objective, but
reasonable people who knew exactly what was needed
and could go about doing it.*

But as Mitroff and Turoff (Ref.24) point out,
engineering knowledge is based mainly on the phil-
osophies of Liebnitz and Locke; and these philos-
ophies, or inquiry systems, are best suited to
dealing with situations that are 'well-structured',
and where a strong consensus exists about the
nature of the problem. Nevertheless, examples of
over-generalization of such inquiry systems come
readily to hand. The Delphi technique itself is
based on a Lockean inquiry system, so that however
scrupulously the technique is applied, and however
technically expert the panel, it cannot guarantee
accurate answers to ill-structured problems (a
category that includes the majority of social and
political questions).

A great deal of the social research into car-
eer choice suffers from the same mismatch of prob-
lems and inquiry systems. The eminent American
psychologist Gordon Allport pointed out more than
twenty-five years ago that the feeling that only
the methods of the established sciences were fully
reputable accounted for the pre-eminence in psy-
chology of Lockean inquiry systems. For many
years, psychology thus exhibited a preference for
'externals rather than internals, for elements
rather than patterns, for geneticism, and for a
passive or reactive organism rather than for one
that is spontaneous and active' (Allport (Ref.5)
p.12). Ironically, the spectacular success of
Liebnitzian and Lockean inquiry systems in the
technological sphere exacerbated this trend and
almost certainly delayed finding the answers to
the riddle of scientific giftedness that were so
urgently sought.

In this light, it becomes less surprising that
it was Hudson, working outside the main paradigm
and on a small scale, who contributed most to our
understanding of vocational choice and career per-
formance. Nor is it accidental that he drew many
of his insights from psychoanalytic theory - the
only major psychological tradition to maintain a
central interest not in the way variables interact
within a large population but in 'what is Johnian
about John', to use Allport's phrase. These pre-
vailing beliefs about the nature of science also
help to explain Anderson and Western's use of a
large sample survey as a basis for recommendations
about such matters as future recruitment into the
professions. While sample surveys undoubtedly
have a place in psychology, it should not be for-
gotten that however well such research reflects
current conditions, 'is' bears no logical rela-
tionship to 'ought'.

3.2 Networks of Connection

There is evidence, too, that the implications
of the engineer's career choice do not stop with
his intellectual stance, but reach into the far-
thest corners of his being. For example, Hudson
and Jacot (Ref.20) found differences between arts
specialists and physical scientists even in the
bald biographical data presented in the British
Who's Who. Analysing the entries for eminent men
born during the period 1900 to 1925, they found
that, for example, physical scientists were less
likely than the arts specialists to remain single,
to marry late, to have childless marriages or to
divorce. Rates for eminent biologists were gener-
ally intermediate between the two (see Table 3).
Finer distinctions could also be drawn within the
physical sciences category. The researchers point
out, for example, that by removing the physicists
from the group (leaving mainly engineers and chem-
ists) the divorce rate, already low compared with

TABLE 3 – Marriage, Divorce and Fertility in the Arts and Sciences
(Percentages)

	Single	Childless	Marry late (35-plus)	Divorce
Arts (n=216)	14.8	16.2	13.4	4.6
Biological sciences (n=147)	2.0	6.1	9.5	12.2
Physical sciences (n=329*)	3.6	11.5	5.5	3.3

*This group includes 109 engineers who were either senior academics or Fellows of the Royal Society.

Note: In each column, the frequencies deviate from chance at the 5% level of confidence (or greater).

Source: Hudson & Jacot (Ref.20).

the arts specialists, was reduced from 3.6% to 1.7%

Hudson (Ref.17) relates these findings to his developmental thesis, arguing that a preference for things rather than people as a subject for study is linked with the social conservatism of the latency stage. Specialists in the arts, he suggests, may be more likely to transgress conventional boundaries, especially those that define the masculine sex role. They are more likely to acknowledge that they are to some degree effeminate or homosexual, and less likely to marry simply because it is conventional to do so.

Research into patterns of sleeping and dreaming also appears to be an improbable source of evidence about the effects of professional socialization. Nevertheless, Hudson (Ref.17) reports that in studies of university undergraduates, convergent thinkers (such as physicists and engineers) differed from divergent thinkers (such as historians and linguists) in the way they experience and process their dreams. Rapid eye movements (REMs), which indicate that a dream is in progress, were found to be more intense among convergers than among divergers; but upon being awakened during REM activity, convergers on as many as half the occasions recalled either nothing at all, or only that a dream had been in progress. Divergers, on the other hand, almost invariably recalled the contents of their dreams. When the dreamers were awakened in the intervals between REM sleep, however, the position changed considerably, with convergers having slightly better recall than divergers. This distinction is important, Hudson argues, because periods of REM sleep are associated with the primary visual experience of a dream, while the intervening periods are devoted to 'secondary cognitive elaboration' – connecting the images into sensible-seeming patterns. Thus, while convergers often fail to recall the vivid visual images of their dreams, they recall perfectly well the more rational thoughts that follow.

These unexpectedly diverse ramifications of cognitive style provide clues to the deep-seated effects of the engineer's socialization. They suggest, for example, that his interpretations of reality follow so closely on the heels of his perceptions that in effect the two are fused into a single experience which assumes the status of the merely obvious - despite the complex philosophies,

goals and values that have contributed to its creation.

4. THE DELPHI REVISITED

The concept of a socialized reality clarifies many aspects of the National Telecommunications Planning Branch's second Delphi study. The concordant readings of the future observed among the engineers are not merely the product of similar personalities gathered together, but are part of a wider group consensus about the nature of reality. This consensus also helps explain the air of simple factuality with which even the more extreme social forecasts were often presented.

For example, in support of his forecast that women would never occupy 25% of jobs carrying the annual salary equivalent of $10,000, one engineer commented:

The average woman will never be as smart nor as capable as the average man. Add to this their role as a wife and mother, and it becomes obvious that they could never compete to this extent.

It is hardly surprising, in view of many of the attitudes already discussed in this paper, that many of the engineers who participated in the Delphi study objected to engaging in debate with 'technologically uneducated housewives'. And, indeed, many of the women were inclined to accept this assessment of their abilities. In the second round of the study, while the engineers largely consolidated the opinions they had offered in the first round (for example, the NEVER vote on the item concerning women in the work force increased from 56% to 64%), many of the women changed their opinions to accord with those of the engineers. This behaviour, together with the essential pessimism on both the 'essence' and 'influence' dimensions of their image of the future, suggests that as power is incorporated into the outlook of the engineers, so powerlessness is incorporated into the outlook of the women. The comments of a housewife interviewed by Albertson and Cutler (Ref.4.) suggest how this powerlessness is experienced:

I wouldn't think of myself as influencing anybody else. I just enjoy my life, and they're free to enjoy their lives, as far as I'm concerned. I mean, if people want to take over the moon, well

and good, that's their business. I suppose if I saw any real evil intent or possibility, then I might jump up and down and do something about it. But my life is busy enough with people.

Given the aggressively masculine image of the physical sciences, it seems almost a natural consequence that women's attitudes towards the future should represent the polar opposite of the engineers', thus defining the domain within which the engineers' power is negotiated. The press report shown as Exhibit 1 surely derives much of its impact from the surprised response of a senior member of the Australian scientific community who witnessed the violation of this fundamental social dynamic.

EXHIBIT 1

SHE'S NO GURU : MONASH DEAN

'Opening the UN Conference on Science and Technology here yesterday, Dr H.C. (Nugget) Coombes introduced Judith Wright as 'Australia's foremost poet'. After listening to her speech, the dean of science at Monash University, Professor John Swan, said she was a disaster as a guru.

Delegates, described as our top scientists, academics and industry representatives gaped as she delivered the most comprehensive attack on the direction of technology they could remember.

Miss Wright said technological determinism - the acceptance that technology would be used simply because it was possible - was an abdication of intellectual and social responsibility.

Shortly after Miss Wright sat down, Professor Swan said that he respected her as a poet, but as a guru she was a disaster.

He angrily challenged her to explain why she was wearing a pseudo-suede jacket and a synthetic shirt - both products of technology.

Miss Wright is reported as saying she was amazed at the emotional level of the outburst'.

(Extract from the Melbourne 'Age', 21 April 1979)

Loye (Ref.21), in discussing the potential implications of his finding that forecasting is linked with personality traits, expresses concern that when there is an imbalance of these traits among a Delphi panel the resulting forecasts will be inaccurate. But given the more serious questions about the validity of the classic Delphi method arising from the analysis by Mitroff and Turoff (Ref.24), such a possibility assumes minor importance. Nevertheless, the demonstration that engineers share a view of the world that is untypical of the community as a whole has potential ramifications that reach far beyond the accuracy of their forecasts.

5. BEYOND PROPHECY AND CONTROL

In his seminal work The Image, the economist Kenneth Boulding suggests that the content of the image of the future might be less important than its quality of optimism or pessimism, certainty or uncertainty, breadth or narrowness. 'The person or the nation that has a date with destiny goes somewhere, though not necessarily to the address on

the label', he argues (Boulding (Ref.10) p.125). Other futures theorists, however, are less sanguine. Russell Ackoff (Ref.1), for example, argues that an organization's image of the future affects its planning mode, and hence its chances of survival in organizational environments that are increasingly characterized by high levels of uncertainty, complexity and change - the kind of environment systems theorists call a 'turbulent field'.

In turbulent fields, according to Ackoff, planning modes based on predicting and controlling the future will not only be inadequate, but are likely to create further instabilities. Under such conditions, he argues, the key to survival is adaptability, which entails increasing the organization's response repertoire to match the increases in variety emanating from the environment. In part, this requisite variety can be achieved by means of re-organizing the workplace, using new organizational forms such as semi-autonomous workgroups. Ackoff and his colleagues (Ackoff & Emery, (Ref.2); Trist (Ref.30)) also emphasize the importance of individual resilience as a resource in organizational survival in turbulent fields.

At base, acceptance of the systems theorists' arguments depends upon the relative persuasiveness of two alternative organizational images. The image that has prevailed since turn-of-the century Taylorism is that of a machine which is largely independent of its environment. The organization's tasks are reduced to their smallest components, and the members are expected to perform them in an essentially mechanical fashion. Responsibility for organizational planning lies entirely with management. The central image of systems theory, on the other hand, is that of a biological organism and its ecology; it emphasizes the whole rather than the parts, and hence points to the resources for survival inherent in the organization's entire membership.

If the systems image is accepted as an appropriate representation of the problem, it follows that the assumptions acquired during socialization into the engineering profession are likely to become increasingly maladaptive in the future. At the corporate level, their essential optimism and belief in man's capacity to influence the future make it likely that the preferred planning mode will be deterministic, rather than adaptive. And, at the level of the individual, the unselfconscious incorporation of these assumptions into the engineer's experience of reality suggests that they will prove inflexible in the face of uncertainty and change.

6. HUMAN RESOURCES AS A KEY TO ORGANIZATIONAL SURVIVAL

Most technology-based organizations are keenly aware of the need for technological advance if they are to survive in the face of external competition. The present paper, however, highlights a threat to organizational survival that is rarely recognized: the probable inflexibility of the assumptive sets of a large and influential segment of the organization's membership. Remedies for this state of affairs are far from simple. As a first step, it is clearly desirable to encourage among engineers a livelier awareness of the assumptions inherent in their knowledge base, and the kinds of problems to which this knowledge is best suited. But to create such awareness represents a major challenge to educators and those responsible

for the continuing education and in-service training of engineers, since these assumptions have become so much a part of the engineer's personality that unless the process of re-assessment and critical review is undertaken cautiously, there is a danger that personality disorganization will result, and that the present positive images of the future will give way to chaos and despair. The task of developing these human resources is thus a formidable one; but if systems theorists are correct in their analysis of the changing organizational environment, it is one that cannot be shirked if technology-based organizations such as Telecom Australia are to survive the environmental turbulence of the late twentieth century.

7. REFERENCES

1. Ackoff, R.L., "Redesigning the Future", Wiley, New York, 1974.

2. Ackoff, R.L. and Emery, F., "On Purposeful Systems", Aldine-Atherton, Chicago, 1972.

3. Albertson, L. and Cutler, T., "Delphi and the Image of the Future", Futures, Vol.8, No.5, October 1976, pp.397-404.

4. Albertson, L. and Cutler, T., "The Human Faces of Technology", Paper presented to the Telepost Engineers Group of the Professional Officers Association, May 1979.

5. Allport, G.W., "Becoming: Towards a Psychology of Personality", Yale University Press, New Haven, 1955.

6. Anderson, D.S. and Western, J.S., "Attitudes of Students Entering Professional Faculties", Australian Journal of Psychology, Vol.21, 1969, pp.291-299.

7. Anderson, D.S. and Western, J.S., "Social Profiles of Students in Four Professions", Quarterly Review of Australian Education, Vol.4, No.3, 1970, pp.3-28.

8. Anderson, D.S. and Western, J.S., "Professional Socialization", In: Hunt, F.J. (ed), "Socialization in Australia", Angus and Robertson, Sydney, 1972, pp.288-306.

9. Barling, C., "Technological Change: Impacts of New Telecommunications Technologies on the Information Society", Telecom Australia Research Laboratories, unpublished paper, 1980.

10. Boulding, K., "The Image", Ann Arbour Paperbacks, Michigan, 1961.

11. Dalkey, N. and Helmer, O., "An Experimental Application of the Delphi Method to the Use of Experts", Management Science, Vol.3, 1963, pp.458-67.

12. Getzels, J.W. and Jackson, P.W., "Family Environment and Cognitive Style", American Sociological Review, Vol.26, 1961, pp.351-9.

13. Goleman, D., "1,526 Little Geniuses and How They Grew", Psychology Today, February 1980, pp.28-53.

14. Hazelrigg, L.E. and Garnier, M.E., "Occupational Mobility in Industrial Societies: A Comparative Analysis of Differential Access to Occupational Ranks in Seventeen Countries", American Sociological Review, Vol.41, June 1976, pp.498-511.

15. Holzner, B., "Reality Construction in Society", Schenkman; Cambridge, Massachusetts, (Revised Edition), 1972.

16. Hudson, L., "Contrary Imaginations", Penguin, Harmondsworth, 1974.

17. Hudson, L., "Human Beings", Triad/Paladin, St. Albans, 1978.

18. Hudson, L., "Personality and Scientific Aptitude", Nature, Vol.198, 1963, pp.914-916.

19. Hudson, L., "Selection and the Problem of Conformity", In: Meade, J.E. and Parkes, A.S., "Genetic and Environmental Factors in Human Ability", Oliver and Boyd, London, 1966, pp.90-94.

20. Hudson, L. and Jacot, B., "Marriage and Fertility in Academic Life", Nature, Vol.229, 1971, pp.531-532.

21. Loye, D., "Personality and Prediction", Technological Forecasting and Social Change, Vol, 16, 1980, pp.93-104.

22. Luten, D.B., "Ecological Optimism in the Social Sciences", American Behavioral Scientist, Vol.24, No.1, 1980, pp.125-151.

23. Parkin, F., "Class Inequality and Political Order", Paladin, London, 1972.

24. Mitroff, I.I. and Turoff, M., "The Whys Behind the Hows", IEEE Spectrum, Vol.10, 1973, pp.62-71.

25. McClelland, D., "On the Dynamics of Creative Physical Scientists", In: H.E. Gruber et al. (eds), "Contemporary Approaches to Creative Thinking", Atherton, 1962, pp.141-174.

26. MacKinnon, D.W., "The Nature and Nurture of Creative Talent", American Psychologist, Vol. 17, 1962, p.834.

27. National Telecommunications Planning Branch. Delphi Forecasting Study Round 2, Telecom Australia, 1975.

28. Roe, A.A., "A Psychological Study of Eminent Psychologists and Anthropologists and a Comparison with Biological and Physical Scientists", Psychological Monographs, Vol.67, No.352, 1953.

29. Schmidt, R.W., Lamm, H. and Trommsdorff, G., "Social Class and Sex as Determinants of Future Orientation (Time Perspective) in Adults", European Journal of Social Psychology, Vol.8, 1978, pp.71-90.

30. Trist, E., "The Environment and System-Response Capability", Futures, April 1980, pp.113-127.

31. Turner, M.L., "Tertiary Education and Socio-economic Class", In: "Report of the Committee on the Future of Tertiary Education", Canberra Vol.1, (Appendix), 1965, pp.43-4.

Reflections In A Crystal Ball

BIOGRAPHY

LESLEY ALBERTSON was a member of Telecom Australia's interdisciplinary 'Telecom 2000' team, and is currently Senior Psychologist with the Telecom Australia Research Laboratories in Clayton, Victoria.

Bayesian Analysis Of Teletraffic Measurements And Simulation Results

R.E. WARFIELD
Telecom Australia Research Laboratories

The purpose of this paper is twofold: to discuss the application of some well known results from the field of Bayesian Statistical Analysis to an estimation problem in Teletraffic Engineering, and to extend those results to allow the estimation of loss factors. For a general traffic process (modelled using birth and death coefficients) offered to a general loss system (modelled using loss factors), a finite dimensional statistic which is sufficient for all unknown parameters is given. The statistic can be computed recursively from real-time observations of group occupancy and unsuccessful call attempts. The resulting estimation procedure is easily applied to the analysis of simulation results, and could also be implemented readily on currently available traffic measuring devices using mini- or microcomputers. Simplified estimation procedures result for various special cases of the general model.

1. INTRODUCTION

1.1 Description of Teletraffic Measurement and Simulation

Teletraffic measurement involves the two phases of modelling and identification. The model is in three parts, namely: a model of the generation of call arrivals, a model of call service times (or, equivalently, call departures), and a model of the system by which calls access the devices that carry all or part of the offered traffic. Identification is carried out by using the results of observations to make statistical inferences about the unknown parameters of the model.

The difference between measurement and simulation, from the point of view of statistical analysis, lies in the classification of parameters into those which are known and those which are to be estimated. For example, a simulation study may be used to determine the properties of a complex switching system - in this case the parameters of the traffic process are considered to be known, and it is desired to estimate the properties of the switch. On the other hand, if measurements are being made of live traffic in an exchange, the parameters of the traffic process (carried or offered) would usually be estimated, and the parameters of the switch may also be estimated from the same data. The analysis of measurement data and simulation results is therefore treated as a whole; in any application only a subset of the analytical results given will be required.

The model of the system, and in particular its unknown parameters, determine what observations ought to be made and also have a bearing on the way the data should be processed. The appropriate degree of complexity of a model is influenced by both the ultimate use to which the model will be put and the complexity and extent of the observations which would be needed to identify the model. For example, it would usually not be practical to use a model in which each of a large number of traffic sources was assigned one or more unknown parameters. The identification of such a model could prove onerous, and, once the unknown parameters were estimated, the applicability of the model to other cases could be of doubtful validity.

Call arrivals and departures may be modelled using the concept of renewal processes, or by using birth and death coefficients. In the former case, the time intervals between successive arrivals and the service times of calls are considered as two separate sequences of independent identically distributed random variables. If the latter alternative is used, namely birth and death coefficients, then the concept of the state of the system is needed. For the present purposes, the state of the system at any instant may be considered as the number of calls in progress. The birth and death coefficients define the probabilities that the state of the system will be incremented or decremented in an infinitesimal interval of time from t to $t+dt$. In general, birth and death coefficients are functions of the state of the system.

The service system to which the traffic is offered may be modelled in various ways. In the following, results are given for loss systems which can be modelled using general loss factors. The loss factors of a system are defined as the probabilities of a call being rejected conditional on the state of the system at the instant of the call arrival. The general results developed below are also applied to the particular case of a geometric group - that is, a loss factor system in which the loss factors form a geometric sequence as a function of the state.

Observations of teletraffic processes can take several forms including: the observation of call arrivals and call departures; the observation of the number of devices occupied as a function of time; the observation of the digits dialled, thus specifying the intended destination of the call.

Bayesian Analysis Of Teletraffic Measurement

Two salient features of a measurement are of interest at this point, namely:

(i) The number of variables to be observed - influenced mainly by whether information must be collected from each individual device or from a group of individuals as a whole,

(ii) The dimensionality of the data stored - influenced by the model of the system and the statistical inferences to be made.

Economic, technological and theoretical considerations all have a bearing, directly or indirectly, on the type of measurement that will be appropriate in any given situation.

Various types of statistical inferences may be made from collected data, depending on the ultimate application. Point or interval estimation is the most commonly required type of inference; hypothesis testing and decision making may also be appropriate in certain cases.

1.2 Problem Statement

Given a model of a teletraffic process and the service system or group of devices to which the traffic is offered, it is desired to estimate unknown model parameters from observations. Moreover, it is desired to estimate the unknown parameters using all available information in the observations and using a fixed, finite amount of data storage space. The above requirements imply that a finite dimensional, recursively computable statistic that is sufficient for all unknown parameters must be constructed. The following problem is considered:

(i) Offered traffic - General birth and death process.

(ii) Group of devices - Loss system with lost calls cleared and general loss factors (including geometric group as a special case).

(iii) Observations - Group occupancy and call attempts are observed.

Note that neither individual calls nor individual circuits are considered to be available for observation. If either were considered available, the observer would be able to treat the individual call holding times as a set of independent, identically distributed random variables. The theory for analysing such observations is well known, and is therefore not considered here.

2. LITERATURE SURVEY

The literature dealing with general problems of statistical inference for birth and death processes (more generally, Markov chains), and, in particular, with the estimation of the probability of loss (congestion) is surveyed below.

Benes (Ref.1) derives a sufficient set of statistics for a simplified system which involves an infinite number of devices with call arrivals modelled as a Poisson process and service times modelled as independent identically distributed random variables with negative exponential distribution (note that this traffic process is a special case in that it can be described as either a renewal process or a birth and death process). With arrival rate and mean holding time unknown, and continuous observation of the process over a finite interval, he demonstrates that the following set of statistics is sufficient for the unknown parameters: number of calls in progress at the start of the interval (initial state); the number of calls arriving during the period of observation; the number of calls terminated during the period, and the average number of calls existing throughout the period.

Billingsley (Ref.2) presents an expository survey of the mathematical aspects of statistical inference as it applies to finite Markov chains. His survey, which has been referred to by many succeeding papers, concentrates on the large sample theory of inference. Billingsley uses the concept of transition count, namely, the matrix with (i,j)'th element equal to the number of transitions from state i to state j in a sample sequence of the Markov chain. He observes that the initial state and the transition count together form a sufficient statistic for the unknown state transition probabilities, and goes on to derive the sampling distribution for this statistic.

Cox (Ref.3) surveys the field of estimation methods applied to queues and again the results are based on likelihood functions similar to those of Billingsley. Cox specifically comments on the fact that there are relatively extremely few papers on problems of statistical estimation in this field compared with the number on analysis.

All of the above studies use the classical approach of maximum likelihood estimation, and the results are essentially applicable to large samples. Reynolds (Ref.4) introduces a Bayesian approach and compares the results obtained with the classical ones. Whereas Billingsley (Ref.2) and others considered only the observation of a sequence of states, Reynolds includes also the times of each transition. Thus his sufficient statistic is:

$$(t_r, m_r, n_r;   0 \le r \le R)$$

where

r is the state of the system

R is the maximum possible value of r

t_r is the time spent in the r'th state

m_r is the number of arrivals while in state r

n_r is the number of departures from state r

Reynolds also assumes that the initial state is known.

For cases where the birth and death coefficients are given by, respectively,

$$\lambda_r = f(r)\lambda \qquad\qquad (1)$$

and

$$\mu_r = g(r)\mu \qquad\qquad (2)$$

with $f(r)$ and $g(r)$ known, and λ and μ to be estimated, Reynolds demonstrates that a Gamma

distribution is appropriate for the prior distribution and derives sufficient statistics and estimator for λ and μ. Reynolds also shows that his results can be used to derive those of, for example, Benes (Ref.1) as a special case, thus showing the link between the Bayesian and classical approaches.

Turning now to the specific problem of estimating the probability of loss in a teletraffic system, Kosten, Manning and Garwood (Ref.5) derive, for the M/M/C loss system with full availability, expressions for the first few moments of the distributions of the number of lost calls and the time congestion observed during a fixed period of time. The expressions they derive are rather complex, and, as stated in their paper, are directly applicable only to full availability systems for which the probability of loss can be derived analytically from the parameters of the offered traffic.

Descloux (Ref.6) gives an expression for the variance of the proportion of blocked calls and the time congestion (scanned or measured continuously) for the same system as that studied by Kosten, Manning and Garwood (Ref.5). The basic formula he uses is (slightly rearranged):

$$\text{Var}\left[\frac{X}{L}\right] = \left[\frac{\text{Var}(X)}{E^2(X)} + \frac{\text{Var}(L)}{E^2(L)} - \frac{2\,\text{Cov}(X,L)}{E(X)\,E(L)}\right]\frac{E^2(X)}{E^2(L)}$$

$$(3)$$

where X is the number of calls blocked and L is the number of calls offered.

Using this same basic formula, Kuczura and Neal (Ref.7) extend the analysis to loss systems with renewal input (GI/M/C) still assuming full availability and a fixed time period of observation. Olsson (Ref.8) extends the analysis to general birth and death processes, giving results for the variance of the number of lost calls, call congestion, and time congestion (scanned and continuous measurement).

Songhurst (Ref.9) considers birth and death processes with negative exponentially distributed service times, but departs from previous work by assuming that observations are made only at the instants of call arrivals. Instead of considering a fixed observation period, he considers a fixed number of call arrivals. He derives the asymptotic variance of a general deterministic function of the state of the system. The examples he gives include the estimation of the probability of loss for the M/M/C system, and the probability of delay, mean delay, delay distribution, and queue length for the M/M/C delay system. In general, his results apply to birth and death processes in loss or delay systems with full availability. Songhurst states that his results might be able to be extended to the case of loss factor models of limited availability systems, but that the results would be expected to be approximate.

The papers above, on the topic of the estimation of the probability of loss or delay, deal with the topic from the point of view of experiment design, and the following limitations apply to them:

(i)   Generally, the formulae given are complex and assume detailed knowledge of the traffic process,

(ii) All the formulae derived apply only to full availability systems with negative exponentially distributed service times. Most involve some degree of approximation, even for the cases for which they were derived.

The problem of the analysis of experimental results, as opposed to experiment design, allows the properties of teletraffic systems to be exploited. Consider the observation of a total of L offered calls divided into n batches of N calls each. If the number and proportion of blocked calls for the i'th batch are denoted, respectively,

x_i is the number of blocked calls

and

b_i is the proportion of blocked calls to call attempts

then, by definition

$$b_i = x_i/N \qquad\qquad (4)$$

If the n values of b are considered as n independent Normal random variables, each with variance σ^2, it is possible to estimate the variance of observed congestion using standard techniques, namely,

$$s_b^2 = \frac{1}{n-1}\sum_{i=1}^{n}(b_i - \bar{b})^2 \qquad\qquad (5)$$

where

$$\bar{b} = \frac{1}{n}\sum_{i=1}^{n} b_i \qquad\qquad (6)$$

By taking advantage of certain properties of teletraffic processes it is possible to improve the accuracy of estimation of congestion, as noted by Rubas (Ref.10), there is a positive correlation between the sample values of the mean offered traffic and the congestion in the individual batches; the variation in the observed congestion is partly due to the variation of offered traffic from one batch to the next. Kümmerle (Ref.11) develops a formula, based on regression analysis, for calculating the confidence interval for congestion, taking into account the correlation between offered traffic and congestion. He reports a typical reduction in the size of the confidence interval of about 30%.

Rubas and Warfield (Ref.12) extend Kümmerle's technique by the use of multivariate regression analysis, using values of both the sample mean and the sample variance of the offered traffic for each batch. They also introduce a technique of re-

Bayesian Analysis Of Teletraffic Measurement

cursive least squares analysis which, if applied on-line, allows the length (and hence cost) of the measurement or simulation to be determined by the actual accuracy obtained. They give practical guidelines for the design of the measurement so as to maximise the accuracy of estimation while preserving the validity of the assumptions on which the regression analysis depends. They also derive an empirical formula for the accuracy (confidence interval width) obtainable using this technique, and show, empirically, that the use of multivariate regression analysis yields an additional improvement in estimation accuracy, especially for the case of rough offered traffic (variance greater than mean).

The general approach of using the observations to compute both estimators of the unknown parameters and the accuracy of those estimators is taken even further by the use of Bayesian methods. In the following section, a method for calculating the conditional probability density function of the unknown parameters will be described. It will be shown that the method uses all the relevant information available in the observations, yet can be implemented practically using a finite amount of computer storage.

3. SOLUTION USING BAYESIAN METHOD

3.1 Notation

In the analysis that follows, it is necessary to distinguish between sequences of vectors (which are recursively computed), and the individual components of those vectors. In order to avoid double subscript notation, which would wrongly imply that the sequences of recursively computed vectors should be treated as matrices, the following abbreviated notation is used. Every vector considered has one component for each possible state of the system from 0 to R, therefore the variable r, which represents the state, is used to index individual components of the vectors. The variable k is reserved to index variables in sequence. Thus s_r denotes the r'th component of the vector s, while s_k denotes the entire vector s at the k'th stage.

3.2 System Model

The offered traffic is assumed to be a general birth and death process with birth coefficients and death coefficients respectively:

$$a = (a_0, a_1, \ldots, a_r, \ldots, a_R)^T \qquad (7)$$

$$d = (d_0, d_1, \ldots, d_r, \ldots, d_R)^T \qquad (8)$$

The traffic is offered to a loss factor system with loss factors:

$$\gamma = (\gamma_0, \gamma_1, \ldots, \gamma_r, \ldots, \gamma_R)^T \qquad (9)$$

Furthermore, it is assumed that a, d, and γ are random variables with known prior probability density function denoted by $f(a,d,\gamma)$.

Every successful call attempt, blocked attempt, and departure is observed. The state, r, of the system after each event, and the time, t, since the occurrence of the previous event are measured.

3.3 Analysis

It is desired to compute the conditional probability density function,

$$f(a,d,\gamma \mid r_1^k, t_1^k)$$

where

r_k is the state of the system after the k'th event (call attempt or departure),

t_k is the time from the $(k-1)$'th event to the k'th event,

$$r_1^k = (r_1, r_2, \ldots, r_k), \qquad (10)$$

$$t_1^k = (t_1, t_2, \ldots, t_k), \qquad (11)$$

with the constraint that the amount of data storage required must be a fixed, finite amount, regardless of how large k becomes. It will also be assumed that the initial state r_0 is known.

A recursive solution is obtained as follows:

$$f(a,d,\gamma \mid r_1^{k+1}, t_1^{k+1})$$

$$= \frac{f(r_{k+1}, t_{k+1} \mid a,d,\gamma, r_1^k, t_1^k) \; f(a,d,\gamma \mid r_1^k, t_1^k)}{f(r_{k+1}, t_{k+1} \mid r_1^k, t_1^k)} \qquad (12)$$

The variable x_k is defined by

$$x_k = r_k - r_{k-1} \qquad (13)$$

Note that x_k is -1, 0, or +1 for a departure, blocked attempt, or successful attempt respectively.

Now

$$f(r_{k+1}, t_{k+1} \mid a,d,\gamma, r_1^k, t_1^k)$$

$$= f(r_{k+1}|a,d,\gamma,r_1^k,t_1^{k+1})\ f(t_{k+1}|a,d,\gamma,r_1^k,t_1^k)$$

$$(14)$$

$$= f(x_{k+i}|a,d,\gamma,r_k)\ f(t_{k+1}|a,d,\gamma,r_k) \qquad (15)$$

Also

$$f(x_{k+1}|a,d,\gamma,r_k) = q(r_k,x_{k+1}) \qquad (16)$$

where the function $q(r_k,x_{k+1})$ is given by

$$q(r,x) = \begin{cases} \dfrac{d_r}{a_r + d_r} & \text{for } x = -1 \\[3mm] \dfrac{a_r}{a_r + d_r}\,\gamma_r & \text{for } x = 0 \\[3mm] \dfrac{a_r}{a_r + d_r}\,(1 - \gamma_r) & \text{for } x = +1 \end{cases}$$

$$(17)$$

Also

$$f(t_{k+1}|a,d,\gamma,r_k)$$

$$= (a_{r_k} + d_{r_k})\ \exp(-t_{k+1}(a_{r_k} + d_{r_k})) \qquad (18)$$

Substituting the above results back into equation (12) yields a recurrence relation for the conditional probability density function of (a,d,γ),

$$f(a,d,\gamma|r_1^{k+1},t_1^{k+1}) = f(a,d,\gamma|r_1^k,t_1^k)$$

$$\dfrac{q(r_k,x_{k+1})\ (a_{r_k} + d_{r_k})\ \exp(-t_{k+1}(a_{r_k} + d_{r_k}))}{f(t_{k+1},r_{k+1}|r_1^k,t_1^k)}$$

$$(19)$$

To aid in computing the probability density functions, a sequence of functions $p_k(a,d,\gamma)$ is defined by:

$$p_0(a,d,\gamma) = f(a,d,\gamma) \qquad (20)$$

that is, p_0 is set equal to the prior density, and

$$p_{k+1}(a,d,\gamma) = p_k(a,d,\gamma)\ q(r_k,x_{k+1})\ (a_{r_k} + d_{r_k})$$

$$\cdot\ \exp(-t_{k+1}(a_{r_k} + d_{r_k})) \qquad (21)$$

Comparing the definition of the sequence of functions p_k with the recurrence relation for the conditional probability density function of the unknown parameters, it can be seen that

$$p_k(a,d,\gamma) = f(a,d,\gamma|r_1^k,t_1^k)\ \cdot\ c \qquad (22)$$

where c is a scaling factor that does not depend on (a,d,γ). Hence the probability density function, f, can be computed by normalising the function p, that is,

$$f(a,d,\gamma|r_1^k,t_1^k) = \frac{p_k(a,d,\gamma)}{\displaystyle\int\ldots\int p_k(a,d,\gamma)\ d(a,d,\gamma)} \qquad (23)$$

A finite dimensional, recursively computable statistic which is sufficient for (a,d,γ) is formed by the statistics

$$(r_0, r_k, s_k, u_k, v_k)$$

where r_0 and r_k are the initial and final states, as previously defined, and s_k, u_k, and v_k are $R+1$ dimensional vectors with r'th components defined by:

s_r is the total time spent in state r,

u_r is the total number of unsuccessful attempts while in state r,

v_r is the total number of successful attempts while in state r,

with all totals computed from stage 1 to stage k inclusive.

The statistic described above is of fixed, finite dimension, and is recursively computable, as is shown formally by the following. The $R+1$ dimensional vectors s_k', u_k', and v_k' are defined to have all components equal to zero, except for their respective (r_{k-1})'th components which are given by:

the (r_{k-1})'th component

of s_k' is equal to t_k;

of u_k' is 1 if x_k is zero (unsuccessful attempt), and zero otherwise;

of v_k' is 1 if x_k is 1 (successful attempt), and zero otherwise.

Hence the vectors s , u , and v are computed recursively from

$$s_k = s_{k-1} + s_k'$$

$$u_k = u_{k-1} + u_k'$$

$$v_k = v_{k-1} + v_k' \qquad (24)$$

The $R+1$ dimensional vector w_k is defined to have r'th component equal to the total number of departures while in state r over the interval from 1 to k inclusive. At any stage k , the r'th component of w can be computed from the $(r-1)$'th component of v and the initial and final states by,

$$w_r = \begin{cases} 0 & \text{for } r = 0 \\ v_{r-1} + \varepsilon(r_0, r_k, r) & \text{for } r = 1, 2, \ldots, R \end{cases} \qquad (25)$$

where

$$\varepsilon(r_0, r_k, r) = \begin{cases} -1 & \text{if } r_0 < r \leq r_k \\ +1 & \text{if } r_k < r \leq r_0 \\ 0 & \text{otherwise} \end{cases} \qquad (26)$$

From the definition of the sequence of functions $p_k(a,d,\gamma)$, at any stage k the components of s_k , u_k , v_k , and w_k can be used to compute the function p using the following equation (from which the subscript k has been dropped for convenience),

$$p(a,d,\gamma) = \prod_{r=0}^{R} \{(1-\gamma_r)^{v_r} (\gamma_r)^{u_r}$$

$$\cdot a_r^{(u_r + v_r)} d_r^{(w_r)}$$

$$\cdot \exp(-s_r(a_r + d_r))\} \qquad (27)$$

Therefore $f(a,d,\gamma | r_1^k, t_1^k)$ is a function of the statistic given above, which demonstrates the sufficiency of that statistic for the unknown parameters.

The practical implications of the results above are as follows. For any birth and death traffic process and any loss factor system, it is sufficient to monitor continuously, in real time, just two quantities for each group of circuits: the occupancy of the group, and the number of unsuccessful call attempts that have been offered to the group (successful call attempts are inferred from changes in occupancy). From these two measurements, and knowledge of the real time as the monitoring proceeds, the sufficient statistic for the unknown parameters can be computed recursively. Storage is required for two $R+1$ dimensional integer vectors, u and v , one $R+1$ dimensional real vector, s , plus two integers for the initial and final state.

At the completion of the measurement, or at any intermediate point, the conditional probability density function of the unknown parameters can be computed. Of course, any form of statistical inference can then be carried out. The form of the natural conjugate prior distribution for a, d and γ is determined from the form of the function $p(a,d,\gamma)$. As discussed by Reynolds (Ref.4), the natural conjugate prior for a and d is the Gamma distribution with a and d independent. By inspection of the formula for f , the natural conjugate prior for γ is seen to be an independent multivariate Beta distribution.

3.4 Special Case

By way of illustration, the special case of pure chance traffic with negative exponentially distributed service times offered to a geometric group is considered. For this case the components of the parameter vectors a, d, and γ are given by

$$a_r = \alpha \qquad (28)$$

$$d_r = r\lambda \qquad (29)$$

$$\gamma_r = \beta^{(R-r)} \qquad (30)$$

where α, λ, and β are unknown parameters. Hence the function p is written as a function of these three scalar parameters, and is computed from the components of s, u, v, and w using the following equation which applies at any stage k :

$$p(\alpha,\beta,\lambda) = \prod_{r=0}^{R} \{(1-\beta^{R-r})^{v_r} (\beta^{R-r})^{u_r}$$

$$\cdot \ \alpha^{(u_r + v_r)} (r\lambda)^{w_r}$$

$$\cdot \ \exp(-s_r(\alpha + r\lambda))\} \tag{31}$$

The MAP (maximum a posteriori probability density) estimators of the unknown parameters are found by maximising the function p, or equivalently its logarithm:

$$\log(p(\alpha,\beta,\lambda)) = \sum_{r=0}^{R} \{v_r \log(1-\beta^{R-r}) + u_r(R-r)\log(\beta)$$

$$+ (u_r + v_r)\log(\alpha) + w_r \log(r\lambda) - s_r(\alpha + r\lambda)\}$$

$$\tag{32}$$

Differentiating with respect to α and λ and equating the derivatives to zero yields the results of Reynolds (Ref.4) which agree with the classical estimators, namely:

$$\alpha' = \frac{\displaystyle\sum_{r=0}^{R}(u_r + v_r)}{\displaystyle\sum_{r=0}^{R} s_r} \tag{33}$$

$$= \frac{\text{Number of calls offered}}{\text{Total time}} \tag{34}$$

$$\lambda' = \frac{\displaystyle\sum_{r=0}^{R} w_r}{\displaystyle\sum_{r=0}^{R} r s_r} \tag{35}$$

$$= \frac{\text{Number of departures}}{\text{Traffic volume}} \tag{36}$$

To find the MAP estimator of β, the expression in (32) is differentiated with respect to β and equated to zero, giving

$$\frac{d(\log(p(\beta))}{d\beta}$$

$$= -\sum_{r=0}^{R-1} \frac{v_r(R-r)\ \beta^{(R-r-1)}}{1 - \beta^{(R-r)}} + (1/\beta)\sum_{r=0}^{R-1} u_r(R-r)$$

$$\tag{37}$$

Hence β' satisfies

$$\sum_{r=0}^{R-1} v_r\ (R-r)\ \frac{\beta'^{(R-r)}}{1 - \beta'^{(R-r)}} = \sum_{r=0}^{R-1} u_r\ (R-r) \tag{38}$$

that is,

$$\sum_{r=0}^{R-1} \frac{v_r\ (R-r)}{1 - \beta'^{(R-r)}} = \sum_{r=0}^{R-1} (u_r + v_r)\ (R-r) \tag{39}$$

The calculation of α', λ', and β' is illustrated by the following example. For a system with two circuits, the number of circuits occupied at the start of the observation period is taken to be 0, and the number occupied at the finish is taken to be 1. That is

$$R = 2$$

$$r_0 = 0$$

$$r_k = 1 \tag{40}$$

Table 1 below gives the observed values of s, u, v, and w — as a function of the state — that will be used for this example.

TABLE 1 — Data for Sample Calculations

r state	s total time (secs)	u unsuccessful attempts	v successful attempts	w departures
0	1500	0	10	0
1	3050	10	10	9
2	1450	10	0	10

Using the data above in equations (33) and (35) gives,

$$\alpha' = 1 \text{ per } 150 \text{ sec} \tag{41}$$

$$\lambda' = 1 \text{ per } 313 \text{ sec} \tag{42}$$

and, from equation (40), β' is given by

$$\frac{20}{1 - \beta'^2} + \frac{10}{1 - \beta'} = 40 \tag{43}$$

hence

$$4\beta'^2 + \beta' - 1 = 0 \tag{44}$$

$$\beta' = 0.39 \tag{45}$$

3.5 Numerical Analysis

Rather than computing point estimators of a, d, and γ it is a simple matter, using a computer, to calculate numerical values for the conditional probability density function for particular values of the parameters. Of course, the re-scaling indicated by equation (23) must be approximated using numerical integration. In principle, the conditional probability density function can thus be computed to any desired accuracy, and any form of statistical inference can be performed using it (point or interval estimation, hypothesis testing, etc.). An example of this type of numerical analysis is given in (Ref.13), pages 84-87.

4. CONCLUDING REMARKS

The essential difference between the technique described above and classical statistical techniques is that it allows the conditional probability density function of the unknown parameters to be computed. This feature, which is the crux of the Bayesian approach, makes use of observations both in computing estimators of the unknown parameters and in determining the accuracy of those estimators.

The practical application of the method is dependent on the existence of the finite dimensional, recursively computable sufficient statistic given in section 3. In practice, all the information in the observations which is relevant to estimating the unknown parameters can be recorded in a finite block of computer memory. For example, 4,000 words of on-line storage would be adequate for a study involving 1,000 circuits in 100 groups.

The conditional probability density function of the unknown parameters, or just estimators of those parameters, can be computed at any stage of the measurement or simulation. For example, a traffic measurement could be performed using a microcomputer to collect and store data, with a large computer analysing the data subsequently. In a simulation study it may be more convenient to compute point estimators, or the entire conditional probability density function, at intermediate stages during the simulation run.

6. REFERENCES

1. Benes, V.E., "A Sufficient Set of Statistics for a Simple Telephone Exchange Model", Bell System Technical Journal, July 1957, pp.939-963.

2. Billingsley, P., "Statistical Methods in Markov Chains", Annals of Mathematical Statistics, Vol.32, 1961, pp.12-40.

3. Cox, D.R., "Some Problems of Statistical Analysis Connected with Congestion", Proceedings of the Symposium on Congestion Theory, University of North Carolina Press, 1964, pp.289-316.

4. Reynolds, J.F., "On Estimating the Parameters of a Birth and Death Process", Australian Journal of Statistics, Vol.15, No.1, 1973, pp.35-43.

5. Kosten, L., Manning, J.R. and Garwood, F., "On the Accuracy of Measurements of Probabilities of Loss in Telephone Systems", Journal of the Royal Statistical Society, Series B, Vol.11, 1949, pp.54-67.

6. Descloux, A., "On the Accuracy of Loss Estimates", Bell System Technical Journal, Vol. 44, 1965, pp.1139-1164.

7. Kuczura, A. and Neal, S.R., "The Accuracy of Call Congestion Measurements for Loss Systems with Renewal Input", Bell System Technical Journal, Vol.51, No.10, 1972, pp.2197-2208.

8. Olsson, K.M., "Statistical Problems in Simulation of Telecommunications Traffic Systems; Some Analytical Results", Fourth International Teletraffic Congress, London, 1976.

9. Songhurst, D.J., "The Variance of Observations on Markov Chains", Eighth International Teletraffic Congress, Melbourne, 1976.

10. Rubas, J., "Traffic Simulation Studies Using an Electronic Computer", Fourth International Teletraffic Congress, London, 1964.

11. Kümmerle, K., "Ein Vorschlag zur Berechnung der Vertrauensintervalle bei Verkehrstests", Archiv Elektrischer Übertragung, Vol.23, No. 10, 1969, pp.507-511.

12. Rubas, J. and Warfield, R.E., "Determination of Confidence Limits for the Estimates of Congestion", Ninth International Teletraffic Congress, Spain, 1979.

13. Warfield, R.E., "A Study of Teletraffic Measurement and Other Estimation Problems", Ph.D. Thesis, Uni. of N.S.W., 1980.

BIOGRAPHY

ROBERT WARFIELD graduated with a B.E. (Hons) in 1970 from the University of New South Wales. In 1981 he received a Ph.D. from the same university for a thesis dealing with applications of Bayesian Statistical methods to Teletraffic Engineering.

He joined the Postmaster General's Department in 1967 as a cadet engineer. Since that time he has held several positions in Telecom, most of them concerned with planning. He is now employed as Senior Engineer, Traffic Engineering Research Section, in the Research Department.

He has published several technical papers, including one which he presented at the 9'th International Teletraffic Congress and another which he co-authored for the same Congress. He is the author of an Engineer Development Programme booklet on Statistics, and has been a lecturer and session leader at various courses in this programme.

Delay Distributions In Digital Switching Networks

S.M. JONG
R. BERMANSEDER
Telecom Australia Research Laboratories

*The introduction of digital switching will marginally increase trans-
mission delays in the telecommunications network. These increased delays are
attributed to the use of time switching. This paper describes the various
sources of delay which can be expected in a network evolving from analogue to
digital working and provides a mathematical treatment for calculating overall
delay distributions in digital switching networks.*

1. INTRODUCTION

Transmission delay in this paper is considered
as the time necessary for voice information to
pass through transmission systems, transmission/
switching interfaces and digital exchanges. In
mixed analogue/digital networks, echo occurs on
any two-wire or combination of two-wire and four-
wire telephone circuits, and for voice working the
degrading effect of this echo depends on the end-
to-end transmission delay. When the transmission
delay exceeds a certain limit, transmission per-
formance is more significantly impaired. An echo
suppressor or canceller is then required to be
connected in the network.

The introduction of digital switching brings
a new source of transmission delay to the net-
work. This delay is introduced mainly by the use
of time switching stages, which store speech sam-
ples in order to reassign the time slot or trans-
mission channel used by a call. For most systems
the delay due to time switching is a random var-
iable. For a particular connection in a network,
statistical methods are needed to derive the over-
all delay distribution.

2. THE SOURCES OF TRANSMISSION DELAY IN A MIXED ANALOGUE/DIGITAL NETWORK

In this section the contributions to trans-
mission delay of the various items of equipment
expected in a mixed analogue/digital network are
analysed, with particular reference to the Aus-
tralian national telecommunications network.

2.1 Transmission Equipment

• Analogue Multiplexing. In analogue FDM trans-
mission systems, the main source of group delay is
the transmit and receive channel filters in the
channel translating equipment (translating the
audio frequency band into the basic group band and
vice versa).

• Digital Multiplexing. In a digital transmission
system (PCM), delay is caused by the sampling-
coding-decoding process and the group delay of low
pass filters.

• Transmission Line. The propagation time of an
electrical signal depends on the transmission med-
ium, e.g. loaded cable, open-wire carrier, radio
system or optical fibre. The presence of (ana-
logue) repeaters or (digital) regenerators will
further increase propagation times.

2.2 Exchange Terminal Equipment

• Phase Alignment in a Plesiochronous Network. In
a plesiochronous network the clocks that control
exchange timing are independent of each other al-
though their frequency inaccuracy is kept within
a specified limit. Therefore slip may occur (loss
or duplication of speech samples, where equipment
handles information at different rates. (Ref.1)).
To reduce slip, it is necessary to arrange that
the time slots coming from different PCM multi-
plexers will as far as possible be kept in con-
stant phase relationship with the exchange time
slots. This is achieved by buffering and re-
clocking. The incoming PCM samples are stored cy-
clically into the buffer store (phase aligner) by
the incoming clock and are read out by the ex-
change clock.

The delay introduced in a phase aligner is the
time difference between writing into the buffer
store and reading out of the store. The maximum
value of this delay is set by buffer store dimen-
sions, usually being about one primary PCM frame
(125 µs).

• Phase Variation in a Synchronous Network. In a
synchronous network the clocks are running ideally
at identical rates or at the same mean rate with
limited relative phase displacement. Hence buffer-
ing to reduce the effect of clock frequency diff-
erences is not necessary. However, there can be
phase variations on the incoming PCM bit stream
due to jitter, wander and propagation delay vari-
ations (Ref.1). To compensate these phase vari-
ations a small "elastic" buffer (commonly up to
40 bits for primary PCM working) is required at
the exchange terminal.

2.3 Switching Equipment

A time switching stage is in principle a ran-
dom access memory where the incoming information
from a PCM system (i.e. a speech sample) is stored
before "switching" or reassignment to an appropri-

ate time slot for read-out. The time difference between this writing and reading is manifested as a delay which behaves as a random variable. It is important to notice that the distribution of this variable delay can be controlled by the designer. If the read-out time slot is randomly selected, as in the L.M. Ericsson digital AXE switch, a rectangular delay distribution results. That is, the delay has a minimum and a maximum value and an equal probability of being anywhere in between. Other systems, e.g. ITT System 1240, minimize delay with a selection algorithm which chooses the next available free time slot for read-out. In any case, delays introduced in each successive time stage behave as independent random variables and statistical methods are needed to derive the overall delay distribution for a particular connection in a network.

3. CALCULATION OF OVERALL DELAY DISTRIBUTIONS

In a digital switching network, the overall transmission delay is composed of fixed delays due to transmission equipment and random delays due to digital exchanges which use buffering and time switch stages. This section provides a mathematical derivation of the overall random delay distribution where the delay is due to a known number of buffers and time switches. Emphasis has been placed on the characteristics of the L.M. Ericsson digital AXE exchange, since this system is coming into use in the Australian telecommunication network.

A delay distribution tells us how often we can expect the delay to take a certain range of values. For example, the "95% point" is a value such that for 95% of connections the delay will be no more than the stated value. In AXE each time switching stage with random path selection contributes a rectangular delay distribution. The following discussion is concerned with overall delays due to switching, and ignores delays due to transmission equipment. These latter are invariant for a given connection and are readily dealt with by the traditional methods of the transmission planner.

3.1 Mathematical Derivation

For a particular connection in a network, a number of time switching stages contribute a number of independent random delays. These delays combine to give an overall delay which has a certain distribution of values. The minimum, maximum and average of the overall delay distribution can be found as simply the sum of the minimum, maximum or average of the contributing delays. However, for other points the overall density is the convolution of the contributing densities.

The convolution problem can be solved easily using Laplace Transforms, since convolution becomes multiplication in Laplace space (Ref.3). The general solution (Appendix 1) takes the form:

$$F(t) = \frac{1}{(N-1)! \prod_n T_n} \sum_{i_1=0}^{1} \sum \cdots \sum_{i_N=0}^{1}$$

$$\cdot \left[\prod_n (-1)^{i_n} \cdot \left(t - \sum_n (i_n T_n) \right)^{N-1} \right],$$

$$t \ge \sum_n i_n T_n \tag{1}$$

where $F(t)$ is the probability density of a delay of duration t

N is the total number of contributing delays

T_n is the maximum value of the nth contributing delay

n is the variable from 1 to N.

If the contributing delays are identical such as in AXE, i.e. all T_n equal, this simplifies equation (1) and it becomes:

$$F(t) = \frac{N}{T} \sum_{i=0}^{N} \frac{(-1)^i (\frac{t}{T} - i)^{N-1}}{i! \, (N-i)!} \, , \quad \frac{t}{T} \ge i \tag{2}$$
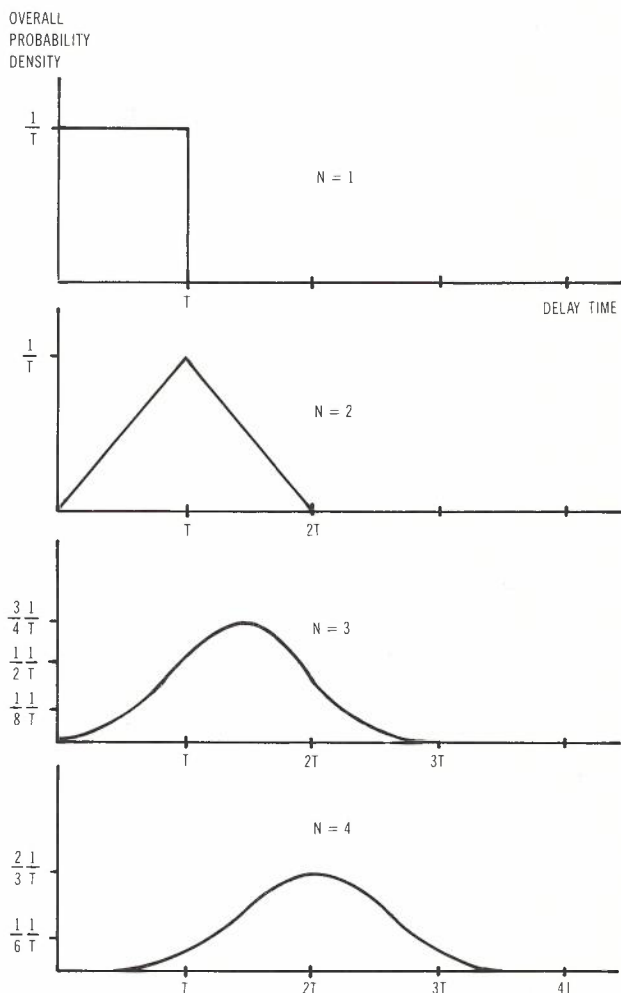

Fig.1 - Overall delay density of N identical rectangular contributing delays.

Digital Switching Networks

The general shape of this probability density function for N=1 to 4 is shown in Fig.1. It shows several interesting features. The overall delay distribution is always symmetric about the average value. As the number N of contributing delays becomes large, the overall distribution becomes more and more like a Normal Distribution (Ref.2). The average value (at the midpoint of the central hump) does increase in proportion to N, but the hump becomes narrower relative to the maximum value. An important consequence of this is that most percentile points tend to stay near the average rather than the maximum value of the overall distribution.

3.2 Computation

At present CCITT Study Group XI specifies single exchange delay distributions in terms of 95% points. In Telecom Australia's studies, a similar convention has been adopted for description of end-to-end network transmission delay. A computer program has been written to generate tables for 95% and 99% points vs the number N of contributing delays, for a specified maximum value of the contributing delays.

The presence of a factorial in the denominator of equation (2) limits the computability of the program for large N(> 20). Approximate values for large N are found by finding the 95% point of a Normal distribution scaled to have the same mean and variance as the true distribution (Appendix 2). A measure of the accuracy of this approximation is found by calculating the ratio of the 95% point of F(t) to its maximum value for a range of N, and comparing this with the ratio of the 95% point of the scaled Normal distribution to the same maximum value. It is shown, Fig.2, that the two ratios are very close in the range N < 20, and can be assumed identical (to 3 figure accuracy) for N > 20.

In interpreting the results shown in Fig.2, it should be remembered that the round-trip delay in a TST (Time-Space-Time) exchange architecture as used in AXE is the delay of 4 time stages plus 2 exchange terminal buffers. If buffer delays are ignored, N = 20 corresponds to 5 switching points. In AXE, the maximum buffer delay is about the same as the maximum delay of a time stage. Therefore the buffer delays are significant. A
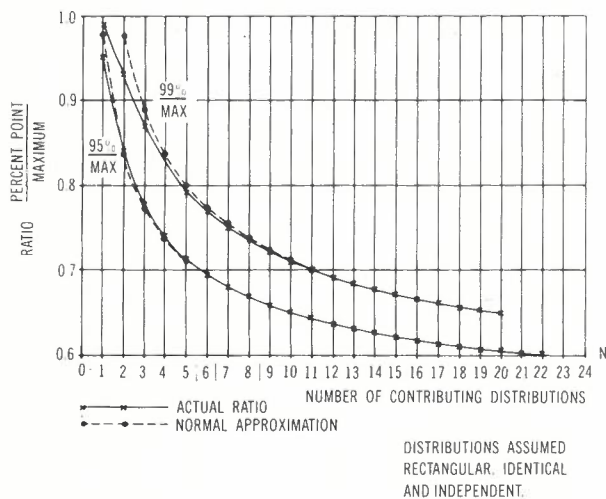
first approximation of their effect can be made by assuming that each switching point has 6 time stages but no buffers. In (Ref.5), more accurate calculations are made by convolving the buffer delays and time stage delays.

4. PRACTICAL APPLICATIONS

Detailed studies have been carried out in Telecom Australia Research Laboratories (Refs.4 &5). The results can be briefly summarized as follows:

• In a mixed analogue/digital metropolitan network, loop delays with AXE digital switches (2 time-stage) may have 95 percentile values of 4-5 ms for some connections. Use of a 4 time-stage digital switch would increase the corresponding delays to 5-6 ms.

• In a national long distance connection, the digital switching plus associated PCM coding-decoding increases the round-trip delay. For example, the 95 percentile round-trip delay of a typical mixed analogue/digital network is increased by about 5 ms compared to a completely analogue network. Therefore the use of digital switching in long distance connections indicates that more echo suppressors will be required in a mixed analogue/digital network than in a completely analogue network. However, the actual use of echo suppression or cancellation depends on many other factors, including economics, as well.

• There appears to be no substantial argument against the adoption of digital switching for the STD network, on delay grounds.

5. CONCLUSIONS

The delay due to the buffers and the time switching stages at a digital switch behaves as a random variable. The distribution of the variable delay depends on the design approach. In any case, delays introduced in each successive time switching stage behave as independent random variables. For a particular connection, the overall end-to-end delay density is the convolution of the contributing delay densities.

In individual AXE time switching stages, random path selection results in a rectangular delay distribution. It is shown that as the number of time switches becomes large, the overall distribution of delay due to switching tends to resemble a Normal distribution with most percentile points appearing to converge towards the average rather than the maximum of overall delay distribution. Similarly, the ratio of any percentile point to the maximum value tends to 0.5.

This paper has described a method of calculating the distribution of the overall transmission delay due to the presence of digital switching in a circuit switched network. In practical terms, the application of these methods (Refs.4&5) shows that digital switching introduces a real but only marginal increase in transmission delay as a network evolves from all analogue to a mixture of analogue and digital switching.

6. ACKNOWLEDGEMENT

Fig.2 - Accuracy of normal approximation.

7. REFERENCES

1. Ericsson, L.M., "Digital Telephony", Sweden, 1977.

2. Hoel, P.G., "Introduction to Mathematical Statistics", Wiley, 1971.

3. Spiegel, M.R., "Laplace Transforms", Schaum's Outline Series, McGraw-Hill, 1965.

4. Jong, S.M., "Sources of Transmission Delay in Mixed Analogue/Digital Networks", Switching and Signalling Branch paper No.31, Telecom Australia Research Laboratories, June 1980.

5. Jong, S.M., "Transmission Delay in Mixed Analogue/Digital Network", Switching and Signalling Branch paper No.32, Telecom Australia Research Laboratories, June 1980.

APPENDIX 1

CONVOLUTION OF PULSE FUNCTIONS

Consider N independent pulse functions :

$$f_n(t) = \frac{1}{T_n} , \quad t \leq T_n$$

$$= 0 , \quad t > T_n$$

Where n is the variable from 1 to N

T_n is the width of the nth pulse

To calculate their combined probability density, they are convolved :

$$F(t) = f_1(t) * f_2(t) * \cdots * f_N(t)$$

The Laplace Transform is taken, since convolution becomes multiplication in Laplace space

$$L[F(t)] = \prod_{n=1}^{N} L[f_n(t)]$$

Now

$$L[f_n(t)] = \int_0^\infty e^{-pt} \cdot f_n(t) dt$$

$$= \frac{1}{T_n} \left[\frac{e^{-pt}}{-p} \right]_0^{T_n}$$

$$= \frac{-1}{pT_n} (e^{-pT_n} - 1)$$

Hence

$$L[F(t)] = \prod_{n=1}^{N} \frac{1}{pT_n} (1 - e^{-pT_n})$$

$$= \frac{p^{-N}}{\prod_n T_n} \cdot \prod_n (1 - e^{-pT_n})$$

$$= \frac{p^{-N}}{\prod_n T_n} \cdot \prod_n \left[\sum_{i_n=0}^{1} (-1)^{i_n} \cdot e^{-i_n p T_n} \right]$$

$$= \frac{p^{-N}}{\prod_n T_n} \sum_{i_1=0}^{1} \sum_{i_2=0}^{1} \cdots \sum_{i_N=0}^{1}$$

$$\cdot \left[\prod_n ((-1)^{i_n} \cdot e^{-i_n p T_n}) \right]$$

$$= \frac{1}{\prod_n T_n} \sum_{i_1=0}^{1} \sum_{i_2=0}^{1} \cdots \sum_{i_N=0}^{1}$$

$$\cdot \left[(\prod_n (-1)^{i_n}) \cdot e^{-\sum_n i_n p T_n} \cdot p^{-N} \right]$$

$$F(t) = \frac{1}{\prod_n T_n} \sum_{i_1=0}^{1} \sum_{i_2=0}^{1} \cdots \sum_{i_N=0}^{1}$$

$$\cdot \left[\prod_n (-1)^{i_n} \cdot L^{-1}[e^{-\sum_n i_n p T_n} \cdot p^{-N}] \right]$$

$$= \frac{1}{(N-1)! \prod_n T_n} \sum_{i_1=0}^{1} \cdots \sum_{i_N=0}^{1}$$

$$\cdot \; [\pi_n (-1)^{i_n} \cdot (t - \sum_n (i_n T_n))^{N-1}] \; , \qquad\qquad \text{where } X_i = (-1)^i \frac{N!}{i! \, (N-i)!}$$

$$t \geq \sum_n i_n T_n \qquad\qquad Y_j = (-1)^j \frac{M!}{j! \, (M-j)!}$$

$$\int F(t) dt = \frac{1}{N! \pi_n T_n} \sum_{i_1 = 0}^{1} \sum \cdots \sum_{i_N = 0}^{1}$$

DERIVATION OF A FORMULA FOR NORMAL DISTRIBUTION PERCENT POINTS

$$\cdot \; [\pi_n (-1)^{i_n} \cdot (t - \sum_n (i_n T_n))^{N}] \; ,$$

Assume the delay distributions are all identical, independent and uniform (rectangular).

$$t \geq \sum_n i_n T_n$$

Central Limit Theorem: The distribution of N independent random variables approaches a Normal distribution as N becomes large.

(1)

If all pulse functions are identical, that is all T_n equal,

The variance of a rectangular distribution is

$$\text{Var} = \frac{(\text{max} - \text{min})^2}{12} \qquad\qquad (2)$$

$$\int F(t) dt = \frac{1}{T^N N!} \sum_{i=0}^{N} \frac{N!}{i!(N-i)!} (-1)^i \cdot (t - iT)^N ,$$

If X and Y are independent random variables, then

$$t \geq iT$$

$$\text{Var} (X + Y) = \text{Var} (X) + \text{Var} (Y) \qquad\qquad (3)$$

$$= \sum_{i=0}^{N} \frac{(-1)^i (t-iT)^N}{T^N \, i! \, (N-i)!} , \qquad t \geq iT$$

In the case of the delay distribution of a single time stage,

$$\text{max} = T$$
$$\text{min} \simeq 0$$

$$= \sum_{i=0}^{N} \frac{(-1)^i (\frac{t}{T} - i)^N}{i! \, (N-i)!} , \qquad \frac{t}{T} \geq i$$

Then (2) becomes:

$$\text{Var} = \frac{T^2}{12}$$

For the special case : N distributions of length T
M distributions of length B,

Also,
$$\text{Mean} = \frac{T}{2}$$

For N identical distributions, (3) gives:

$$\int F(t) dt = \frac{1}{T^N B^M (N+M)!} \sum_{i=0}^{N} \sum_{j=0}^{M} X_i Y_j$$

$$\text{Var} = N \cdot \frac{T^2}{12}$$

Also,
$$\text{Mean} = N \cdot \frac{T}{2}$$

$$\cdot \; [t-(iT + jB)^{N+M}] \; , \qquad t \geq iT + jB$$

Consider a Normal distribution having mean = $\frac{NT}{2}$, variance = $\frac{NT^2}{12}$ i.e. Normal $(\frac{NT}{2}, \frac{NT^2}{12})$ and find the (say) 95% point of this distribution.

From tables, the 95% point of Normal (0,1) is at 1.645 standard deviations. Hence by scaling Normal (0,1), i.e. by multiplying by $\sqrt{\frac{NT^2}{12}}$ and then adding $\frac{NT}{2}$, we generate Normal $(\frac{NT}{2}, \frac{NT^2}{12})$ and find the required 95% point.

$$95\% \text{ point} = 1.645 \sqrt{\frac{NT^2}{12}} + \frac{NT}{2} \qquad (4)$$

Now, the maximum value of the actual delay distribution is simply NT . The ratio of the 95% of the scaled Normal distribution to the actual maximum value becomes:

$$\text{Ratio} = \frac{1.645 \sqrt{\frac{NT^2}{12}} + \frac{NT}{2}}{NT}$$

$$= 0.500 + 0.475/\sqrt{N} \qquad (5)$$

NOTE: As $N \rightarrow$ infinity, Ratio $\rightarrow$ 0.5

The ratio of the 95% of the actual distribution to its maximum value is found empirically to be very close to (5) in the range N < 20 , and can be assumed identical (to 3 figure accuracy) for N > 20 .

When two types of delays are involved such as buffer delays and time stage delays in an AXE digital switch, the Normal distributions are convolved together simply by summing the individual means and variances.

Let N = number of delays of type 1
     T = length of delays of type 1
     M = number of delays of type 2
     B = length of delays of type 2

Then

$$\text{Mean} \quad = \frac{NT + MB}{2}$$

$$\text{Variance} = \frac{NT^2 + MB^2}{12}$$

95% point (2 variables)

$$= 1.645 \sqrt{\frac{NT^2 + MB^2}{12}} + \frac{NT + MB}{2}$$

Ratio (2 variables)

$$= 0.500 + 0.475 \frac{\sqrt{NT^2 + MB^2}}{NT + MB}$$

BIOGRAPHIES

SOE MEI JONG graduated from Monash University with a Bachelor of Engineering degree in 1969. She joined Telecom Research Laboratories as an Engineer in 1970. She was involved in the design and development of the Laboratories model SPC digital exchange and Remote Switching Unit. She is currently working in the Network Studies Section on design studies for DDN Time Division Cross Connect.

ROBIN BERMANSEDER graduated with a Bachelor of Science degree from Griffith University (Queensland) in 1978. During 1979-1980 he worked as a Research Officer with the Switching and Signalling Branch, Telecom Research Laboratories. His work was mainly concerned with the use of computers to solve telecommunication network problems. In January 1981 he left Telecom to join the Australian Regular Army.

The Multiplexing Factor In Digital Transmission Systems

R.A. COURT
R.B. COXHILL
P.G. POTTER
Telecom Australia Research Laboratories

The error performance of digital networks is currently under study by telecommunications administrations and organisations. The factor which complicates error performance specifications is the occurrence of errors in bursts. This paper discusses the effect of error bursts on the relation between Error-Second performance at multiplexed rates (e.g. 2048 kbit/s) and at tributary rates (e.g. 64 kbit/s). This relationship is known as the Multiplexing Factor (MF). Experimental results are presented and analysed for digital line systems and DAV radio systems. For digital line systems a MF=10 gives an adequate margin while for DAV systems MF is much closer to 1.

1. INTRODUCTION

The question of how to set objectives for the performance of digital networks is becoming increasingly important to telecommunications administrations and organisations (Ref.1). In particular the error performance of digital networks is currently under study (Refs.2&3). The factor which complicates the specification of error performance is that errors occur, not only as single events, but also as bursts of varying lengths containing a mixture of bits in error and correctly transmitted bits. It is difficult to precisely define an error burst, however the number of correctly transmitted bits between errors may be used to identify separate bursts on a particular system, i.e. if this number is greater than some predetermined value then the errors are not in the same burst. How such a value should be determined is a matter for study.

There are two major complications caused by error bursts. In the first place the performance provided at customer rates (e.g. 64 kbit/s and lower) cannot be determined directly from measurements at multiplexed rates (e.g. 2048 kbit/s and above). This problem is the subject of this paper and will be discussed in more detail later. The second complication arises when one network is carrying a number of services (Ref.2) or when several networks are sharing the same transmission facilities. The services being carried may each require a different measure of error performance (e.g. bit error rate, error-free-seconds) in their specifications. It would be advantageous to be able to relate these different measures and emerge with a single specification to guide the design of transmission systems. However this is not possible, in general, without a detailed knowledge of error burst structures on the systems in question. This problem is beyond the scope of this paper.

In what follows the first of these two complications will be outlined. A data test set (Ref.4) developed by Telecom Australia to assist in performance studies for the Australian Digital Data Network (Ref.5) has been adapted to make measurements related to the problem. Results from measurements on digital line transmission systems and Data-Above-Voice (DAV) radio transmission systems are presented and analysed.

2. THE MULTIPLEXING FACTOR

One method of expressing the error performance of digital transmission systems is in terms of error-free-seconds (EFS) or conversely error-seconds (ES). An EFS is a second which contains no errors, i.e. the bit error rate (BER) equals 0, when measured over that second. Because of the burst nature of errors the EFS performance of de-multiplexed tributary bit streams cannot be determined directly from the EFS performance of the higher order stream. The relation between the EFS (or ES) performances at the two bit rates is known as the multiplexing factor (MF), where, defining %ES as the ratio of ES to available seconds (×100),

$$MF = \frac{\%ES \text{ (high order stream)}}{\%ES \text{ (tributary stream)}}$$

Most error specifications are written in terms of customer bit rates and in particular 64 kbit/s is chosen. This may be regarded as a fast customer rate and the performance at lower speeds will, at worst, be the same as the 64 kbit/s performance. If the performance of the main transmission bearer, operating at the higher order bit rate, is to be specified then MF must be known.

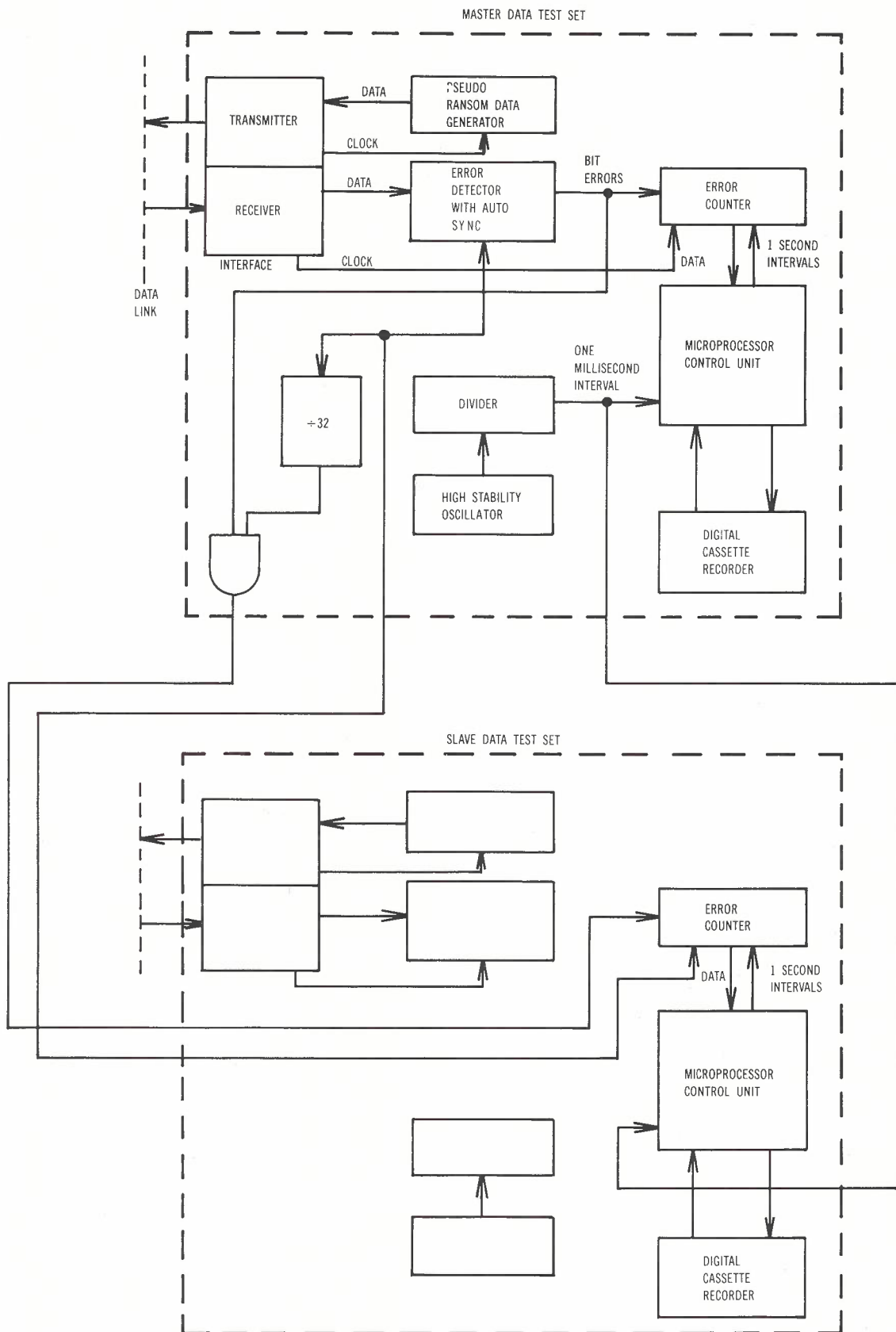To illustrate the effect of the MF, consider firstly the case of single errors separated by

MASTER DATA TEST SET

TRANSMITTER

PSEUDO RANSOM DATA GENERATOR

DATA

CLOCK

RECEIVER

DATA

ERROR DETECTOR WITH AUTO SYNC

BIT ERRORS

ERROR COUNTER

INTERFACE

CLOCK

DATA

1 SECOND INTERVALS

DATA LINK

÷ 32

DIVIDER

ONE MILLISECOND INTERVAL

MICROPROCESSOR CONTROL UNIT

HIGH STABILITY OSCILLATOR

DIGITAL CASSETTE RECORDER

SLAVE DATA TEST SET

ERROR COUNTER

DATA

1 SECOND INTERVALS

MICROPROCESSOR CONTROL UNIT

DIGITAL CASSETTE RECORDER

Fig.1 - Arrangement of test sets to measure multiplexing factor.

more than one second, and the relation between EFS (or ES) performance at 2048 kbit/s and 64 kbit/s. The 2048 kbit/s stream is made up of frames containing 32 time slots (i.e. 30 channels + framing + signalling), each of which contains 8 bits belonging to one of the 64 kbit/s tributaries. In this instance there will be, on average, one ES in each of the tributaries for every 32 ES in the main stream and the MF = 32. However if the errors are not single random events but occur as bursts longer than 248 bits, and with at least one error every 8 bits, then every time slot and hence every tributary will have errors due to the burst. This means that every ES in the 2048 kbit/s stream will result in an ES in each of the 64 kbit/s streams and MF = 1.

Rather than having error bursts of one type as in the two extreme cases quoted above, each transmission system will have a distribution of error bursts in terms of length, composition and frequency of occurrence. As a result MF cannot be determined analytically without detailed information on the error bursts for the system in question. An experimental programme has been undertaken to measure the 2048/64 MF directly to ascertain the potential use of the relationship.

3. TEST EQUIPMENT

As mentioned in the introduction, a data test set developed by Telecom Australia has been adapted to make measurements of MF. The set is designed to make long term measurements of the per-
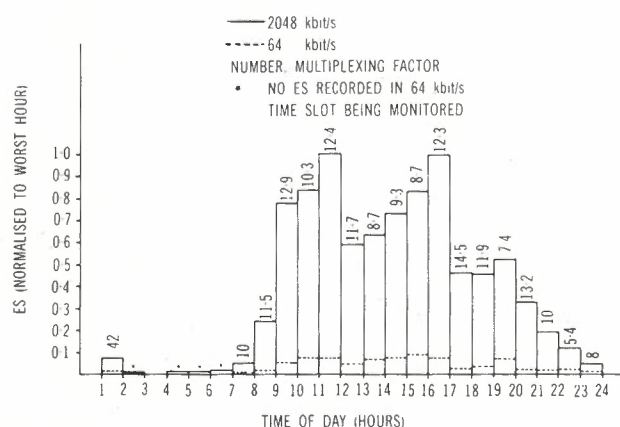
Fig.2 - Error performance of digital line system averaged over five consecutive weekdays.

formance of digital transmission systems. The measurements are based on error-seconds whereby an independent clock generates consecutive one second intervals during each of which the digital signal is monitored for bit errors. Detection of any bit error during a second causes that interval to be counted as an error-second. Conversely, if no bit error is detected, it causes an error-free-second to be counted. This information is collated and stored on a digital cassette recorder for later analysis on a central computer.

Two identical test sets are used to allow simultaneous measurements at 2048 kbit/s and 64 kbit/s. One set (the "master") performs measurements at 2048 kbit/s while the other (the "slave") measures at 64 kbit/s via a "pseudo demultiplexer". A block diagram illustrating the arrangement is shown in Fig.1. The master set supplies the independent timing and data clock for both its own use and that of the slave set. The slave receives bit errors via a gate which is only active for a period equivalent to one 64 kbit/s tributary i.e. 1/32 of the period of the master set.

4. DIGITAL LINE SYSTEMS

Using the equipment described above the ES performance of 2048 kbit/s PCM junction cable systems has been monitored. Figure 2 shows a typical histogram of ES performance averaged over a period of 5 consecutive weekdays. Also included in the figure are the hourly variations in MF during the period. The overall MF for the entire 5 days was 10.4. The systems are operating in a predominately analogue environment and as it can be seen from the figure the ES performance varies with traffic, clearly indicating the effects of impulse noise (coupled through crosstalk paths from switching or signalling events on adjacent pairs). Similar figures for other periods and other bearers have similar shapes varying only in scale as the long term ES performance changes.

Table 1 shows variations in the overall MF on another bearer obtained by altering the traffic adjacent to the PCM bearer and thereby altering the long term ES performance. Also monitored at the same time was the distribution of bit errors per ES in the decoded 2048 kbit/s stream and these results are shown in Table 1. This data was stored in binary groups (i.e. 1-2, 3-4, 5-8 etc.) as shown in the table. Note that in period B the overall MF was 44.8 which is higher than the calculated maximum of 32. Such values are explained by the statistical distribution of errors over the

TABLE 1 - Result of Altering Long Term %ES Performance

Period	Long Term % ES	Overall MF	Distribution of Bit Errors per ES (%)			
			1-2	3-4	5-8	9-16
A	0.13	28.5	88	11	1	
B	0.09	44.8	90	9	1	
C	0.53	22.7	60	27	12	1
D	0.54	16.7	58	26	14	2
E	0.49	16.6	57	25	16	2
F	0.52	15.6	54	28	15	3
G	0.19	29.1	71	25	4	
H	0.17	22.5	87	13		

time slots, i.e. over a particular period the time slot being monitored may receive less than the number of errors in the 2048 kbit/s stream averaged over the 32 time slots.

Table 2 shows the hourly variation in MF both in the same period and between periods. The four periods used were C, D, E and F because of their similar %ES performance. The overall MF for the four periods was 17.4. Only the hours between 0900 and 1700 are included in Table 2 because few errors were recorded in the 64 kbit/s stream outside these hours.

TABLE 2 - Busy Hour Variations in MF

HOUR PERIOD	9- 10	10- 11	11- 12	12- 13	13- 14	14- 15	15- 16	16- 17
C	18.5	16.2	53.3	24.0	22.5	15.7	23.3	15.0
D	14.4	10.0	16.2	20.0	25.0	13.7	12.0	20.0
E	16.6	12.7	28.0	46.6	13.3	11.3	20.0	11.3
F	26.6	10.0	8.6	22.5	80.0	17.1	20.0	16.6

To consider the results, it is obvious that MF has considerable short term variation and rather less long term variation. A significant trend is for MF to decrease as traffic increases (i.e. as long term %ES increases). The results that have been obtained on this system together with other similar tests indicate that no one MF can be used to characterize digital line systems of this type. Rather a lower limit may be put on MF, associated with the error performance of an in-service bearer. A MF of 10 would seem to give an adequate margin, i.e. the %ES performance of a 64 kbit/s stream is at least 10 times better than the %ES performance of the 2048 kbit/s.

An insight into the burst structure of the errors can be made by examining the distribution of bit errors per ES in Table 1. There are two major groups, i.e. those with %ES ≈0.1 and those with %ES ≈0.5. In those cases with %ES of the order of 0.1 the occurrence of more than one bit error in a second can be explained by the error multiplication due to the decoding of the HDB3 line code (Ref.6). This process causes one line error to become as follows:

0 bit error with a probability of 0.023,

1 bit error with a probability of 0.628,

2 bit errors with a probability of 0.215,

3 bit errors with a probability of 0.134.

Using these figures if all error seconds were caused by single line errors then the distribution of bit errors per ES would be,

1 or 2 errors, $\frac{62.8}{100-2.3} + \frac{21.5}{100-2.3} = 86.3\%$

3 errors, $\frac{13.4}{100-2.3}$ $= 13.7\%$

which agrees with the measured results shown for periods A, B and H in Table 1.

However for those cases with %ES of the order of 0.5 the relative proportions of bit errors per ES has changed and it appears that in some seconds more than one line error is occurring. Calculations indicate that only 60% of ES are due to single line errors. A random arrival process with such low ES probability (.005) would not result in enough multiple line errors to account for the change which is observed. It must therefore be concluded that the line errors are somehow grouped in time. It is possible to estimate the fractions (P_1, P_2 and P_3) of "one line error", "two line error" and "three line error" ES from the decoder error multiplication factors listed previously and the distribution of bit errors per ES shown in Table 1. If it is assumed that the multiple line errors in a second do not occur in the same time slot, then the average number of time slots which are affected per ES(2048) is N, where

$$N = P_1 + 2P_2 + 3P_3 .$$

Therefore, considering only line errors, on average there will be N ES(64) for every 32 ES(2048). In addition one line error may cause bit errors in two time slots due to error multiplication when decoding, for example one line error may cause two bit errors separated by three bits (see (Ref.6)). The bit errors in this case will occur in two different eight bit time slots fifty percent of the time. If all such possibilities are included there will be a 12 percent increase in the number of decoded time slots with bit errors when compared to the number of time slots with line errors. Thus,

$$MF = \frac{32}{1.12N}$$

This yields a value of ≈18 which compares with the overall MF for periods C, D, E and F (i.e. those periods with %ES ≈0.5) of 17.4. Thus we now appear to have multiple line errors in a second which are grouped but separated by at least one time slot.

The reasons for this behaviour are not altogether clear although the following explanation may be considered. The events which produce line errors are most likely to be dial pulses on pairs adjacent to the PCM bearer. These occur in groups of from 1 to 10 in less than 1 second. The increased number of "multiple line error" ES in the higher %ES cases may be due to,

(i) Overlap of dial pulses on adjacent disturbing pairs

or

(ii) Increase in traffic on a disturbing pair for which there is a higher probability of a dial pulse causing an error than previously, where the errors had been caused by dial pulses on other disturbing pair(s). Thus the error rate and the proportion of "multiple-line-error" seconds have increased.

Digital Transmission Systems

5. DATA-ABOVE-VOICE (DAV) SYSTEMS

Tests have been conducted on a DAV radio system operating in the 6 GHz band. The system comprises four sections, one of which has space diversity switching. As expected the MF behaviour is quite different from that found on line systems. Table 3 gives the overall MF and long term %ES measured over four weekly periods.

Figure 3 shows the 2048 kbit/s error performance averaged over each of the four periods. Also included in this figure is the hourly variation in MF. Table 4 gives the distribution of bit errors per ES for the four periods.

TABLE 3 - Variation in MF for DAV System

Test Period	Overall MF	Long Term %ES
A	6.6	.011
B	6.4	.014
C	3.3	.027
D	11.0	.016

The variation in MF shown in Table 3 is once again quite large. These variations can be explained by the distribution of bit errors per ES shown in Table 4. There are two significant error mechanisms in operation one which produces short bursts and one which produces long bursts. Possible explanations are diversity switching and radio propagation fading respectively. The effect of these two mechanisms can be illustrated by the following two examples.

(i) For a period where 90% of the ES contain short bursts which cause errors in only one time slot per frame and 10% of the ES contain long bursts which cause errors in all time slots per frame, then

$$MF = \frac{100 \times 32}{90 \times 1 + 10 \times 32}$$

$$= 7.8 \text{ (e.g. periods A, B \& D)}$$

(ii) As in (i) with 90% and 10% replaced by 80% and 20% respectively

$$MF = \frac{100 \times 32}{80 \times 1 + 20 \times 32}$$

$$= 4.4 \text{ (e.g. period C)}$$

The fading in period C can be seen in Figure 3 as MF, between 1500 and 2100 hours, is almost 1.

Fig.3 - *Error performance of DAV bearer averaged over four weekly periods.*

TABLE 4 - % Number of Bit Errors per ES for DAV System

Period	| 1-2	3-4	5-8	9-16	17-32	33-64	65-128	129-256	257-512	513-1024	1025-2048	2049-4096	4097-8192	8193-16384	>16385
A	83	3	3					2				3			6
B	79	5	4	2	3			1	1	1		1	2		1
C	59	6	4	2	2	2		1	2	2		1	2	1	3	13
D	83	10	2	1							1		1		2

The results given above show that if only a small fraction (1/5) of the ES are due to fading, and consequently include error bursts which are longer than one frame, then MF will be close to 1. This, in turn, means that unless the radio bearer is adequately protected then the ES performance at 64 kbit/s may only be slightly better than that at 2048 kbit/s.

6. CONCLUSIONS

This paper has discussed the error performance of digital transmission systems with particular reference to the relation between the ES perform- ance at 2048 kbit/s and that at 64 kbit/s, i.e. the Multiplexing Factor (MF). On a digital line system, measurements indicate that for the error performance associated with in-service bearers, a MF of 10 gives an adequate margin. Results from a DAV system indicate a MF much closer to 1 is needed to ensure a margin against fading.

7. REFERENCES

1. CCITT Study Group XVIII, Question 9.

2. CCITT Recommendation G821.

3. Jones, W.T. and Pullum, G.G., "Error Perform- ance Objective for Integrated Services Digital Networks Exhibiting Error Clustering", IEE Second Int. Conf., "Telecommunication Trans- mission into the Digital Era", London, 17-20 March 1981.

4. Duc, N.Q., Coxhill, R.B., English, K.S. and Webster, R.I., "A Performance Monitoring Sys- tem for Data Transmission Circuits", Telecom. J. of Australia, Vol.30, No.2, 1980, pp.110- 117.

5. Beare, C.T., Falkovitz, Y. and Poussard, T.J., "An Introduction to the DDN", to be published in the Telecom Journal of Australia.

6. Bréant, Pierre, "Influence of a Single Error on HDB3 Code Transmission. Comparison with the Bipolar Code", (In French), Câbles et Trans- mission. Vol.28, No.1, Jan. 1974, pp.3-36.

BIOGRAPHIES

ROBIN A. COURT graduated with a B.Sc. degree from Melbourne University in 1969. He then joined the Australian Post Office as a Cadet Engineer and studied at Monash University graduating with a B.E.(Hons.) degree in 1971 and a M.Eng.Sc. degree in 1974. In 1973 he commenced with the Radio Systems Section of the APO (now Telecom Australia) Research Laboratories where he remained until 1979 working on various aspects of mobile radio and digital radio systems. In 1979 he joined the Line and Data Systems Section of the Laboratories where he is a Senior Engineer working mainly in the area of local transmission aspects of ISDN access. Other interests include the error performance of digital transmission systems.
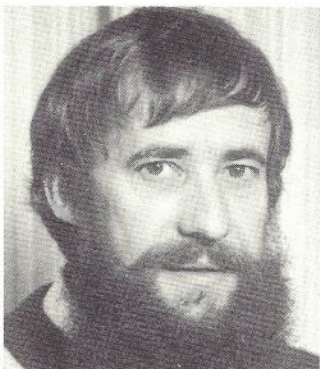
RICK COXHILL joined the Australian Post Office in 1963 as a Technician- in-Training. On completion of this training he was appointed as Technician in the Line and Data Systems Section of the Australian Post Office Re- search Laboratories. Since then he has worked on various projects to study transmission related aspects of the Australian Telecommunications Network. He is currently employed as a Senior Technical Officer and is engaged in developing instrumentation to investigate local transmission aspects of ISDN access.
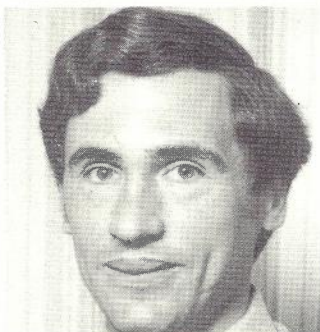
PHILIP G. POTTER graduated with a B.E. degree in 1974 and a Ph.D. in 1979 from Monash University. He joined Telecom Australia in March 1979 and has worked since then as an Engineer with the Line and Data Systems Section in the Transmission Branch of the Research Laboratories. He is interested in statistical modelling of crosstalk and impulse noise interference with application to the estimation of the error performance of digital trans- mission systems. He is currently working in the area of local trans- mission aspects of ISDN access.

Synthesised Phase Locked Local Oscillator Design For Mobile Field Strength Receiver

P.R. HICKS
Telecom Australia Research Laboratories

This paper describes the theory and design of a phase locked synthesiser that has been developed to be used as the local oscillator for a Mobile Field Strength Receiver. The method of frequency synthesis is that of prescaling using a two modulus prescaler.

The loop uses a novel voltage controlled oscillator consisting of a wideband amplifier with a resonant cavity and delay line in the feedback path. A resonant cavity exists for each frequency band. The design of the control logic is such that frequency bands between 100 MHz and 1 GHz may be covered by provision of suitable cavity resonators and appropriate delay lines.

In addition to describing the components of the synthesiser the paper discusses the design and choice of various types of loop filter.

1. INTRODUCTION

Electronic phase locked loops (PLL) came into vogue in the 1930s when they were used for radar synchronisation and communication applications. This technique for electronic frequency control is widely used today and is most suitable for frequency synthesis, synchronisation of digital signals and clock recovery from encoded digital data streams.

The basic PLL technique compares the frequency and phase of the incoming data (or reference signal) to the output of a voltage controlled oscillator (VCO). If the two signals differ in frequency and/or phase an error voltage is generated and applied to the VCO causing it to correct in the direction required for decreasing the difference. The correction procedure continues until lock is achieved after which the VCO will continue to track the incoming signal. The basic analogue phase locked loop is shown in Fig.1.
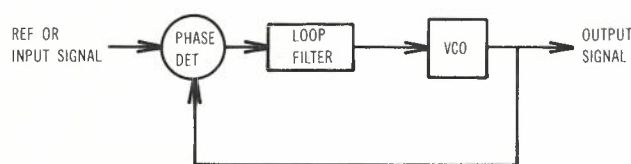
Fig.1 - Basic phase locked loop.

One of the major applications of the PLL is frequency synthesis in the many systems which require discrete frequencies or fixed channel spacing - such as a receiver suitable for the mobile radio bands with a fixed channel spacing of 25 kHz. This paper describes the design of a synthesiser used as a local oscillator in a receiver used to measure field strength for mobile radio services. Reference (1) describes techniques of measuring field strength.

2. SYNTHESIS USING DIGITAL PHASE LOCKED LOOP

With the development of digital hardware the use of digital phase locked loops for frequency synthesis have attracted much attention and have been extensively discussed in print (Ref.2).
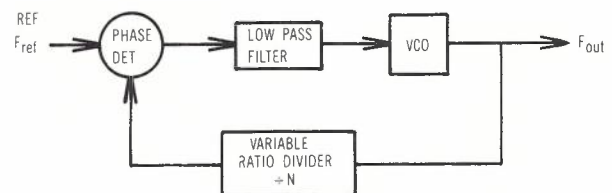
Fig.2 - Digital phase locked loop synthesis - basic configuration.

The basic form of the digital PLL is shown in Fig.2. The loop consists of a VCO, a variable ratio frequency divider, phase comparator and a low pass filter. The VCO output is divided and compared with a stable reference frequency. Error voltages derived from the phase comparator maintain the VCO on frequency. For locking to occur

$$f_{out} = Nf_{ref} \qquad (1)$$

Equation (1) indicates that the smallest frequency increment generated by the loop is equal to the reference frequency f_{ref}.

The system shown in Fig.2 is considered to be the direct approach. While this is the simplest form that the loop can assume it does have some associated design problems. Assuming that we can produce a VCO capable of operating at the required output frequency (in the range 100-1000 MHz), we are faced with the problem of designing a complex programmable counter which is required to operate at the VCO output frequency. Since high frequency (>25 MHz) programmable counters are difficult and expensive to realise, special

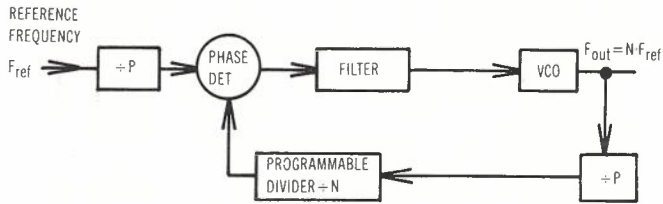techniques to programme the output frequency are required.

REFERENCE FREQUENCY

Fig.3 - *Frequency synthesis by prescaling.*

One approach is to prescale (÷P) the output of the VCO before applying it to the programmable counter. The block diagram for such a synthesiser is shown in Fig.3. The input frequency into the programmable divider is low and likewise the loop response is slow. When the loop is locked the output frequency is given by

$$f_{out} = N.P.f_{ref} \qquad (2)$$

The disadvantage of using a fixed modulus (÷P) prescaler in high frequency phase locked loops is that it also requires the reference frequency to be divided by P if the relationship given by equation (1) is to hold. To overcome this disadvantage a technique known as synthesis by variable modulus prescaling may be used.

3. SYNTHESIS BY VARIABLE MODULUS PRESCALING

The technique of variable modulus prescaling allows a simple two modulus prescaler to be controlled by a relatively slow programmable counter. The two modulus prescaler can be implemented using high speed emitter coupled logic (ECL) while the relatively slow programmable counter can be implemented using TTL.

The use of the variable modulus prescaling technique permits direct high frequency prescaling without any sacrifice in resolution since it is no longer necessary to divide the reference frequency by the modulus of the high frequency prescaler.

The theory of variable modulus prescaling may be explained by considering the system shown in Fig.3 (Ref.3). The governing equation for the loop shown is

$$f_{out} = N.P.f_{ref} \qquad (2)$$

where P is fixed and N is variable (N and P both integers). For a change of 1 in N the output frequency changes by $P.f_{ref}$, i.e. the channel spacing is $P.f_{ref}$

From equation (2) it is easily seen that only every P channel may be programmed simply since N is always integer. To obtain intermediate channels P must be multiplied by an integer plus a fraction. The problem of how to programme intermediate channels is found by considering equation (2).

If we define

$$N = N_p + A/P \qquad (3)$$

where N_p, A and P are integers; substitute into equation (2).

$$f_{out} = (N_p + A/P).P.f_{ref} \qquad (4)$$

i.e.

$$f_{out} = (N_p.P + A)f_{ref} \qquad (5)$$

Adding ± A.P to the coefficient of f_{ref} in equation (5) and factoring gives:

$$f_{out} = (N_p.P + A - AP + AP)f_{ref}$$

i.e.

$$f_{out} = \{(N_p-A).P + A(P+1)\}f_{ref} \qquad (6)$$

From equation (6) it is apparent that the fractional part of N can be synthesised by using a two modulus counter (P and P+1) and dividing by the upper modulus A times and by the lower modulus (N_p-A) times. Equation (6) also suggests the circuit configuration shown in Fig. 4.
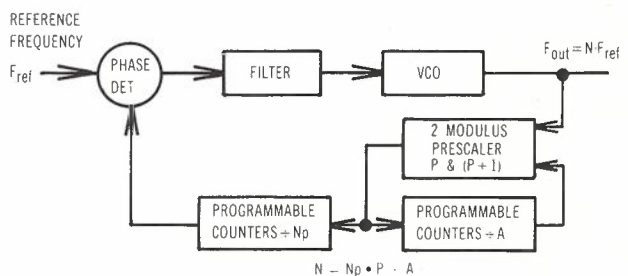

REFERENCE FREQUENCY

Fig.4 - *Frequency synthesis by two modulus prescaling.*

In operation the prescaler divides by (P+1), A times. For every P+1 pulses into the prescaler both the A counter and the N_p counter are decremented by 1. The prescaler divides by P+1 until the A counter reaches the zero state; (after (P+1).A pulses). At the end of (P+1).A pulses the state of the N_p counter equals (N_p-A). The modulus of the prescaler then changes to P and the prescaler divides by P until the remaining count (N_p-A) in the N_p counter is decremented to zero. When the zero state is

reached both the A and the N_p counters are reset, the prescaler modulus resets to P+1 and the cycle repeats.

The theory of "variable modulus prescaling" presented so far examined the case where the magnitude of the upper and lower modulus of the prescaler differed by 1 . In some applications the ready availability of two moduli prescalers capable of operating at certain frequencies, makes it desirable to use moduli other than P/P+1 .

From equation (5) we have $f_{out} = (N_p.P + A)f_{ref}$.

Consider an additional prescaler (÷M) placed in the loop

thus

$$f_{out} = (N_p P + A).M.f_{ref} \qquad (7)$$

i.e.

$$f_{out} = (N_p P' + AM).f_{ref} \qquad where\ P' = M.P \quad (8)$$

By algebraic manipulation as previous

$$f_{out} = \{(N_p-A).P' + A.(P' + M)\}.f_{ref} \qquad (9)$$

Equation (9) is the general case of equation (6); the moduli of the two modulus prescaler are P' and P'+M . The operation of the P'/P'+M prescaler is similar to that described above for the P/P+1 prescaler.

4.   DESIGN OF A TWO-MODULUS PRESCALER

For receivers operating in the mobile radio bands the required channel spacing is 25 kHz ; thus f_{ref} = 25 kHz . The required output frequency is in the range 100-1000 MHz . The choice of the value of the prescaler modulus P is determined to some extent by the available hardware. However if we choose P = 40 ($P.f_{ref}$ = 10^6 Hz) the programming of the synthesiser is somewhat simplified.

From equation (5) we have

$$f_{out} = (N_p.P.f_{ref} + Af_{ref}) \qquad (10)$$

With P = 40 and f_{ref} = 25 × 10^3 Hz; N_p is then the integer part of the output frequency in MHz and $A.f_{ref}$ is the fractional part of the

output frequency in MHz. For example if f_{out} = 501.425 MHz : N_p = 501 and A = 17 . Since these design conditions have been obtained from equation (5) the moduli of the prescaler are 40/41.

From equation (8) or (9) if P' = 80 M = 2 and f_{ref} = 12.5 kHz N_p and A have the same meanings as before. Thus it is seen to be most convenient if we choose the prescaler moduli to be 40/41 or 80/82 with the reference frequency being 25 or 12.5 kHz respectively.

At the time of design there were two UHF programmable dividers that could be used to implement the required two modulus prescaler. The first divider was a 500 MHz ÷ 10/11 UHF divider from which a 40/41 prescaler could be realised. The second was a 1 GHz ÷ 20/22 divider from which an 80/82 prescaler could be realised.

A block diagram of the UHF 40/41 prescaler is shown in Fig.5. The divide by 40 sequence is (÷10 ÷10 ÷10 ÷10) while the divide by 41 sequence is (÷10 ÷10 ÷10 ÷11). The 80/82 prescaler could be readily obtained by just interchanging the ÷10/11 divider for a ÷20/22 divider.
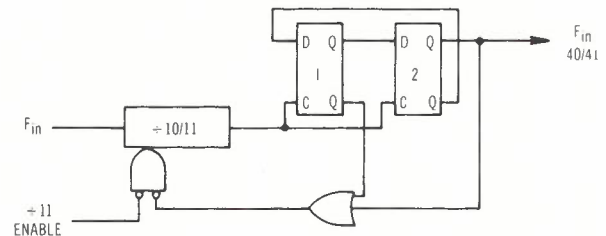

Fig.5 - UHF 40/41 prescaler - block diagram.

5.   25/12.5 kHz REFERENCE FREQUENCY

The 25/12.5 kHz reference frequency is derived from a 5 MHz oven controlled crystal oscillator. This 5 MHz oscillator is a commercially available unit and provision exists for fine frequency adjustment. The ageing rate of this oscillator is typically 5 parts in 10^9/day and the level of the RF output is 1.5 V peak-to-peak into a 50 ohm load.

The 25/12.5 kHz reference is obtained by dividing the 5 MHz signal by 200 or 400 respectively. A simplified block diagram of the dividing circuit is shown in Fig.6. The 5 MHz signal is initially divided by either 2 or 4 and then further divided by 100 using a two decade counter. Both TTL and ECL outputs are available.
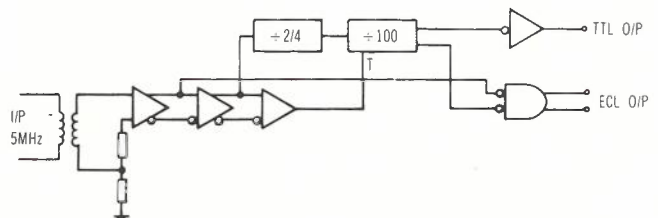

Fig.6 - Frequency reference diving circuit.

6.   PROGRAMMABLE DIVIDER

A block diagram of the programmable divider is shown in Fig.7. This divider is the implementation of the ÷N_p and ÷A programmable counters of Fig.4. The N_p and A counters in conjunction with the counter control logic block provide the

controlling (enabling) signal for the two modulus prescaler. The operational sequence of the counters and the prescaler is as described in section 3. The N_p and A counters each consist of a cascade of programmable decade counters.

When the loop is locked the divider output signal f_{var} equals the reference frequency f_{ref}.

7. PHASE CONTROLLER

The purpose of the phase detector is to determine the lead or lag phase relationships and the time difference between the leading edges of the reference and feedback signal.

The phase detector used is a commercially available unit (MC 12040); which is a four terminal sequential logic circuit. The input terminals are designated R and V and the output terminals are designated U and D. The gain of the phase detector is .16 Volts/radian.

Operation of the device may be illustrated by assuming two input waveforms R and V of the same frequency but differing in phase as shown in Fig.8. If the logic had established by past history that R was leading V the U output of the detector would produce a positive pulse whose width is equal to the phase difference and the D output would simply remain low.

Alternatively it is possible that V was leading R in which case a positive pulse will
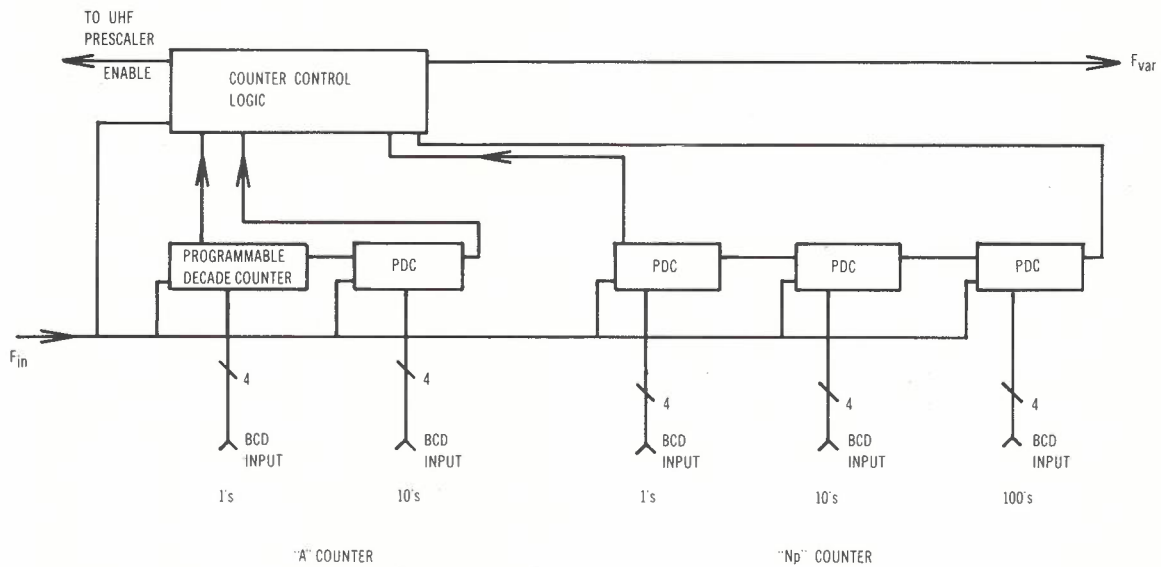
Fig.7 - *Programmable divider.*
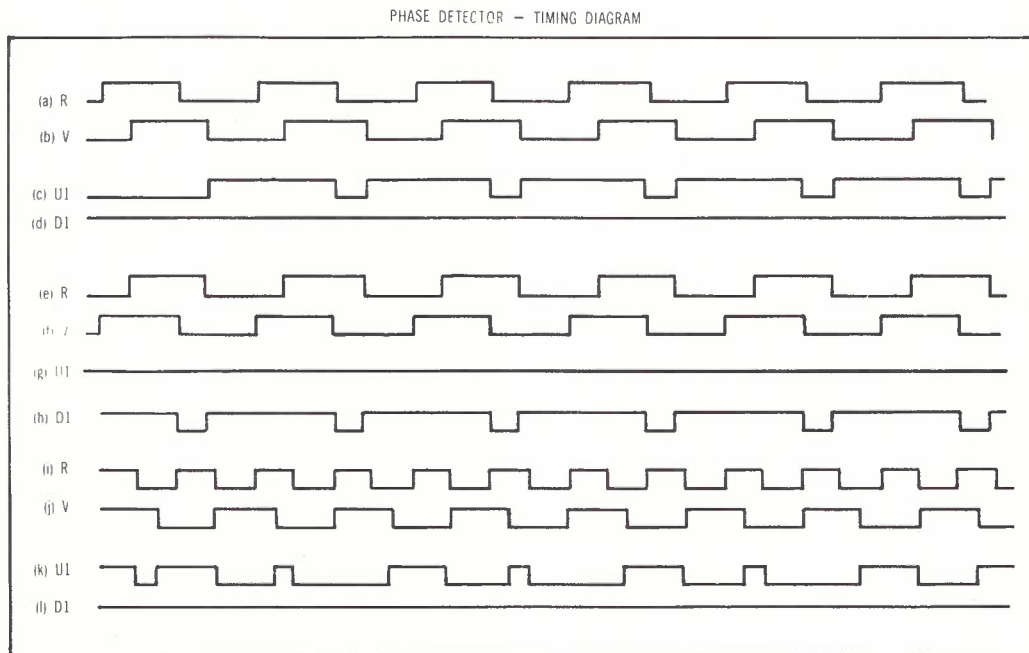
Fig.8 - *Phase controller - timing diagram.*

occur on the D output and the U output would remain low.

Phase error information is contained in the output duty cycle - that is, the ratio of the output pulse width to total period. By integrating or low pass filtering the outputs of the detector and shifting the level to accommodate ECL swings usable analogue information for the voltage controlled oscillator can be developed.

Level shifting is accomplished by differentially driving an operational amplifier from the normally high outputs of the phase detector i.e. $\bar{U}$ and $\bar{D}$, as shown in Fig.9. Phase error summing is accomplished through resistors connected to the outputs of the operational amplifier. Some R-C filtering is imbedded in the input network since the very narrow correctional pulses of the phase detector would not normally be integrated by the amplifier.

In order that the VCO varactor diode is always reversed biased the output of the summing amplifier is offset such that the VCO control voltage always remains positive.

8. LOOP FILTER

The purpose of the loop filter is to integrate the output pulses of the digital phase detector. The filter output is then applied to the Voltage Controlled Oscillator. As will be shown in Appendix 1 fundamental loop characteristics such as the loop bandwidth, capture time and transient response are controlled primarily by the loop filter. The design of the loop filter is discussed in detail in Appendix 1.

The filter has the effect of attenuating the high frequency error components of the phase comparator output, thus enhancing the interference rejection characteristics.

In addition to the primary low pass loop filter it may be necessary to provide filtering to suppress reference frequency components which feed through the loop filter. The suppression of spurious outputs is discussed in Appendix 2. In order to suppress reference frequency components a low pass filter with a deep notch at 25 kHz was provided. The response of this filter is shown in Fig.10.

9. THE VOLTAGE CONTROLLED OSCILLATOR

The design of efficient low noise, high power, high frequency oscillators operating over an adequate tuning range is fraught with many problems.

The voltage controlled oscillator (VCO) used in the synthesiser is quite simple and is based on fundamental concepts rather than going to more sophisticated designs.
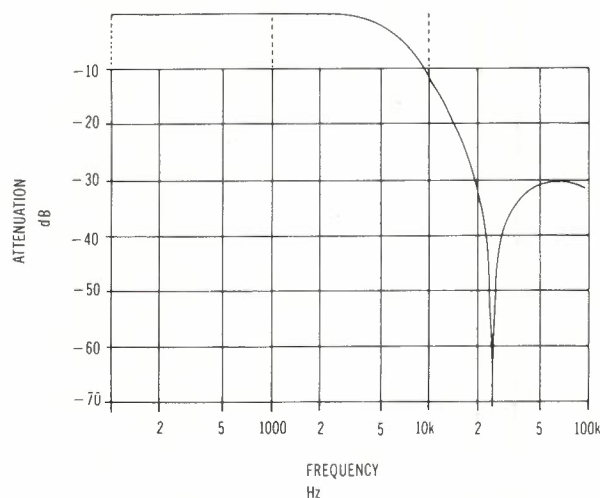
Fig.10 - *Response of reference frequency suppression filter.*

Fig.9 - *Phase controller - block diagram.*

The basic requirements for the VCO were:

    power output - +15 dBm

frequency ranges - 168 - 196 MHz, 490 - 540 MHz

    Also it was desirable that additional frequency ranges could be added at a later date as required; upper limit of 1 GHz.

    This last requirement together with the frequencies involved suggest an oscillator based around a number of cavity resonators.

    Before proceeding with a description of the design it will be an advantage to review the general conditions necessary for oscillation to occur.

9.1 Feedback Requirements for Oscillation

    An oscillator may be represented and studied as a form of feedback amplifier, see Fig.11. For oscillation to occur special requirements are placed on the amplifier block A and on the feedback block β .

    The feedback voltage supplies the entire amplifier input.

Hence

$$E_{in} = E_{fb} = \beta E_o = \beta A E_{in} \qquad (11)$$

i.e.

$$(1 - A\beta)E_{in} = 0 \qquad (12)$$

In order that an output be obtained $E_{in} \neq 0$

Thus for the circuit to produce output

$$(1 - A\beta) = 0 \qquad (13)$$

i.e.

$$A\beta = |1| \underline{/0^o} \qquad (14)$$

This relation is known as the Barkhausen criterion for oscillation.
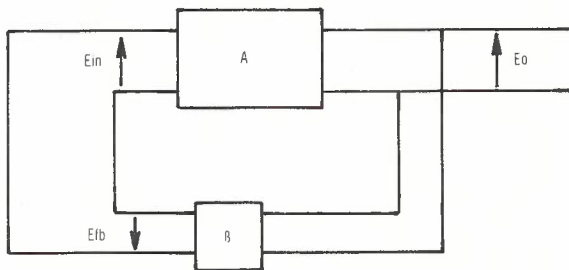
Fig.11 - Basic feedback oscillator.

    The expression emphasises two basic requirements for oscillation: that the gain and phase shift of the blocks A and β , over the frequency range of interest must be such that the overall loop gain is unity and the overall phase shift around the loop is zero or a multiple of 2π radians.

9.2 The Directional Coupler Oscillator

    The block diagram of Fig.11 together with the Barkhausen criterion suggests the configuration shown in Fig.12.

    The output of a wideband amplifier whose gain is G is connected to the input of a matched directional coupler with a coupling numerically slightly less than the gain of the amplifier. The coupled port, port 4, is returned to the amplifier input through the appropriate length of transmission line to provide a net zero phase shift.

    In order to control the frequency of oscillation, a cavity resonator can be inserted in the feedback path. Since the cavity may introduce some loss it may be necessary to increase the gain of the amplifier. Also, since it is required to feedback the VCO output signal to the PLL prescaler, a second directional coupler is used to provide isolation between the VCO and the prescaler. Finally the output is amplified to the required level. A block diagram of the overall VCO is shown in Fig. 13.
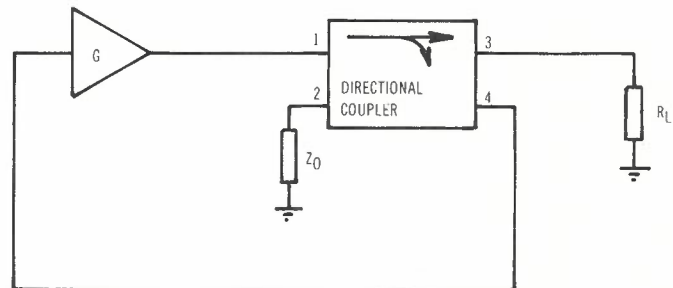

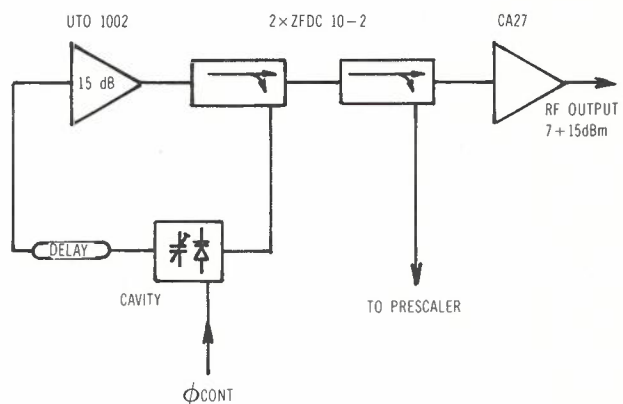*Fig.12 - Suggested configuration of feedback oscillator.*

Fig.13 - Voltage controlled oscillator - block diagram.

Phase Locked Local Oscillators

This approach to oscillator design is now quite attractive in view of the ready availability of low cost stable wideband amplifiers and low cost wideband directional couplers. Also it is only necessary to have one amplifier and coupler to cover all frequency ranges. The frequency band of the oscillator is changed by simply connecting the appropriate cavity and delay line in the feedback loop.

Also it is now possible, with the aid of a vector voltmeter, to conveniently and accurately make the necessary high frequency phase and gain measurements that such an approach requires. The procedure used in the construction and tuning of the VCO is described below.

9.3 The Cavity Resonator

The cavity resonator used for the VCO is of the so called helical resonator type. The advantage of the helical resonator over say coaxial line quarterwave resonators is one primarily of size. Helical resonators have been used extensively in such applications as preselection filters, interstage filters and as the resonant elements in oscillators at VHF and UHF.

The resonator used in the VCO consists of a helix of 16 SWG wire (approximately 11 mm in diameter and 25 mm in length) mounted in a cylindrical cavity. The cavity is 25.4 mm in diameter and 36.5 mm in length and is machined from a solid block of brass. Course frequency tuning of the cavity is accomplished by means of a mechanical tuning capacitor tapped approximately 4 turns from the earth end of the helix. Fine tuning is via the control voltage, derived from the phase locked loop, applied to a varactor diode through a feed through capacitor. The varactor diode is tapped approximately 2 turns from the earth end of the helix. The lid of the cavity provides a mechanically rigid platform on which are mounted the input and output coaxial connectors (sma type), the helical coil and coil former, the variable capacitor and the variator diode and feed through capacitor.

The feed through filter is required to keep the varactor diode dc lead at ac ground and to keep RF from filtering back to the control voltage circuitry. A schematic diagram of the mechanical arrangement is shown in Fig.14. This
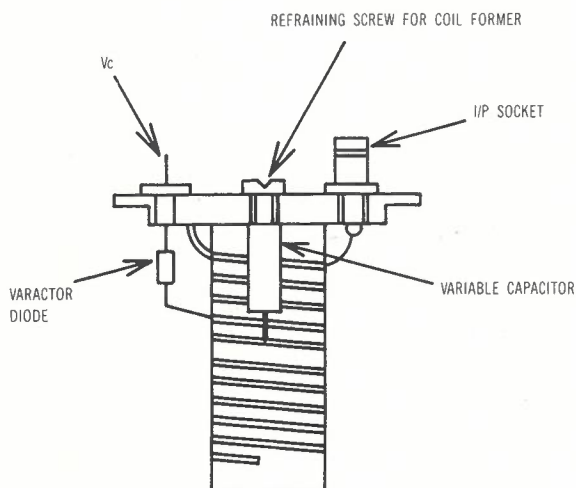
arrangement simplified construction of the resonators and enabled adjustments of the tap positions and trimming of the coil length to be readily accomplished. The helical coil was wound on a Rexolite former to ensure mechanical rigidity of the coil. Ideally it is best if the use of a dielectric former can be avoided. However bench tests indicated that the vibration and shock that the equipment was likely to experience in use, (mounted in a vehicle), would cause movement in the coil and a change of resonant frequency.

The pertinent design equations and nomographs relating the basic parameters of a helix resonator (coil diameter, conductor diameter, axial length of helix, winding pitch etc.) are given in (Refs. 4&5). Having chosen the dimensions of the cavity, the coil diameter is then restricted to a certain range. Having fixed the coil diameter it is then only necessary, (assuming a centre frequency) to solve for the number of turns and the winding pitch.

The design parameters obtained are for operation at one frequency. Since we require the cavity to operate over a band of frequencies a convenient starting point is to choose the centre frequency of the band. Further, the design equations relate to a resonator consisting of a single layer helix on a low loss former and enclosed in a cylindrical shield. They do not make allowance for a mechanical tuning capacitor and/or a varactor diode tuner. Thus some adjustment may be necessary to account for their physical inclusion in the cavity. The most convenient adjustment is the helix length. A recommended procedure is to wind several additional turns above the number indicated by the design equations – this will have the effect of lowering the resonant frequency. The resonant frequency can then be slowly increased by trimming the length of the helix. A second adjustment available is the helix coil pitch. The helix can be either stretched (increases frequency) or compressed (decreases frequency). This procedure is not recommended since it is difficult to obtain a uniform coil pitch and repeatability is low. The other adjustment available is the position of the taps for either the mechanical tuning capacitor or the varactor diode.

9.4 Tuning of the Cavity and Delay Line

Section 9.3 described the cavity resonator used in the VCO and made mention of the adjustments necessary. This section describes the procedure used to adjust the cavity resonator and the delay line length in order to obtain oscillation over the required range.

9.4.1 Adjustment of the Cavity Using the test set up shown in Fig.15 the cavity is adjusted to have minimal insertion loss and a phase shift of approximately $-5°$ at the centre frequency of the band. The procedure used was to trim back the coil at the band upper frequency and then adjust the tap position of the variable capacitor to give an approximately symmetrical phase change across the band. Once the cavity has been adjusted the required length of delay line can be determined using the test set up shown in Fig.16.

9.4.2 Adjustment of Delay Line Length In order to account for the phase change through the interconnecting cables the vector voltmeter is first zeroed with the VCO components removed from the

Fig.14 - Mechanical arrangement of helical resonator.

test set up (i.e. points X and Y connected). The generator output power is adjusted to obtain a convenient magnitude reading on the vector voltmeter. The phase angle reading is then zeroed using the offset and/or vernier adjustment.

With a convenient length of delay line inserted in the loop the signal generator is set to the centre frequency of the band. A convenient operating voltage (say 4-5 volts) is applied to the varactor diode. The variable capacitor was adjusted to give minimum loss around the loop and the phase change around the loop measured.

If the phase angle is positive the delay line is too short and needs to be lengthened. If the phase angle is negative the delay line needs to be shortened.

The amount by which the delay needs to be changed is given by

$$\Delta L \simeq V_f \times \frac{3 \times 10^8}{f} \times \frac{\text{phase angle}^{\circ}}{360} \qquad (15)$$
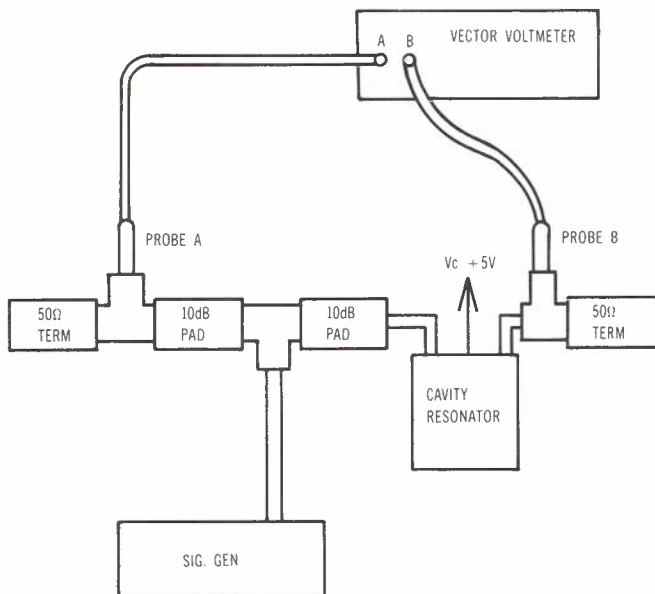
Fig.15 - *Test set up for adjustment of cavity resonator.*
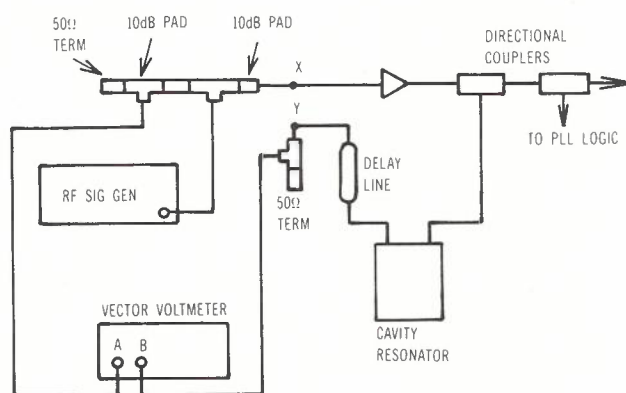
Fig.16 - *Test set up for adjustment of delay line length.*

where ΔL is the change in length in metres

V_f is the velocity factor of the cable (for RG174 $V_f \simeq 0.66$)

f   frequency in Hz.

To facilitate this testing procedure a number of standard lengths of RG174 coaxial line together with SMA M-M / F-F cable adaptors were used to obtain the required length of delay line.

Once the delay line length had been adjusted to achieve zero phase change at the centre frequency the phase and gain of the loop at other frequencies was measured by adjusting the variable capacitor and RF signal generator frequency. The vector voltmeter was rezeroed at each frequency. When satisfactory oscillator performance had been achieved permanent delay lines were constructed.

For the 168-197 MHz cavity, it was found that a single delay line would not produce the conditions for oscillation over the whole band. This problem was overcome by using two delay lines to cover the band.

During the testing procedure it was also found that the 168-197 MHz oscillator had a tendency to oscillate at an overtone frequency of approximately 450 MHz. To overcome this problem a simple L-Section lowpass filter was inserted in the feedback loop. The delay lines were adjusted with this filter in the loop.

9.5 The VCO Characteristic

A plot of the frequency/voltage characteristic at the approximate centre frequency of each band is shown in Fig.17. The characteristic is moved in frequency by manual adjustment of the variable capacitor. Thus it is seen that the loop is only fully automatic over a limited range and the synthesiser can only be considered to be semi-automatic with some manual adjustment necessary.
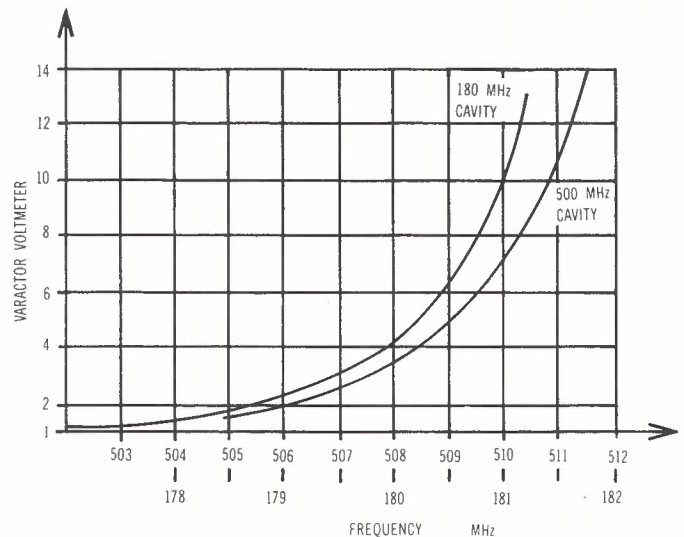

Fig.17 - *VCO characteristic.*

10. FREQUENCY DIFFERENCE DECTOR/TUNING INDICATOR

To assist in the manual tuning of the cavities a tuning indicator is provided. The indicator consists of a frequency difference detector; to measure the difference to frequency between f_{ref} and f_{var} (programmable divider output); an LED display and a tuning meter.

Manual adjustment of the frequency is made by firstly operating a switch which opens the loop, at the phase comparator output, and applies a constant voltage to the cavity varactor diode through the reference frequency suppression filter, and then setting the required frequency on the programmable divider.

The LED display indicates if the cavity is tuned too high or too low in frequency. The variable capacitor is then adjusted as required. As the frequency error is decreased the deflection on the meter is increased. When maximum deflection has been achieved the switch is again operated to close the loop and lock is achieved.

11. CONCLUDING REMARKS

The design of the major components of a phase locked synthesiser that employs a novel VCO have been described. The synthesiser's frequency range can be readily expanded by the inclusion of further suitable cavity resonators and appropriate delay lines. The penalty for this feature is that the synthesiser is not fully automatic. However this is not seen as a serious restriction since the manual tuning procedure is relatively simple and requires no external test apparatus. Also, since the synthesiser is to be used as a local oscillator in a field strength receiver, frequent changes to the operating frequency are not envisaged.

12. ACKNOWLEDGEMENTS

13. REFERENCES

1.   Lawson, I., Hicks, P. and De Jong, H., "Field Strength Survey Techniques for Mobile Radio Services", ATR Vol.15, No.1, May 1981.

2.   Colloquium on Phase Locked Techniques - Proceedings, Presented by IEE Professional Group E10, London, March 1980.

3.   Phase-Locked Loop Systems Data Book, Motorola Semiconductor Products Inc., 1973.

4.   Macalpine, W.W. and Schildknecht, R.D., "Coaxial Resonators with Helical Inner Conductor", Proc. IRE, 47, December 1959, p.2099.

5.   Macalpine, W.W. and Schildknecht, R.D., "Helical Resonator Design Chart", Electronics, 12 August, 1960, p.140.

6.   Gardner, F.M, "Phaselock Techniques", Pub. Wiley, 1966.

APPENDIX 1 : Loop Analysis and the Design of the Loop Filter

This appendix discusses the calculation of the time constants for various types of filter. The phase locked loop can be represented by the functional block diagram of Fig.A1 (Ref.6). This assumes that the loop is locked and the phase detector is linear.

Applying elementary control systems theory the closed loop response is given by

$$\frac{\theta_o(s)}{\theta_i(s)} = \frac{k_p.F(s).k_v}{s + \dfrac{k_p.F(s).k_v}{N}} \tag{16}$$

where $k_p.$, $F(s)$, k_v and $1/N$ are the gain constants of the various blocks as shown in Fig.A1.

From equation (1) it is seen that the loop filter will to a large extent determine fundamental loop characteristics such as loop bandwidth, transient time and capture time.

In some applications it may be necessary to consider the phase error that exists, in the phase detector, between the reference/input signal $\theta_i(s)$ and the feedback signal $\theta_o(s)/N$

It can be shown that

$$\frac{\theta_e(s)}{\theta_i(s)} = \frac{1}{1 + \dfrac{k_v k_p F(s)}{sN}} \tag{17}$$

where

$$\theta_e(s) = \theta_i(s) - \frac{\theta_o(s)}{N} \tag{18}$$

Consider the situation of applying an input frequency that is different to the VCO output.
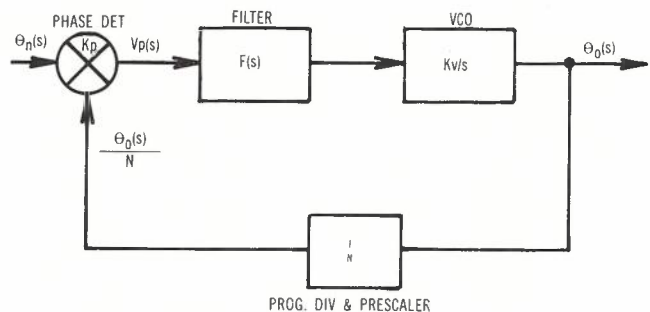

Fig.A1 - Functional block diagram of phase locked loop.

Since frequency is the derivative of phase this is equivalent to applying an input signal $\theta_i(t)$ where

$$\theta_i(t) = C_v \cdot t \quad t \geq 0 \quad ; \quad \text{so called step velocity input}$$

$$(19)$$

and C_v is the magnitude of the rate of change of phase in rad/sec.

Applying the Final Value Theorem we have

$$\lim_{t \to \infty} \theta_e(t) = \lim_{s \to 0} \left\{ s \cdot \frac{1}{1 + \dfrac{k_v k_p F(s)}{sN}} \cdot \frac{C_v}{s^2} \right\} \quad (20)$$

If $F(s)$ is of the form

$$F(s) = \frac{k_f(s+a)}{s} \quad (21)$$

then

$$\lim_{t \to \infty} \theta_e(t) = 0 \quad (22)$$

Thus it is seen that if it is desired for the PLL to track a reference frequency (step velocity input) with zero phase error the open loop gain of the system should have at least two poles located at the origin. Such a system is known as a type 2 system. The filter zero at $s = -a$ is required to provide stability.

The design of a phase locked synthesiser would not generally demand phase coherency between the VCO output and the reference input. However a type 2 system offers some design advantages which will be discussed later. Alternatively a simple lag-lead filter may be adequate if phase coherency is not required.

Having specified the general form of the filter transfer function it is then only necessary to specify the filter time constant to complete the phase locked loop design. The time constants are calculated primarily from stability considerations.

Consider the following cases.

Case (i)

$$F(s) = \frac{T_2 s + 1}{T_1 s} \quad (23)$$

This function can be realised by the circuit of Fig.A2.

The characteristic equation of the resulting type 2 system is given by

$$s^2 + \frac{k_p k_v T_2}{N\, T_1} s + \frac{k_p k_v}{N.T_1} = 0 \quad (24)$$

i.e.

$$s^2 + 2\xi\omega_n s + \omega_n^2 = 0 \quad (25)$$

Equating coefficients we have

$$\omega_n = \frac{k_p k_v}{N\, T_1}^{\frac{1}{2}} \quad (26)$$

ω_n is known as the natural frequency

$$\xi = \frac{1}{2} \frac{k_p k_v}{N\, T_1}^{\frac{1}{2}} \cdot T_2 = \tfrac{1}{2}\omega_n T_2 \quad (27)$$

ξ is known as the damping factor.

The response of the type 2 second order system to a step of phase input can be readily calculated. The normalised step response is given by

$$\theta_o(t) = 1 + \frac{\exp(-\xi\omega_n t)}{\sqrt{1-\xi^2}} \cdot \text{Sin}\{\omega_n t \sqrt{1-\xi^2} - \phi\}$$

$$\text{for} \quad \xi \neq 1 \quad (28)$$

where

$$\tan\phi = \sqrt{1-\xi^2}/\xi \quad (29)$$

and

$$\theta_o(t) = 1 + \exp(-\omega_n t) \cdot \{\omega_n t - 1\} \quad \text{for} \quad \xi = 1.$$

$$(30)$$

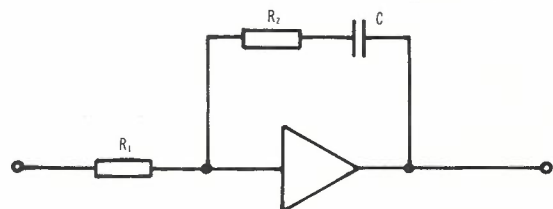*Fig.A2 - Loop filter* $F(s) = T_2 s/(T_1 s + 1)$

The above expressions are plotted as a family of curves for various values of damping factor ξ in Fig.A3. Each curve is plotted as a function of normalised time $\omega_n t$. For a given ξ and a required lockup time the ω_n required to achieve the desired results can be determined. Thus we see that for a loop with this filter we can independently choose ξ and ω_n.

However in choosing the filter time constants we must take into consideration that the factor k_V/N will vary as the synthesiser operating frequency is changed. The usual case will be that k_V will vary with both frequency and control voltage. The value adopted in calculations was the average gradient of the VCO characteristic over the expected control voltage range.

Without going to the complication of designing an adaptive filter the following design procedure was used. From lock-up time considerations an ω_n is chosen. For a selected value of ξ the filter time constants can then be calculated, from equations (26) and (27), using the values of k_V and N applicable when the synthesiser operating frequency is a maximum. Using these values for the time constants the stability of the loop is then checked at other frequencies as N and k_V vary. (The natural frequency, damping factor, and closed loop pole positions were calculated.) The calculations are then performed for a different value of ξ.

This procedure can be most readily carried out using a programmable desktop calculator and will provide the designer with a number of suitable filter designs.

An alternative starting point is to select the desired -3 dB closed loop bandwidth. It can be shown that for a type 2 second order system the -3 dB bandwidth of the locked loop is given by

$$\omega_{-3dB} = \omega_n \{1 + 2\xi^2 + (2 + 4\xi^2 + 4\xi^4)^{\frac{1}{2}}\} \qquad (31)$$

Thus for a given damping ratio and a desired loop bandwidth (at the maximum operating frequency) the required value of ω_n and hence the filter coefficients can be determined.

Case (ii)

$$F(s) = \frac{T_2 s + 1}{(T_1 + T_2)s + 1} \qquad (32)$$

This transfer function can be realised by the circuit of Fig.A4.

For this filter the characteristic equation is given by equation (25)
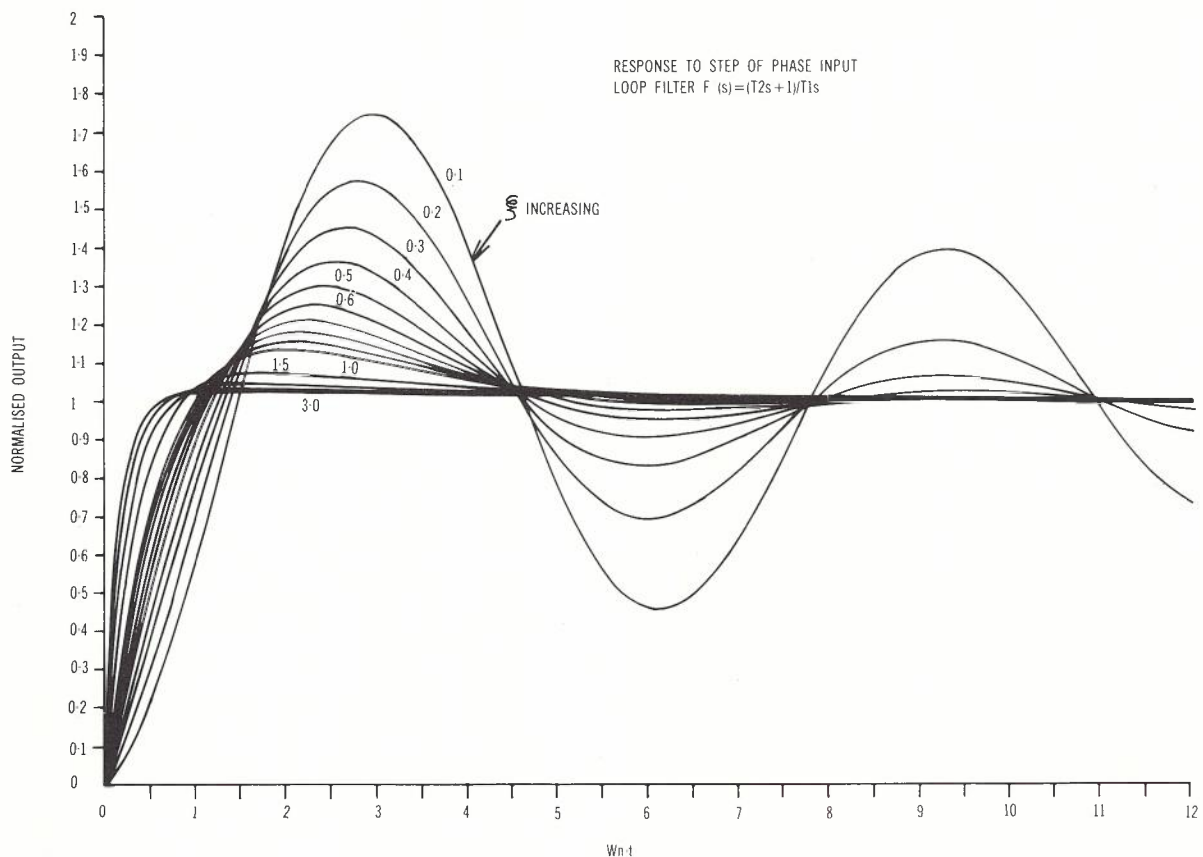

Fig.A3 - Response of PLL for step of phase input (Filter Fig.A2)

where

$$\omega_n^2 = \frac{k_p k_v}{N(T_1 + T_2)} \qquad (33)$$

and

$$2\xi\omega_n = \frac{k_p k_v T_2}{(T_1 + T_2)N} + \frac{1}{T_1 + T_2} \qquad (34)$$

$$\xi = \frac{\omega_n}{2}\left[T_2 + \frac{N}{k_p k_v} \right] \qquad (35)$$

For a realisable filter $T_2 > 0$

and thus

$$\frac{2\xi}{\omega_n} > \text{max value}\left[\frac{N}{k_p k_v} \right] \qquad (36)$$

Equation (36) places a restriction on the value of ω_n assuming a value of ξ. However ω_n and ξ can still be selected independently.

The normalised response of the loop to a step of phase input is given by

$$\theta_o(t) = 1 + \frac{\exp(-\xi\omega_n t)}{\sqrt{1-\xi^2}}\left\{ (T_2\omega_n - \xi)Sin\omega_n\sqrt{1-\xi^2}t \right.$$

$$\left. - \sqrt{1-\xi^2}\ Cos\omega_n\sqrt{1-\xi^2}t \right\} \qquad \text{for } \xi < 1$$
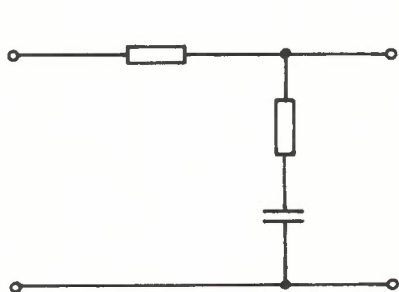
$$(37)$$

Fig.A4 - Loop filter
$$F(s) = (T_2 s + 1)/((T_1 + T_2)s + 1)$$

This response can only be readily plotted for differing values of ξ against normalised time $\omega_n t$ assuming a value of $T_2.\omega_n$ as shown in Fig. A5.

The design procedure used to determine the time constants was as follows. For an initial value of ξ the maximum integer value of ω_n was calculated such that inequality of equation (36) was satisfied. Using these initial values the time constants were then calculated using the values of N and k_v applicable at the maximum frequency. The stability of the loop at other frequencies was then confirmed. The whole procedure can then be repeated for a different initial value of ξ. This procedure was readily performed on a desktop calculator.

It is to be noted that the achievable closed loop bandwidth for the locked loop is considerably less than that which can be achieved by the filter of case (i).

Case (iii)

$$F(s) = 1/1 + T_1 s \qquad (38)$$

For this filter we have following a similar procedure to the above

$$\omega_n^2 = \frac{k_p k_v}{N T_1} \qquad (39)$$

$$2\xi\omega_n = 1/T_1 \qquad (40)$$

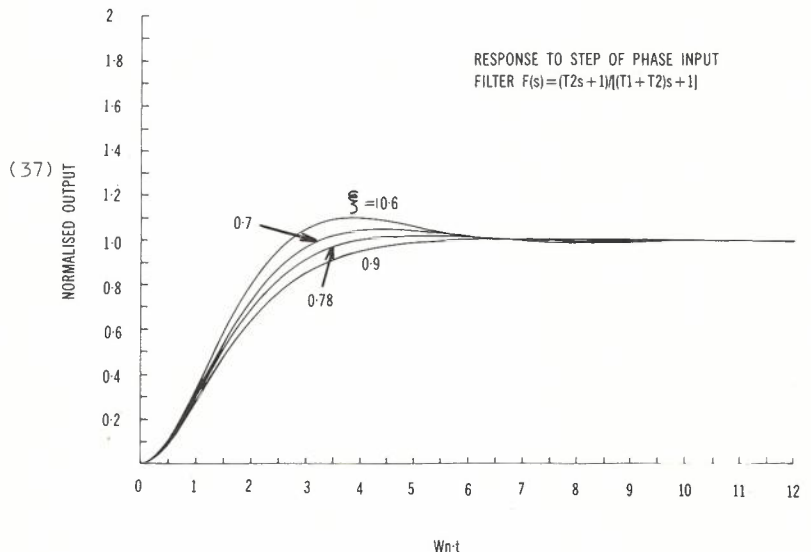$$\therefore \quad \omega_n = \frac{2\xi k_p k_v}{N} \qquad (41)$$

Fig.A5 - Response of PLL for step of phase input (Filter Fig.A4)

Thus we see that ω_n and ξ are not independent.

$$\frac{S}{C} = V_\phi \frac{\xi \omega_n N}{k_p \omega_{ref}} \tag{46}$$

APPENDIX 2 : Suppression of Spurious Outputs

In addition to defining loop gain and assuring stability under operating conditions, consideration to minimizing spurious spectral components may be required. The worst of the spurious signals is often the reference frequency sidebands.

Any steady state signal on the VCO control line will produce sidebands in accordance with FM theory. For small spurious deviations the relative sideband-to-carrier levels are given by

$$\frac{\text{sidebands}}{\text{carrier}} \simeq \frac{V_{ref} \cdot k_v}{2\omega_{ref}} \tag{42}$$

where V_{ref} is the peak voltage of the spurious frequency on the VCO control line.

The most likely cause of unwanted control line modulation is from the phase detector pulse components feeding through the loop filter.

If V_ϕ is the peak value of the reference frequency voltage at the phase detector output and V_{ref} is the peak value of the reference frequency at the VCO input:

$$V_{ref} = V_\phi \cdot F(s) \Big|_{s=\omega_{ref}} \tag{43}$$

For the filter

$$F(s) = T_2 s + 1/T_1 s \tag{44}$$

$$\frac{\text{sideband level}}{\text{carrier level}} = V_\phi \frac{T_2}{T_1} \frac{k_v}{2\omega_{ref}} \tag{45}$$

substituting for T_2 and T_1 from expression in Appendix 1.

For the filter

$$\frac{T_2 s + 1}{(T_1 + T_2)s + 1} \tag{47}$$

We have from Appendix 1

$$T_1 + T_2 = \frac{k_p k_v}{N\omega_n^2} \tag{48}$$

$$T_2 = 2 \xi/\omega_n - N/k_p k_v \tag{49}$$

$$\therefore \quad V_{ref} = V_\phi \frac{N\omega_n^2}{k_p k_v} \left\{ \frac{2\xi}{\omega_n} - \frac{N}{k_p k_v} \right\} \tag{50}$$

$$\therefore \quad \frac{S}{C} = V_\phi \frac{N\omega_n^2}{2k_p \omega_{ref}} \left\{ \frac{2\xi}{\omega_n} - \frac{N}{k_p k_v} \right\} \tag{51}$$

Consider the case $\xi = 8$, $\omega_n = 52$, $N = 22000$. Assuming $V_\phi = 10$ mV and substituting into equations (5) and (10) we find that the filter of equation (47) provides approximately 47 dB sideband suppression; $\simeq 38$ dB more than the filter of equation (44).

Since it is difficult to estimate V_ϕ and in cases where phase coherency of reference and output signal are required (filter given by equation (44)) it is advisable to provide additional loop filtering to increase the sideband suppression. Any lowpass roll off must be removed from ω_n and yet be well below ω_{ref}. The response of the suppression filter used is shown in Fig.10. With this filter the sideband suppression was greater than 58 dB.

BIOGRAPHY

PETER R. HICKS - see previous paper in this issue.